Ability of a non-invasive sensor to improve soil management of paddy rice fields

Mohammad Monirul Islam

Promotor **Prof. dr. ir. Marc Van Meirvenne**
Department of Soil Management
Faculty of Bioscience Engineering
Ghent University

Dean **Prof. dr. ir. Guido Van Huylenbroeck**

Rector **Prof. dr. Paul Van Cauwenberge**

MOHAMMAD MONIRUL ISLAM

ABILITY OF A NON-INVASIVE SENSOR TO IMPROVE SOIL MANAGEMENT OF PADDY RICE FIELDS

Thesis submitted in fulfilment of the requirements for the degree of Doctor (PhD) in Applied Biological Sciences: Land and Forest Management

Cover: Photograph of a FloSSy mobile survey on a flooded paddy rice field in Bangladesh.

Reference:

M.M. Islam. Ability of a non-invasive sensor to improve soil management of paddy rice fields. PhD thesis, Ghent University, November 2012.

ISBN-number: 978-90-5989-562-1

ACKNOWLEDGEMENTS

First, I would like to express my heartfelt respect and immense indebtedness to my promoter Prof. dr. ir. Marc Van Meirvenne, Department of Soil Management, Faculty of Bioscience Engineering, Ghent University for teaching me the creativity and the science of solving problems. I thank him for accepting me as a PhD candidate and for building up the research project; next, for his worthy guidance, valuable suggestions, helpful comments and continuous supervision throughout the research work and for the preparation of this thesis.

I take pleasure to express my deep sense of gratitude and appreciation to my colleagues of the ORBit (Onderzoeksgroep Ruimtelijke Bodeminventarisatietechnieken) research group of the Department of Soil Management for supporting me in various ways. For that I am grateful to all of them. I especially thank Timothy, Philippe, Eef and Ellen, "your unbound help, comments and suggestions have helped me a lot to carry out this research". I thank Valentijn for helping me in the field work under the scorching sun. I am also thankful to Sam (Samuel) for being a nice collaborator during my stay in ORBit.

I thank all members of the Department of Soil Management for providing a friendly and interactive research environment which inspired me to continue the work with sincerity and devotion. Special thanks to Mathieu and Luc for showing me the laboratory procedures of analyzing my soil samples.

The financial and administrative support of BOF-UGent (Bijzonder Onderzoeksfonds - Universiteit Gent), Belgium is highly acknowledged. The administrative and physical help of the Bangladesh Agricultural University, Mymensingh in Bangladesh and the Department of Agronomy of the same university are undoubtedly acknowledged. I would like to thank the University for using the paddy rice fields to conduct my research.

I would like to acknowledge the many people who have helped me in various ways throughout the realisation of the study and the writing of this thesis. I thank all of them for their general support. I express my heavenly love to my beloved wife Kamrun Nahar (Nipa) and my son Muhammad Fatanul Islam (Fatan). Last but not the least, I express my ever indebtedness to my parents who sacrificed their happiness for my higher education and gave me continuous inspiration and encouragement during my study and research.

Mohammad Monirul Islam

Table of contents

List of figures

List of tables

List of abbreviations and acronyms

CEC = Cation Exchange Capacity

CV = Coefficient of Variation

EC = Electrical Conductivity

EC_a = Apparent Electrical Conductivity

EC_a-d = Apparent Electrical Conductivity in dry condition

EC_a-H = Apparent Electrical Conductivity in Horizontal orientation

EC_a-V = Apparent Electrical Conductivity in Vertical orientation

EC_a-w = Apparent Electrical Conductivity in wet (flooded) condition

EC_e = Soil paste Electrical Conductivity

EC_p = Solid phase Electrical Conductivity

EC_w = Soil solution Electrical Conductivity

EMI = Electromagnetic Induction

ET = Evapotranspiration

FloSSy = Floating Soil Sensing System

FPI = Fuzziness Performance Index

GPS = Global Positioning System

GUI = Graphical User Interface

MEE = Mean Estimation Error

MPE = Modified Partition Entropy

NCE = Normalized Classification Entropy

OC = Organic Carbon

OK = Ordinary Kriging

OM = Organic Matter

PA = Precision Agriculture

PR = Penetration Resistance

PVC = Polyvinyl Chloride

RMSEE = Root Mean Square Estimation Error

RNE = Relative Nugget Effect

SD = Standard Deviation

SK = Simple Kriging

SKlm = Simple Kriging with varying local means

SSSM = =Site Specific Soil Management

USDA = United States Department of Agriculture

Samenvatting

Precisiebodembeheer richt zich voor het maken van beheerbeslissingen op het kwantificeren van de binnen-perceels variabiliteit. Hierbij is het verwerven van gedetailleerde bodeminformatie een noodzakelijke voorwaarde, maar in de meeste gevallen is de beschikbaarheid van dergelijke informatie ontoereikend. De kosten, inspanning en tijd nodig voor het verzamelen en analyseren van bodemstalen zijn dan ook algemeen bekende beperkende factoren voor de gedetailleerdheid van bodeminformatie. Dit gebrek aan informatie vormt een van de voornaamste hinderpalen voor plaatsspecifiek beheer in paddy rijstvelden.

De karakterisering van paddy rijstvelden is traditioneel gebaseerd op een beperkt aantal bodemstalen die worden verzameld onder droge of onverzadigde omstandigheden, wat overeenstemt met de gebruikelijke bemonsteringsomstandigheden voor akkerland. Paddy rijst wordt echter geteeld in natte of overstroomde omstandigheden waarbij de fysische, chemische en biologische eigenschappen van de verzadigde bodem anders zijn dan in de droge periode. De karakterisering van paddy velden onder teeltomstandigheden is een sleutel tot precies en duurzaam beheer van bodemgrondstoffen ter ondersteuning van gewasteelt. De verzameling van bodeminformatie onder teeltomstandigheden wordt echter sterk bemoeilijkt door de overstroomde omstandigheden. Desondanks is er nood aan gedetailleerde en kwantitatieve informatie over bodemeigenschappen die de paddy oogst beïnvloeden, en dus zouden aanvullende gegevens die informatie over deze bodemeigenschappen kunnen verstrekken welkom zijn. In deze context hebben recente technologische ontwikkelingen het mogelijk gemaakt om in hoge resolutie bodeminformatie te verzamelen door toepassing van niet-invasieve proximale bodemsensoren.

Deze scriptie gaat in op de ontwikkeling en de studie van een bodemsensor voor paddy rijstvelden. Deze sensor is gebaseerd op elektromagnetische inductie (EMI), zoals de EM38 of de EM38-MK2 sensor. Deze sensoren meten de schijnbare (*apparent*) elektrische geleidbaarheid (EC_a) van de bodem op basis van het EMI principe. De afstand tussen de zend- en ontvangstspoel bepaalt de diepte tot waarop bodeminformatie kan verkregen worden. Metingen kunnen zowel in de horizontale oriëntatie (EC_a-H) als de verticale oriëntatie (EC_a-V) worden gemaakt, elk met hun eigen dieptegevoeligheid. De EM38 meet steeds in een enkele spoelconfiguratie, terwijl de EM38-MK2 de twee configuraties

combineert. Beide sensoren zijn niet-invasief, wat betekent dat ze geen direct contact met de bodem vereisen. Het doel van dit onderzoek was het ontwikkelen van een bodemsensor, en om via verschillende casestudies het potentieel ervan te onderzoeken voor gedetailleerd beheer van paddy velden. De paddy velden die hiervoor werden gebruikt zijn gelegen in de Brahmaputra overstromingsvlakte.

Eerst werd gefocust op de ontwikkeling van een drijvende bodemsensor voor overstroomde paddy velden. Er werd een *Floating Soil Sensing System* (FloSSy) ontworpen dat in staat is om in dergelijke omstandigheden gedetailleerde geogerefereerde informatie te verzamelen en realtime te verwerken. De FloSSy is opgebouwd uit een EMI bodemsensor, een GPS, een veldlaptop en software voor realtime verwerking van sensordata en stuurbegeleiding, een waterdichte behuizing voor de bodemsensor en een drijfplatform voor de sensor en de GPS. De FloSSy kan realtime EC_a en GPS informatie verwerken en deze converteren naar het vereiste gebruikersformaat. Het systeem beschikt over een software component, de FloSSy logger, die toelaat om in een volautomatische mobiele set-up te werken. De grafische gebruikersinterface (GUI) van de logger toont de verplaatsingsweg van de sensor in realtime zodat een constante afstand kan behouden worden tussen de verschillende meetlijnen die het veld doorkruisen. Het gewicht van het sensorplatform is laag genoeg om probleemloos getrokken te kunnen worden door een typische paddy veld cultivator. Als dusdanig werd het systeem voorbereid om te functioneren onder paddy groeiomstandigheden, wat meteen ook de aanleiding was naar het onderzoek rond de inzetbaarheid van het systeem.

Aangezien overstroomde paddy velden duidelijk verschillende fysisch-chemische eigenschappen ontwikkelen gedurende het groeiseizoen, werd onderzocht hoe representatief de resultaten voor een veld opgemeten onder droge omstandigheden zijn voor de overstroomde omstandigheden tijdens het groeiseizoen. Daartoe werd via de FloSSy uitgerust met de EM38 de EC_a-H van een alluviaal veld van 1.4 ha opgemeten, zowel onder droge als onder overstroomde omstandigheden en werden de resultaten van beide surveys vergeleken. Omwille van het gladde wateroppervlak onder overstroomde omstandigheden, die een verhoogde stabiliteit van het sensorplatform verzekerden, vertoonden de resultaten van de survey een aanzienlijk gereduceerde EC_a variabiliteit. Verder leverden de resultaten voor de overstroomde omstandigheden betrouwbaardere bodemgerelateerde informatie, voornamelijk door de afwezigheid van bodemvochtdynamiek. De verschillen tussen EC_a onder droge en

overstroomde omstandigheden werden toegekend aan verschillen in bodemtextuur, en dan hoofdzakelijk aan de variatie in zandgehalte die een beduidend effect heeft op bodemvochtverschillen bij overstroming van een droog veld. Daarom worden de grootste verschillen in EC_a tussen droge en overstroomde omstandigheden teruggevonden in de delen van het veld met een hoog zandgehalte. De studie toonde aan dat een EC_a survey onder overstroomde omstandigheden een toegevoegde waarde heeft voor precisiebodembeheer.

Een volgende studie doelde op het testen van het potentieel van het systeem voor het verkrijgen en verwerken van gedetailleerde geogerefereerde bodeminformatie van overstroomde velden met het oog op bodembeheer op veldschaal. In deze studie werd een alluviaal paddy veld van 2.7 ha gebruikt. De EC_a survey met de FloSSy werd uitgevoerd na de gebruikelijke voorbereiding van het veld door puddle-bewerkingen en vóór de seizoensbeplanting met rijstzaailingen. Op het moment van de metingen stond het water op het veld ongeveer 0.18 tot 0.20 m hoog. De rijsnelheid was circa 3.6 km h^{-1} en de metingen werden uitgemiddeld tot één waarde per vierkante meter. De resolutie van de verwerkte data was dus 1 observatie per m^2. Er werden tevens bodem- en gewasstalen verzameld ter interpretatie van de gemeten EC_a. De verkregen hoge-resolutie EC_a data werd ingedeeld in drie klassen via een fuzzy *k*-means classificatie. De variatie tussen deze klassen kon worden toegeschreven aan verschillen in de schijnbare dichtheid van de ondergrond (0.15 - 0.30 m onder het grondoppervlak), waarbij de kleinste EC_a waarden overeenstemmen met de laagste dichtheid. Dit effect werd verklaard door verschillen in compactie van de ploegzool wegens verschillende puddle-bewerking. Er werd eveneens een significant verschil in rijstoogst waargenomen tussen de verschillende EC_a klassen. Met deze casestudy werd aangetoond dat de FloSSy toelaat om relevante bodeminformatie te verzamelen, wat perspectieven opent voor de toepassing van precisielandbouw op overstroomde landbouwvelden. Hierop steunend, werd de focus van deze scriptie verschoven in de richting van evaluatie van de FloSSy voor bodembeheeraspecten van paddy velden.

Onze volgende doelstelling betrof het beheer van bodemwater voor paddy teelt. Het in stand houden van een aangewezen waterhoogte is cruciaal om voldoende waterbeschikbaarheid te verzekeren voor het paddy gewas. Deze vereiste vormt een uitdaging voor snelle identificatie van zones gevoelig voor percolatie. Het doel van deze studie was het evalueren van een methodologie die gebruikmaakt van de EMI sensor in de FloSSy om gebieden met waterlekkage te identificeren, om bij te dragen aan precisiebeheer van

bodemwater op een binnen-perceelsschaal. De EC_a-V van een paddy veld met een oppervlakte van 1.4 ha werd geregistreerd onder zowel droge als overstroomde omstandigheden. Vergelijking van deze twee EC_a datasets toonde opnieuw aan dat EC_a metingen onder overstroomde omstandigheden (EC_a-w) sterker gerelateerd waren met bodemeigenschappen, omwille van de afwezigheid van variatie in bodemvocht en de verhoogde stabiliteit van het drijvende sensorplatform. Daarom werd verder gewerkt met de EC_a-w metingen, die in twee klassen werden gegroepeerd via een fuzzy *k*-means classificatie. Deze klassen vertoonden significante verschillen in waterinfiltratie: lagere EC_a waarden vertegenwoordigden een hogere infiltratiesnelheid en vice versa. Dit effect werd toegekend aan verschillen in bodemtextuur, meer bepaald aan het zandgehalte, en het effect ervan op de waterretentie. Deze resultaten bewezen dat een EC_a-w survey met de FloSSy toeliet om de bodemheterogeniteit gelinkt met neerwaartse waterfluxen te detecteren, wat potentieel het beheer van bodemwater in paddy velden kan ondersteunen. Dit toonde het potentieel van de EMI sensor in de FloSSy configuratie aan om overstroomde omstandigheden in paddy velden te behouden door de aanpassing van bodembeheerpraktijken.

Paddy velden worden herhaaldelijk gepuddled onder quasi-waterverzadigde omstandigheden om de bovenste bodemlaag los te maken en een uniform gecompacteerde ploegzool te vormen die vereist is om het verlies van water en nutriënten te beperken. Onder paddy groeiomstandigheden vormt het echter een uitdaging om de compactievariatie binnen de ploegzool op een niet-invasieve manier te detecteren. Daarom werd in een volgende studie de methodologie geëvalueerd waarbij door toepassing van de FloSSy wordt getracht om gebieden te identificeren die zijn gecompacteerd door verschillende intensiteiten van puddling. Een paddy veld van 1.6 ha werd hiervoor geselecteerd. Het veld werd opgesplitst in drie gebieden met een variabele compactie door graduele toename van de puddlingintensiteit. Van elk gebied werden de bodemeigenschappen gekarakteriseerd en werd de EC_a opgemeten via de FloSSy. Daarnaast werden de effecten ingeschat van compactie van de ploegzool op verliezen via waterpercolatie en op paddy oogst. De resultaten geven weer dat de gebieden met verschillende compactie significant verschilden qua schijnbare dichtheid van de bodem, gerelateerd met de penetratieweerstand van de bodem. Vergelijking van de EC_a datasets toont dat de EC_a waarden systematisch toenemen met toenemende compactie. Voldoende bodemcompactie werd vastgesteld wanneer percolatieverliezen het laagst waren en paddy oogst het hoogst. Er werd aangetoond dat een niet-invasieve EC_a survey gebruikmakend van een EMI bodemsensor toelaat om de bodemheterogeniteit, gelinkt met

bodemcompactie door puddle-bewerkingen, te detecteren. Dit creëert interessante mogelijkheden voor precisiebeheer van puddling and landvoorbereiding in paddy velden.

In een laatste studie werd verder onderzoek gedaan naar het potentieel van de FloSSy om de binnen-veld variabiliteit van de gecompacteerde bodemlaag te modelleren. Een sleutelkenmerk van overstroomde paddy velden is de ploegzool die ontstaat door puddling. Dit is een bodemlaag in de ondergrond met hogere compactie en schijnbare dichtheid, die waterverlies door percolatie beperkt. De dikte van deze gecompacteerde laag kan echter ruimtelijk variëren, met gevolgen voor het beheer van de waterhuishouding binnenin het veld. Om die reden werd een methodologie ontwikkeld om de verticale variatie i van de gecompacteerde laag te bepalen. De niet-invasieve EMI sensor EM38-MK2 werd daarvoor gemonteerd in de FloSSy en een paddy veld van 2.7 ha opgemeten, waarbij de EC_a van de natte paddy bodem werd geregistreerd in hoge resolutie (1.0 × 0.5 m). De schijnbare dichtheid van de bodem en de diepte van de gecompacteerde laag werden verkregen door zowel klassieke staalname van ongeroerde bodemkernen als penetrometermetingen. Er werd een sterke relatie gevonden tussen de diepte van de gecompacteerde laag en de EC_a (n = 10), gemeten met de EM38-MK2 sensor in de verticale oriëntatie met 0.5 m spoelafstand. Deze relatie werd gevalideerd door onafhankelijke observaties (n = 18) van de diepte van de gecompacteerde laag resulterend in een Pearson correlatiecoëfficiënt van 0.87 en een RMSEE waarde van 0.03. De EC_a metingen lieten toe om een nauwkeurige schatting te maken van de diepte van de ploegzool onder de waterverzadigde bodemlaag. Het verband tussen waterverlies en diepte van de gecompacteerde laag werd bevestigd door metingen van de waterpercolatie, waarbij een inverse relatie werd gevonden met een Pearson correlatiecoëfficiënt van 0.89. Dit opent nieuwe perspectieven om de ploegzool gedetailleerd te karakteriseren, waardoor bodembeheer in paddy rijstvelden geoptimaliseerd kan worden.

Uit deze studie bleek dat een niet-invasieve EMI bodemsensor in een mobiele configuratie een waardevol hulpmiddel is voor het verkrijgen van bodeminformatie van overstroomde paddy rijstvelden, en dus van grote betekenis is voor het introduceren van precisielandbouwpraktijken in paddy teeltsystemen.

Summary

Precise soil management aims at quantification of within-field soil variability to take management decisions. Obtaining detailed soil information is a pre-requisite. But in most cases the availability of soil survey information does not meet the requirements. The cost, effort and time needed to collect and analyze soil samples already limit the detail of soil information. Lack of information is one of the key obstacles that potentially prevent site-specific soil management in paddy rice fields.

Characterization of paddy fields is based on the limited number of soil samples collected under dry or unsaturated soil conditions, which is also the usual condition of sampling an arable field. Paddy rice is grown in wet or flooded condition when the saturated soil is different than in the dry period, in physical, chemical and biological properties. The characterization of paddy fields in growing condition is a key to precise and sustainable management of soil resources to support crop growth. Obtaining soil information in this condition however is obstructed by the flooded field conditions. But there is a need for detailed and quantitative information on soil properties influencing paddy yield. The use of ancillary data to provide information on soil properties of interest should be welcome. In this context, recent technological developments enable the collection of high-resolution soil information through the application of non-invasive proximal soil sensors.

This thesis comprises the development and exploration of a soil sensing system for paddy rice fields. The sensor is based on electromagnetic induction (EMI), such as the EM38 or the EM38-MK2 sensor. These sensors measure the soil apparent electrical conductivity (EC_a) based on the EMI principle. The distance between the transmitter and receiver coil determines the depth of investigation to acquire soil information. Measurements can be made in horizontal orientation (EC_a-H) and vertical orientation (EC_a-V), each having different depth sensitivity. The EM38 measures in one coil configuration while the EM38-MK2 in two. Both sensors are non-invasive i.e. do not require a physical contact with the soil. The goal of this research was developing a soil sensing system and examining its potential for precise management of paddy fields through several case studies. Paddy fields located in the Brahmaputra floodplain of Bangladesh were used for this.

First, we focused on the development of a floating soil sensing system for flooded paddy fields. Therefore, a Floating Soil Sensing System (FloSSy) to acquire and process in real time

detailed geo-referenced soil information under such conditions was developed. The FloSSy consists of an EMI soil sensing instrument, a GPS, a field laptop, a real time sensor data processing and path guidance software, a waterproof housing for the soil sensor, a floating platform for the sensor and the GPS. The FloSSy can simultaneously process real-time raw EC_a and GPS information and convert these to the format required by the user. It has a software component, the FloSSy logger, to function in fully automated on-the-go mode. The graphical user interface (GUI) of the logger displays the traversing path of the sensor in real-time to track the previously measured path in order to keep a constant distance between measured lines in a flooded field. The sensing platform is light enough and so can be easily pulled by a typical paddy field cultivator such as the power tiller. As such the system was made ready to be operated under paddy growing conditions and therefore further investigation on the system at work was underway.

As flooded paddy fields develop distinct physico-chemical characteristics during crop growing season, a field measured under dry condition was investigated for representativeness of the results are for the flooded crop growing conditions. Therefore, the EC_a-H of a 1.4 ha alluvial paddy field was measured in both dry and flooded conditions by the FloSSy using the EM38 and compared both surveys. Due to the smooth water surface under flooded conditions which ensured increased stability of the sensing platform, the results of the survey showed considerably reduced micro-scale variability of EC_a. Furthermore, the flooded survey results more reliably furnished soil-related information mainly due to the absence of soil moisture dynamics. The differences between EC_a under dry and flooded conditions were attributed to differences in soil texture, mainly the sand content variation having considerable effect on soil moisture differences when flooded following drying the field. Accordingly, the largest differences between EC_a under flooded and dry conditions were found in those parts of the field with a large sand content. The study proved that an EC_a survey on flooded fields is appropriate for paddy fields and has an added value to precision soil management.

A next study aimed at testing the potential of the system to acquire and process detailed geo-referenced soil information within flooded fields which could be used to support soil management at a within-field level. Therefore, an alluvial paddy field of 2.7 ha was used. The EC_a survey with FloSSy was conducted after the usual field preparation by puddling and

before the seasonal plantation of rice seedlings. At the time of measurements, the water height on the field was approximately 0.18 - 0.20 m. The traversing speed was approximately 3.6 km h^{-1} and the measurements were averaged to one value per square meter. So the processed data resolution was 1 observation per m^2. Soil and crop samples were also collected to interpret the measured EC_a. High resolution EC_a data were obtained and classified into three classes using the fuzzy *k*-means classification method. The variation among the classes could be attributed to differences in subsoil (0.15 - 0.30 m below soil surface) bulk density, with the smallest EC_a values representing the lowest bulk density. This effect was attributed to differences in compaction of the plough pan due to differential puddling. There was also a significant difference in rice yield among the EC_a classes, with the smallest EC_a values representing the lowest yield. It was shown that the FloSSy allowed the collection of relevant soil information, opening potential for precision agriculture practices in flooded crop fields. Based on this, the focus of the thesis was shifted more towards evaluating the FloSSy for soil management aspects of paddy fields.

Our next aim was on soil water management aspects for paddy cultivation. Maintenance of standing water at a recommended depth is crucial to ensure sufficient water availability to the paddy crop. This requirement is challenging to achieve because of the lack of suitable technologies to detect rapidly percolation prone zones within these fields. The objective of this study was to evaluate a methodology using the FloSSy to identify water leakage areas to support precision soil-water management at a within-field level. The soil EC_a-V of a 1.4 ha paddy field was recorded both under dry and inundated conditions. Comparison of EC_a data sets obtained under inundated and dry conditions again showed that the EC_a measurements under inundated condition (EC_a-w) were more strongly related to soil properties due to the absence of variability in soil moisture and the increased stability of the floating sensing platform. Therefore, we proceeded with the EC_a-w measurements and grouped them into two classes using a fuzzy *k*-means classification method. These classes showed significant differences in water percolation: lower EC_a values represented a higher percolation rate and vice versa. This effect was attributed to differences in soil texture, more specifically the sand content, and its effect on water retention. These results proved that an EC_a-w survey with the FloSSy allowed the detection of soil heterogeneity linked to downward water fluxes which has a potential to support precision soil-water management in paddy fields. This further

opened the scope of investigating the potential of the FloSSy to maintain flooded conditions in paddy fields through adjustment of soil management practices.

Paddy fields are repeatedly puddled at near water saturation to loosen the top soil and to form a uniformly compacted plough pan required to reduce losses of water and nutrients. In paddy growing conditions however, the non-invasive detection of compaction variation within the plough pan layer is challenging. Therefore our next study evaluated a methodology based on the application of the FloSSy to identify areas compacted by different intensities of puddling to support precise land preparation. Therefore, a 1.6 ha alluvial paddy field was selected. Three areas within the field were variably compacted through gradually increasing the intensity of puddling and characterized by soil properties and EC_a. The FloSSy was used to record the EC_a dynamics of the soil for each of the puddling intensities. The effects of plough pan compaction on water percolation losses and paddy yield were assessed. The results show that the variably compacted areas had significant differences in soil bulk density linked to the soil penetration resistance. Spatial comparison of EC_a data sets showed that the EC_a values increased systematically under increased compaction. Sufficient soil compaction could be identified when percolation losses were significantly the lowest and paddy yield was significantly the highest. It was demonstrated that a non-invasive EC_a survey using electromagnetic induction based soil sensing allowed the detection of soil heterogeneity linked to soil compaction caused by puddling, which offers an interesting potential for precise puddling and land preparation in paddy fields.

The final study was focused on further investigating the potential of the FloSSy to model the within field variation of the compacted soil layer. A key characteristic of flooded paddy fields is the plough pan resulting from puddling, which is a sub-soil layer having higher compaction and bulk density to restrict water losses through percolation. However, the thickness of this compacted layer can be spatially variable with consequences on the within field soil and water management. Therefore we evaluated a methodology to identify the variation in the vertical extent of the compacted soil layer. The non-invasive electromagnetic induction sensor EM38-MK2 was used in the FloSSy. A 2.7 ha alluvial paddy rice field was measured and EC_a of the wet paddy soil was recorded at a high resolution (1.0 × 0.5 m). Soil bulk density and depth of the compacted layer was obtained by classical soil sampling using

undisturbed soil cores and penetrometer measurements. A strong non-linear relationship (R^2 = 0.89) was found between the depth of the compacted layer and the EC_a (n = 10) measured with the EM38-MK2 sensor used in the vertical orientation with 0.5 m transmitter-receiver coil separation. These predictions were validated by independent observations (n = 18) of the depth of the compacted layer resulting in a Pearson correlation coefficient of 0.87 with an RMSEE value of 0.03. The EC_a measurements allowed a detailed estimation of the plough pan depth beneath the water saturated soil layer. The link between water losses and depth of the compacted layer was confirmed by water percolation measurements where an inverse relationship with a Pearson correlation coefficient of 0.89 was found. The rapid non-invasive, time and cost-effective system offers new perspectives to measure the plough pan in detail. This has potential for adjustment of soil management practices in paddy rice fields.

Finally, it was concluded that a non-invasive soil sensing system such as the FloSSy is valuable to obtain soil information from flooded paddy rice fields. EC_a data obtained by the FloSSy proved its usefulness to provide adequate information on soil attributes. The system has a large value to introduce precision agriculture practices in paddy cultivation systems.

1

Introduction

1.1 Background of using sensors in soil management

Understanding soil properties is the key to successful soil management. However, the heterogeneous nature of the soil complicates the management of soil resources in a sustainable way. Historically, soil information from particular areas of interest has been collected and documented as maps. The first civilization to develop measuring devices to survey land areas and produce maps of land and soil resources was probably the ancient Egyptians. In course of time, other civilizations gradually improved the measuring devices and included land slope measurements in soil survey. Such improvements allowed the Romans to produce soil maps of greater detail and accuracy than the previous civilizations (Dilke, 1985; Dorling and Fairbairn, 1997). Farmers of ancient times were also keen observers of crop performance. They observed benefits from spreading different amounts of manure and liming materials on different kinds of soils. In the 1620s, colonists observed specific fertilizer practices of Indian farmers who placed fish directly at the roots of each corn plant (Kellogg, 1957). In 1929, Bauer and Linsley suggested to mark a field at fixed intervals to determine field position for application of limestone materials using different rates (Goering, 1993). All these early works contributed to soil management and paved the way of soil knowledge base. In recent times, improvements in precise soil survey equipments and methods of soil analysis played a key role in soil description. Modern information technologies have the potential to generate sophisticated assessments of heterogeneity in soil properties. Extension of soil boundaries beyond the sample area has already become possible with the interpretation of aerial photographs using photo-grammatic techniques and topographic measurements (Jensen, 2007). Gradually our knowledge of soil is increasing and flourishing.

Our knowledge to manage soil resources is commonly based on an individual profile or a pit excavation and site descriptions, which are translated to qualitative soil maps across a landscape. Therefore, this conventional approach eventually relies on extrapolation of limited sampling sites or locations, to make a generalized soil management scheme and recommendation packages. In fact, soils are highly heterogeneous and variable in space, both laterally and vertically, due to having a complex interaction among soil forming factors inherent to edhaphic and climatic roots (Jenny, 1941). As the only and ultimate usage of soil resources across arable landscapes is for cropping, soil spatial variability exerts a direct consequence on crop productivity. Until recently, the problematic issue of managing spatially

variable soil properties has been rooted to sampling effort, limited data, information quality and uncertainty in decision making (McBratney, 1992). However, with an increasing flow of awareness among the soil scientists and agriculturists and with the advent of new technologies and soil sensors, the demand to adapt the limited-sampling-based soil management approach to an exhaustive-information-based management approach is evolving. This is opening a new era where soil sensors can play a pioneering role to provide quantitative, ancillary and complementary information on soil variability.

Proximal soil sensors are operated close to the terrestrial surface (Viscara Rossel et al., 2008). In contrast to air or space borne remote sensors intended for similar objectives, the proximal soil sensors collect soil information at a much finer spatial resolution. In addition to collecting high resolution soil information, they reduce the costs of operation and data acquisition. Over the last decade, the most widely used proximal sensors are based on electrical and electromagnetic induction (EMI) techniques (Adamchuk et al., 2004). These sensors are perfectly suited for detailed investigation of arable fields. The sensor collected information can be combined in a geographical information system (GIS) to take site specific decisions, realizing an extra advantage both in terms of crop performance as well as in reducing the environmental impact. As an additional advantage, the sensors provide the possibility for a mobile survey configuration, hence, making them time efficient. Among proximal sensors, the EMI based sensors have been found to be useful inferring a wide range of soil properties. The EMI sensors measure the apparent electrical conductivity (EC_a) of the soil, which varies with a number of soil properties like soil moisture, salinity, clay, organic matter, depth to contrasting soil layers and bulk density variation (Kachanoski et al., 1988; McBride et al., 1990; Doolittle et al., 1994; Jaynes et al., 1994; Jaynes, 1996; Davis et al., 1997; Brevik and Fenton, 2002; Hezarjaribi and Sourell, 2007; Cockx et al, 2009; Saey et al., 2011).

This dissertation focuses on the management of paddy rice fields. These fields dominate 135 million ha of the earth's surface and have a profound impact on our subsistence, as they, either directly or indirectly, support 60 % of the world's population (Kyuma, 2005). For most of the growing season paddy fields remain flooded which makes them inaccessible for obtaining direct soil information. Sensors requiring a direct contact with the soil, such as electrical resistance instruments, are not suitable in paddy field conditions wherein inundation and flooding are common. Therefore, the use of a non invasive sensor, EM38, based on EMI

is considered. This sensor does not require a direct physical contact with the soil being measured. The EM38 sensor is designed to be used in either horizontal or vertical orientation. Each orientation receives a dominant influence from different soil depths, and therefore, can provide crucial soil information from the depth of interest in a layered soil system. An adapted version of the EM38 is the EM38-MK2, which consists of two receiving coils at 0.5 and 1 m distance from the transmitting coil. The multiple coil configuration of this sensor allows simultaneous measurements of soil EC_a using multiple signals. This feature offers a wide range of potential for applications in soil management of paddy rice fields because soil properties of different layers are addressed simultaneously.

1.2 Aim and research questions

The rationale of this research comes from site specific soil management concept of the 20th century when mobile soil sensing systems were introduced in countries such as the United States, Australia and Western Europe for precision agriculture practices. In many cases, these sensing systems are able to identify soil variability within a field that can be targeted and managed for near-optimal crop production. When this concept of precise soil management is considered for paddy rice fields we are faced with the limitations of our soil information systems. The mobile sensing systems used in standard configuration for arable fields (Cockx et al, 2009; Saey et al., 2008a & 2012) are also not applicable as such in flooded field conditions. While paddy fields lack soil information collected in growing conditions, the use of a non-invasive proximal sensor to improve soil management in these fields is yet to be addressed.

The general aim of this dissertation is to develop a mobile sensing system to be used under flooded paddy field conditions and to evaluate its potentials to characterize in detail soil properties at a high resolution for soil management within these fields.

To reach the general aim, the following research questions were put forward:

- *Can a soil sensing system be offered for flooded field conditions?*
- *How is the quality of the EC_a data set obtained under flooded conditions?*
- *Is there a benefit of surveying a field in flooded conditions compared to dry conditions?*
- *Is it complementary to characterize top and sub soil properties?*

- *How does EC_a measured under flooded condition provide information relevant for paddy field management and crop yield improvement?*
- *Can apparent electrical conductivity be used to identify compaction variability?*
- *Which sensor and signal is appropriate to model the variability of thickness of the compacted layer?*

1.3 Outline of the dissertation

The outline of this dissertation is schematically presented in Fig. 1.1. The first three chapters are written to give a background on the subject: a general introduction to the research topic, the state of the art and formulation of the research problem is given in chapter 1. Chapter 2 describes the management of soil variability in the context of paddy rice fields using sensors and chapter 3 describes the methodology to analyze high resolution soil information from a proximal sensor. The next six chapters were organized to address the research objective and answer the research questions.

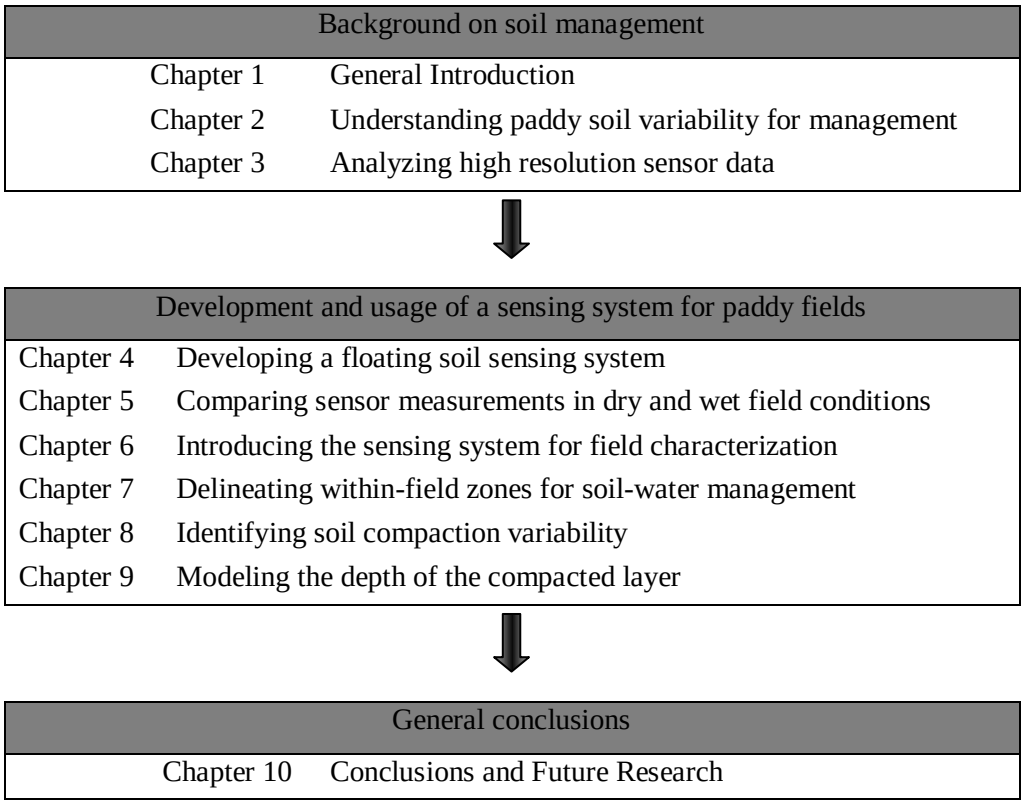

Figure 1.1 Outline of the dissertation.

Chapter 4 deals with the development of a proximal soil sensing system that can be used in flooded conditions of a paddy rice field. Mobile soil sensing configurations used in dry arable fields are discussed and the need for a similar technology for paddy fields is explained. A protocol for real time processing and georeferencing of sensor information is also described. Chapter 5 evaluates the measurements of a paddy field in growing conditions. The differences in soil EC_a, which relate to soil texture variability observed in dry and wet field conditions were investigated and compared. Assessment EC_a data quality using both survey conditions was also discussed. In chapter 6, the processed EC_a measurements were used to characterize a paddy field in growing conditions. The use of the sensor to delineate classes having similar EC_a values was evaluated. Finally, the within-field soil classes were characterized in terms of the soil bulk density and the relationship between EC_a and paddy yield was modeled.

The next two chapters aim at investigating the potential of the sensing system for paddy soil management. Chapter 7 addresses the complications of homogeneous land preparation where differences in soil texture occur. Therefore, we developed a strategy to locate the water leakage zones within a paddy field. These zones were interpreted in terms of water percolation measurements. In chapter 8 soil compaction variability caused by puddling of paddy fields was investigated. A field was puddled at different intensities and the EC_a dynamics were characterized. Soil bulk density and penetration resistance were used to characterize the field, and water percolation and paddy yield observations were used to interpret the compaction differences. EC_a measurements were proposed to identify compaction differences. Variability in the depth of the compaction layer was the topic under investigation in chapter 9. A field survey was performed and the simultaneously measured horizontal and vertical EC_a were used to obtain information from different soil layers. The multiple signals were compared to relate the compaction depth and the extent of the vertical heterogeneity was modeled. The sensitivity of the model to changes in the depth of the compacted layer was assessed in terms of the accuracy of the prediction.

The last chapter summarizes the results from the different case studies according to the research questions. General conclusions are drawn concerning the use of a noninvasive sensor for paddy soil management.

2

Management of paddy rice fields: making sense with sensors

2.1 Soil information and soil variability

Obtaining soil information for the evaluation of soil properties is typically performed by taking a limited number of soil samples. Typically, the samples are pooled (ignoring their locations), analyzed in the laboratory and the resulting values are averaged and used as one value across the entire study area (Wollenhaupt et al., 1997). The number and location of sampling points across a field are determined by a sampling design. Randomizing sample locations or overlaying a uniform grid of fixed size on the boundaries of a field is common (Earl et al., 2003). Because inherent field variability is frequently not pre-understood, determination of sample resolution is based mostly on costs and expected return. Eventually, no single sampling methodology has been determined to be optimum, and this continues to be a problem due to differential soil properties and field characteristic (Hollands, 1996).

Scientists are aware that soil varies in space either gradually or continually or sometimes even abruptly at short distance. Soils vary significantly as a result of differences in climate, origin, topography, parent material, time and past and present cultural practices (Sommer, 2006). The variability of soil physical, chemical, and biological properties has dramatic effects on crop production. Limited auger observations are in no way able to capture the detailed information required to manage within field variability. However, a detail quantitative understanding of soil variability is necessary for sustainable management of soil properties. In this context, increasing availability of advanced tools and technologies that can deal with spatially variable data is creating awareness among the soil scientists.

2.2 Managing soil variability

Management of soil spatial variability for crop production systems involves many decisions, all of which are interrelated and ultimately affect crop yield. Often, crop yield is subject to uncertainty due to both stochastic processes (primarily weather) and unmeasured variability in agronomic conditions (Lark, 2005). Precise soil management tools may improve decisions related to specific site conditions, thereby reducing this aspect of uncertainty in the management system. However, the performance depends on the interaction between site conditions and stochastic factors such as climate (Yang et al., 1998). If site specific management is to be successful, it must be based on techniques that allow exhaustive information collected to encompass the simultaneous effects of the most important factors influencing yield, rather than individual factors taken in isolation. For instance, successful

strategies will likely be based on soil characteristics that relate to nutrient response curves, weather conditions, and other factors in addition to applied fertilizer.

The ability to respond to changing and dynamic conditions is likely to be as important as understanding temporal variability in the beginning of the crop season. Intelligent management of soils that allow the producer to adjust initially for a lower yield goal and still respond to seasons in which yield potential is greater than normal could substantially ameliorate the effects of temporal variation (Ferguson et al., 2002). Such an ability to respond to temporal variability would be particularly desirable for handling weather related risk. For irrigated paddy production areas, perhaps the greatest threat to crop production is lack of sufficient water to support the aquatic crop (De Datta, 1981). Low water supplies often causes paddy growers to opt for lower initial fertilizer application rates and thus forego the expected return. Similar situations occur when the potential for water losses through percolation and nutrient leaching in light sandy soils limits the amount of nitrogen that can be applied in a single application (Booltink et al., 1996).

In the past, uniformity trials have been used to study soil heterogeneity by simply planting a crop that was uniformly managed throughout the growing season (Sanders, 1930). The field was divided into small segments and crop yield was measured on each segment. Crop yield variability among segments was the measure of varying levels of soil fertility in the field. Crop yields obtained from a uniformity trial were plotted on a map, and field segments having similar yields were connected by smooth lines. These yield maps were interpreted as soil fertility contour maps. LeClerg et al., (1962) made two general conclusions from these early uniformity trials:

- Soil variation is not distributed randomly but is to some degree systematic; contiguous field segments are more likely to be connected in space rather than segments separated by some distance.
- Soil variation is often distributed systematically; it could be described by a statistical model.

The traditional strategy in soil management is to match fertilizer inputs with crop needs. The goals of this mass balance approach are to increase nutrient uptake efficiency and minimize fertilizer losses (Chang et al., 2003). Fertilizer rate recommendations for immobile nutrients (i.e., phosphorus, potassium, and zinc) are based almost entirely on soil test levels

calibrated for a specific crop, soil type, and climate. Nitrogen fertilizer rates are based on estimates of yield potential (average or spatial) with corrections or credits for nitrogen in soil profile, legume, manure, and soil organic matter sources (Schroeder et al., 2000). Recently, producers have been encouraged to adjust timing of fertilizer applications to reduce environmental risks. For example, nitrogen losses due to leaching can be reduced by minimizing the time between application and plant uptake (Killorn et al., 1995). Improved crediting of residual nutrients remaining in the soil after a crop is harvested works best for less mobile soil chemical properties such as phosphorus and potassium concentrations or pH. Nitrogen is more mobile and requires more frequent sampling to assess the appropriate credit levels (Chang et al., 2004). Nitrogen remaining in the soil after harvest may be available to the next crop, unless temperature and rainfall conditions result in leaching or volatilization. Precise management of nutrients can reduce costs and environmental load where over applications would have occurred, and can improve yields for locations that would have been under treated. Moreover, precision management of soil nutrients allows the producer to set variable yield goals for fields that do not have a uniform productive potential (Hergert et al., 1997).

Conventional approaches to manage soil management based on averages alone are inadequate for characterizing temporal and spatial variation of soil properties. Soil management deserves a holistic approach to address the entire farming system towards a low-input high-efficiency optimized agriculture (Zhang et al., 2002). The approach is best considered as a suite of technologies targeted to a specific site wherein numerous variables from land, soil, and cropping practices interact at varying degrees. Consequently, soil scientists require new tools that are designed explicitly to improve understanding of the complex interactions between multiple factors affecting soil properties and crop growth. The availability of sensor derived information about the landscape, production fields and crop yields opens the door to new ways of managing our soil resources.

2.3 Proximal soil sensors

Proximal soil sensors are able to collect soil data at high spatial density, allowing the determination of soil properties almost continuously. The term ‘proximal sensing’ was coined in 1998 to describe devices that collect data from a distance that is in close proximity (1 m or less) to the object of interest (Viscarra Rossel and McBratney, 1998). A number of proximal soil sensors have been developed for use in a mobile configuration [Fig. 2.1 (b) and 2.2 (b)],

allowing on-the-go soil measurements (Adamchuk et al., 2004). Among them, two types of sensors are widely used in a mobile configuration: electrical resistivity (ER) and electrical conductivity (EC) based sensors. They use electrical circuits to determine the ability of soil to conduct electrical charge. When the soil becomes part of the circuit, its physical and chemical properties influence the measured electrical parameters. Since the ability of a soil volume to resist or conduct the current flow depends on differences in soil properties, soil variability can be measured (McNeill, 1980b). The ability of the soil to conduct electricity is usually quantified by ER or EC. Both values are related to the voltage and electric current ratio for a known configuration of transmitting and receiving electrodes or coils. Both the ER and EC based techniques are well suited as a soil information gathering tool because their sphere of influence covers the soil depth in which the roots of many crops are concentrated.

2.3.1 Electrical resistivity sensors

Schlumberger introduced electrical resistivity in 1912 to study subsurface rocks (Meyer de Stadelhofen, 1991). The basic configuration of an invasive ER sensor is referred to as a Wenner array, which has four electrodes inserted into the soil at equal distances [Fig. 2.1 (a)]. A DC current is applied to the two transmitter or coulter electrodes introducing an electrical current in the soil (Samouelian et al., 2005). The resistance in current flow through the soil is measured by two receiver electrodes (potential electrodes). When the four electrodes are equally spaced in a straight line at the soil surface, the outer electrodes act as the current transmitting electrodes and the inner electrodes as the receiving electrodes (Corwin and Lesch, 2003). The depth of soil investigation is determined by the electrode spacing. The greater the spacing between the outer current electrodes, the deeper the electrical currents will flow into the soil, allowing a greater depth of exploration.

The ER sensing concept forms the basis of a widely used commercial product, the Veris 3100 (Veris Technologies., Salina, USA). This mobile measuring system [Fig. 2.1 (b)] uses six rolling coulters for electrodes and simultaneously measures shallow (0 - 30 cm) and deep (0 - 100 cm) depths (Lund et al., 1999). If more than two or multiple electrodes are used multiple depths can be explored simultaneously. The Multidepth Continuous Electrical Profiling (MUCEP) system is able to explore three depths of investigation at the same time (Panissod et al., 1997). A drawback of ER sensing is that the electrodes need a contact with the soil. This is difficult to achieve under very dry soil conditions or in soils with a lot

of stony material at the surface. As the method targets the resistance to current flow, saturated or wet soil conditions also limits its application.

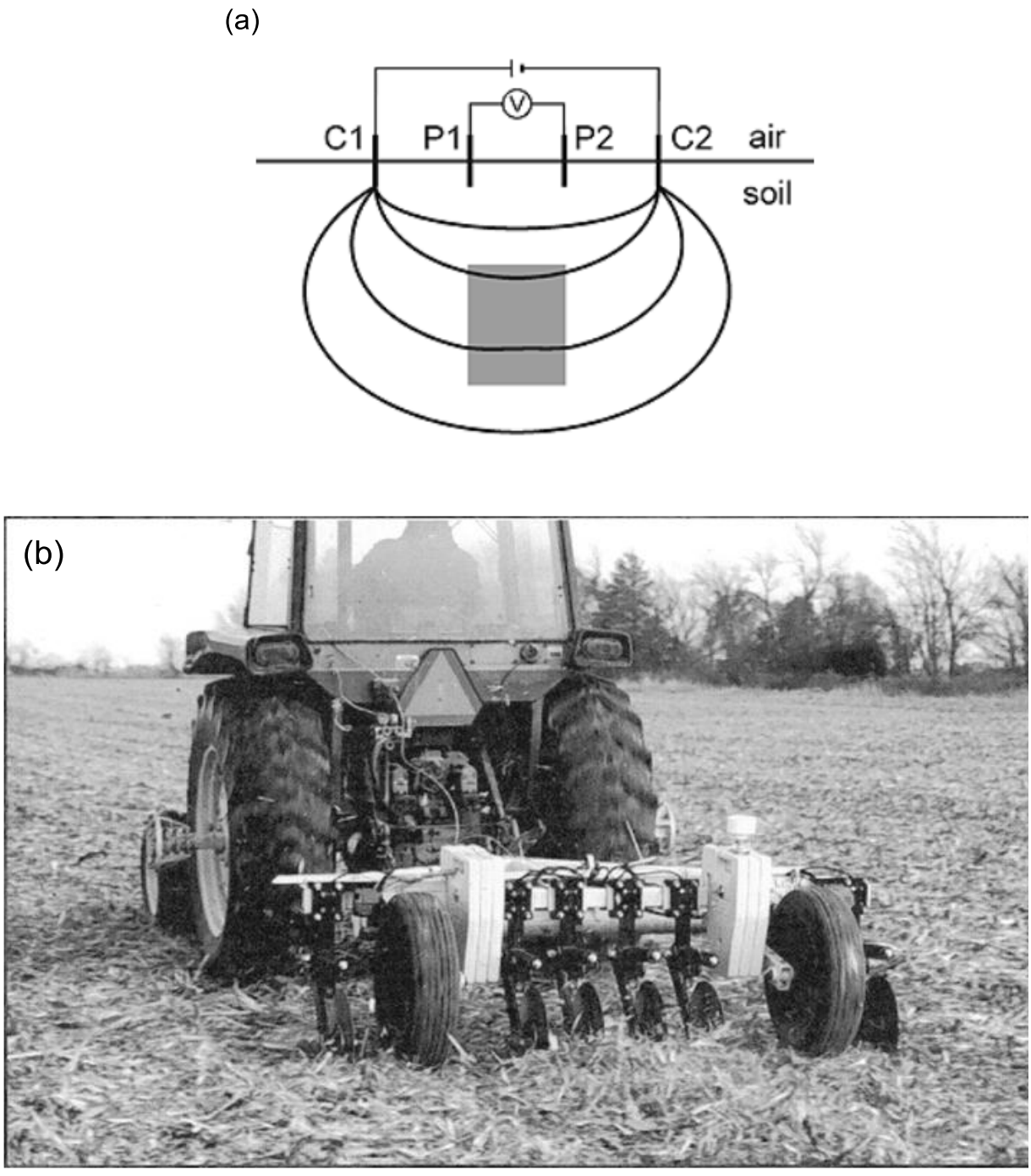

Figure 2.1 (a) Basic principles of galvanic electrical resistivity measurements and (b) illustration of a mobile ER survey equipment: the Veris 3100 system.

2.3.2 Electromagnetic induction sensors

The non-invasive EC sensors are based on electromagnetic induction (EMI) and use the principle of the propagation of alternating magnetic fields through the soil to measure soil conductivity (Corwin and Lesch, 2003). Therefore, there is no need of direct contact between the soil and the sensor to obtain measurements. An EMI sensor uses a transmitter coil with an alternating current which produces a low frequency magnetic field propagating through the soil. As a soil is composed of materials which have electrical properties carrying electric charges, differences in soil properties can be measured. The distance between the two coils (inter-coil spacing) and their orientation determines the effective depth of measurement. An example of a mobile EMI survey equipment is shown in Fig. 2.2.

Figure 2.2 Illustration of a mobile EMI survey equipment.

EMI instruments are sometimes called terrain conductivity meters and they operate at very low induction numbers (Spies and Frischknecht, 1991). Low induction numbers imply that the charge flowing in any loop of the magnetic field is completely independent of the charge that passes in any other loop since they are not magnetically coupled (McNeill, 1980a). The induction number (β) is linked to the electrical skin depth (δ). The skin depth is the depth at which the primary magnetic field has been attenuated to e^{-1} (37%) of its original strength at the surface of the soil. The induction number is deducted from this skin depth and defined as the ratio of the inter-coil spacing to the skin depth (McNeill, 1980a):

$$\beta = \frac{s}{\delta} = \frac{s}{\sqrt{\frac{2}{\sigma\omega\mu_0}}} \tag{2.1}$$

where s = inter-coil spacing (m)

σ = Soil conductivity (mS m^{-1})

$\omega = 2\pi f$

f = frequency (Hz)

μ_0 = permeability of free space, which is $4\pi.10^{-7}$ H^{-1}

An induction number much less than unity is obtained when the skin depth is much larger than the inter-coil spacing. This is ensured in the design of the soil conductivity sensors and implemented by the manufacturers. For soils where δ does not exceed 100 mS m^{-1}, $\beta \leq 1$ is also satisfied. This condition is known as operating at low induction numbers. Then the conductivity measured by the soil sensor becomes proportional to the ratio of the out-of-phase component of the secondary field to the primary field (McNeill, 1980a):

$$\sigma = \frac{4}{\omega\mu_0 s^2}\frac{\mathrm{Hs}}{\mathrm{Hp}} \tag{2.2}$$

where, Hs = secondary magnetic field at the receiver coil (H m^{-1})

Hp = primary magnetic field at the receiver coil (H m^{-1})

Most EMI sensors are lightweight and require little power to pull through the field and make it possible to collect data under wet or dry soil conditions. Unlike the ER sensor, the instrument operation is not restricted by the internal nature of soil material. Also, it is possible to collect data even under crop growing conditions. The most often used EMI based sensor is the EM38 (Geonics Ltd., Mississauga, Ontario, Canada). The other common EMI instruments from the same manufacturer include, EM31, EM34 and EM38-MK2. Other manufacturers are the DUALEM instruments (DAULEM Inc., Milton, Ontario, Canada) and GEM instrument series (Geophex Ltd., Raleigh, NC, USA). Those sensors show differences in depth densities and physical construction, but the operating principle is common to all. Therefore, details of the operating principle of EMI sensor category is provided in chapter 3 using the EM38 sensor, which was used in this research.

The measured conductivity by an EMI sensor is called apparent electrical conductivity (EC_a) (apparent resistivity for the ER sensors), since the soil is rarely uniform and the exact sample size cannot be determined. EC_a is the electrical conductivity of a homogeneous half-space, averaged to the depth of investigation that would yield the observed instrument response. This depth-weighted average is also known as the bulk soil electrical conductivity (Cook and Walker, 1992; Greenhouse and Slaine, 1983). In other words, it is the average of the electrical conductivity integrated over different depths in the soil, these depths being dependent on the instrument used to make the measurement.

Soil EC_a measured by EMI has been used to indicate and quantify many soil properties. Conrad Schlumberger was the first to use electric current in 1920s to map subsurface properties (McNeill, 1980b). There are many agricultural uses as well as military and environmental applications. The measured EC_a values are affected by more than one physical or chemical soil property: soil salinity, clay content and mineralogy, cation exchange capacity (CEC), soil pore size and distribution, soil moisture content and temperature (McNeill, 1980b; Mueller et al., 2003; Samouelian et al., 2005).

2.3.2.1 Soil electrical conductivity: types

Soil electrical conductivity (EC) is the ability of the soil to conduct an electric current (McNeill, 1980b).

There are four types of soil EC. Three types of EC are measured in the laboratory and the fourth type can be measured in the field. The three laboratory methods are: (i) soil solution EC, (ii) saturated paste extract EC and (iii) soil solid EC. Apparent soil EC can be measured in the field (Rhoades, 1990a; 1990b).

(i) Soil solution electrical conductivity (EC_w) is another type of EC. Soil solution is the pore water that is extracted from soil samples by a variety of centrifuge and non-polar liquid displacement (Cook and Williams, 1998). The moist soil is taken into the lab and it is centrifuged. The liquid is removed and the EC is measured.

(ii) Soil paste electrical conductivity (EC_e) is the EC measured on a soil and water paste. The soil is taken into the lab and air dried. Then the soil is saturated with distilled water. Once the paste is formed, it is scooped into a Buchner funnel above an Erlenmeyer flask

connected to a vacuum pump for extraction. The extract is then collected and used to determine EC using a conductivity meter. The saturated paste can also be centrifuged. The solution from the paste is then removed and its EC of the water can be measured (Rhoades, 1990b).

(iii) Solid phase electrical conductivity (EC_p) is due to the presence of exchangeable cations and anions on the surfaces of clay particles (Cook and Williams, 1998). The soil is taken into the lab and dried similar to the paste extract method. Distilled water is added to the soil to make a paste. The EC is then measured by direct contact with the actual solid of the paste and not the extract like above (Brady and Weil, 2000).

Soil EC_a includes the conductance through the soil solution, the solid soil particles, and the exchangeable cations that are located on the soil-water interface of clay minerals (Corwin and Lesch, 2003). It can be determined by above ground measurements from a ground conductivity meter. Electromagnetic induction is an easy and time efficient way to measure soil EC_a. The method is virtually non-invasive and non-destructive to the soil (Corwin and Lesch, 2003). However, some ground-truthing is required in order to accurately assess the data collected.

2.3.2.2 Factors affecting soil apparent electrical conductivity

In order to affect the soil EC_a, certain factors must be able to conduct electricity or affect the materials that do conduct electricity. Depending on physical and chemical properties, soil can exhibit different electrical properties (Hedley et al., 2004). Most soil solids and rocks are insulators of electrical current. In general, electrolytes in soil water are the main contributors to conductivity (McNeill, 1980b). Therefore, salinity, soil water content, and clay content and mineralogy are the three main studied factors that contribute to soil EC_a. Rhoades et al., (1999) have also indicated that cation exchange capacity (CEC), soil pore size and distribution, and temperature affect EC_a.

Sudduth et al. (2003) stated that CEC is a primary driver of EC_a. Increasing CEC causes an increase in EC_a (Kachanoski et al., 1988; Rhoades et al., 1976; McKenzie et al., 1997). Organic matter is a collection of plant and animal remains. The remains further break down into fine-colloidal particles called humus. These particles have a large surface area per unit volume. They absorb large amounts of water and can have a negative charge. There is a lack

of information on the electrical conductivity of organic matter. However, water content does play a part in soil conductivity (McNeill, 1980b).

Changes in temperature affect the conductivity of soil and soil solution (McNeill, 1986; McNeill, 1992; Rhoades et al., 1999; Doolittle et al., 2000). When temperature increases, viscosity of a fluid decreases and ion agitation increases. Therefore, when temperature increases, conductivity increases. For every degree Celsius increase in temperature, the conductivity increases by 2% between 15 and 35 degrees Celsius (Samouelian et al., 2005). Measured EC_a is reduced with air temperatures at or below 12°C and/ or soil temperatures at or below 8°C (Allred et al., 2005).

Changes in bulk density can alter the soil EC_a. A greater bulk density indicates that more soil particles are packed into a unit volume of soil, and, therefore, particles have more of their surface in contact with other particles (Rhoades and Corwin, 1990; Malicki et al., 1989). This change also alters soil water content; a more dense soil will have less pore space for water (Brevik and Fenton, 2004). The study of Brevik and Fenton (2004) study resulted in higher EC_a readings with higher soil bulk densities. The size and amount of soil pores affect the EC_a of soil (McKenzie et al., 1997; McNeill, 1980b). Low and high conductivity values are related to macro- and meso- porosity respectively (Samouelian et al., 2005). The pores filled with solution can contribute to the soil EC_a. Larger pores allow solution to drain out while smaller pores hold water in the soil. Greater porosity allows for greater moisture content. Therefore, a porous soil tends to be more electrically conductive (McNeill, 1980b). The air in soil pores acts as an insulator (Samouelian et al., 2005).

2.3.2.3 Pathway of soil apparent electrical conductivity

As described earlier, the electromagnetic induction process involves the flow of eddy currents in the soil. Corwin and Lesch (2005a) described three pathways of current flow that contribute to the EC_a of a soil, namely: (i) a solid-liquid phase pathway primarily via exchangeable cations associated with clay minerals, (ii) a liquid phase pathway via salts contained in the soil moisture occupying the large pores and (iii) a solid phase pathway via soil particles that are in direct and continuous contact with one another (Fig. 2.3).

The study of Rhoades et al. (1989) revealed that the movement of electrons through a soil solution is complex and they identified that soil structure does not provide enough direct

particle-to-particle contact to form a continuous pathway for current flow. Hence, they identified the major contributors in soil EC_a measurement as the electrical conductivity of the soil particles (EC_s); the electrical conductivity of the soil solution associated with discontinuous pores (EC_{ws}); the electrical conductivity of the mobile soil solution associated with large, continuous pores (EC_{wc}); the volumetric soil moisture content of the small, discontinuous pores (θ_{ws}); the total volumetric content of moisture in the soil (θ_w); and the volumetric content of soil particles (θ_s). Among those the vital ones influencing EC_a are θ_w (Rhoades et al., 1976; Nadler, 1982); EC_s, influenced by cation exchange capacity (Shainberg et al., 1980); θ_s per unit of soil, initially influenced by soil texture and bulk density (Rhoades and Corwin, 1990); and EC_{ws} and EC_{wc}, influenced by the amount of dissolved salts in the soil solution (Malicki and Walczak, 1999). Nevertheless when only within-field measurements are concerned, the absolute EC_a values are not of major interest. It is the relative changes in the soil EC_a that indicate the soil spatial variability.

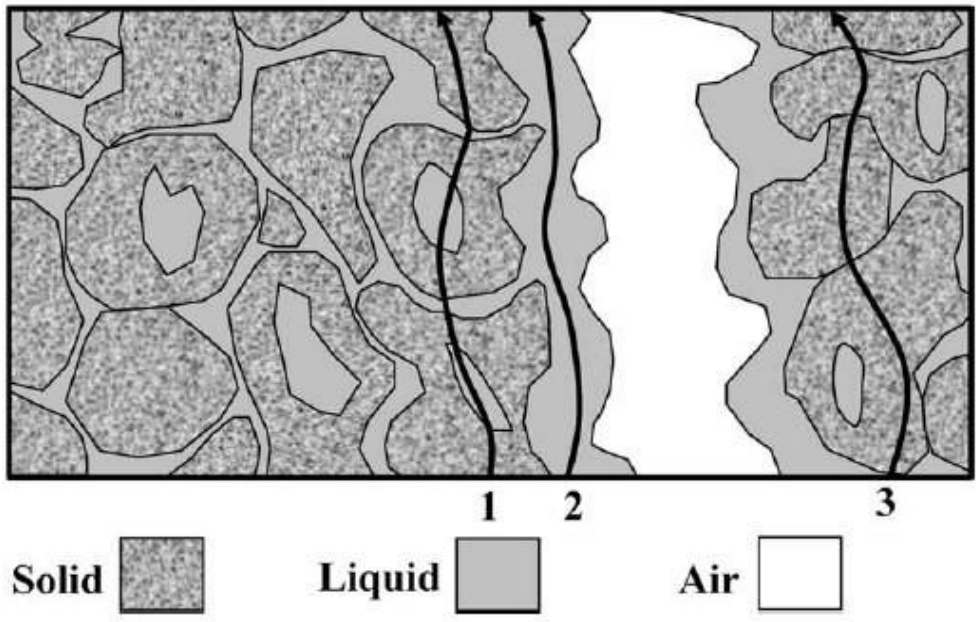

Figure 2.3 The cross section of a soil showing the three-phase electrical conductance pathways for the EC_a measurement (Corwin and Lesch, 2005a).

In general, the magnitude and spatial heterogeneity of EC_a in a field is dominated by one (or two) soil properties (Corwin and Lesch, 2003). If the within-field changes are large enough with respect to the variation of the other EC_a influencing soil properties then the EC_a can be calibrated as a direct measurement of that dominant property. In cases where dynamic soil properties (salinity, water content and temperature) dominate the EC_a measurements, the

spatial patterns exhibit more temporal changes than systems dominated by static factors (texture) (Corwin, 2004). In the latter case, the relative spatial patterns remain consistent since the dynamic properties only affect the magnitude of the measured EC_a.

High resolution information such as EC_a offers an unparalleled ability to characterize the nature and extent of soil variation occurring in agricultural fields and to develop optimized management strategies for these varying conditions. At the field and subfield scale, information about the spatial heterogeneity of field characteristics opens the possibility to manage the variation rather than attempting to overcome the variation with sufficiently high uniform rates of resource inputs. Because of the complex interactions of factors affecting agricultural production, a spatially variable management strategy becomes a part of sustainable soil management (McBratney, 1992). A spatially variable management strategy intended to reduce heterogeneity, however, is to divide the farmland into sub-fields or zones that are relatively homogeneous within, permitting an optimized sorts of gains over uniform management.

2.4 Paddy soils

According to IRRI (2002), some 11% of the total area cultivated for rice worldwide is in uplands, the rest being in wetlands, either as rainfed, deepwater, or irrigated paddies. As upland rice is generally much less productive, rice production in paddy soils exceeds 95% of the total global production.

There are about 135 million ha of paddy lands in the world, of which 126 million ha, or 93%, are in monsoon Asia, or in humid East, Southeast, and South Asia (IRRI, 2002). Climate and landforms are the two determinants for this strongly biased distribution of paddy lands (Kyuma 2004). Monsoon climate is characterized by a yearly inversion of wind direction and this accompanies alternating rainy and dry seasons. Therefore, rainfall is concentrated during the rainy season, often bringing more than 1 000 mm of rain in less than half a year, thus enabling cultivation of a rice crop. In terms of landforms, monsoon Asia features an exceptional abundance of lowlands. Being in the region of active orogeny and volcanism, in combination with high rainfall, monsoon Asia undergoes severe erosion in its high mountainous lands and deposition in its riparian and coastal lowlands, producing extensive floodplains and deltas in the middle and lower reaches of gigantic rivers such as the Yangtze, Mekong, Brahmaputra, and Ganges. These lowlands are naturally inundated with

monsoon rains during the rainy season. As depicted above, monsoon Asia, with its high seasonal concentration of rainfall and its exceptionally extensive area of lowlands, provides *Oryza sativa*, a plant species native to the region, with the most adapted natural habitat. Thus, rice culture originated as an adaptation to the given natural settings of monsoon Asia. Later expansion of paddy lands has been made possible mainly by the provision of irrigation. A small share of indigenous rice culture with *O. glaberrima* is known to exist in West Africa, but it has been narrowly confined to its place of origin throughout history, for the climate and landforms of the region are not favorable for its propagation.

2.4.1 Paddy field management

Rice grows on a wide range of landforms affected by an equally wide range of hydrologic conditions. The term upland rice in rice cultivation is used in the sense that rice is grown on nonbunded, nonleveled fields that are prepared and seeded dry and depend on rainfall for moisture. The crop is grown in nonflooded fields although may be transplanted, but still be considered upland. Upland rice grows as a dryland crop like any other cereal crop, or it can grow in contrast to paddy rice where the soil is kept under water during most of its growing cycle.

Any field that is used for growing aquatic rice can be called a paddy field. The field is suited to grow rice where sufficient water is available to submerge the soil for the necessary length of time needed by the crop (Kyuma, 2004). Paddy soil in this definition is related directly to land use, but not to any particular type of soil in a pedological sense. Paddy soils occur basically in lands with an aquic (this is a technical term used in U.S. Soil Taxonomy and widely recognized as a term to denote hydromorphic conditions) moisture regime, in floodplains, deltaic plains, fans, and terraces. Paddy soils commonly connote a class of soils occurring on land brought under wetland rice cultivation that is used for the crop growing and of which the surface is submerged during all or part of the crop-growing season. Therefore, a soil moisture regime is present naturally or imposed artificially on the upper part of the profile, but the lower horizons remain largely unchanged, reflecting the free drainage of the original profile. Modification of the natural water regime, if required for soil-water management, towards a more aquatic regime basically involves two management practices:

- The leveling and bunding of individual fields, which leads to retention or ponding of water. Such leveled and bunded rice fields are designated as paddy fields.

- Irrigation of rice fields, either by water brought in from elsewhere or by overflow from a higher to a lower paddy field.

The advantages of growing rice in an aquatic milieu are several, and their relative importance is locale specific in that each advantage operates to a varying degree depending on soil, climate, hydrology, soil fertility, biotic factors, etc. A few advantages, however, seem to operate in most circumstances (Moormann and van Breemen, 1978):

- Sufficient water supply for the rice plant, which among food crops is one of the least drought-resistant plants.

- Ease of land preparation in moist to wet soils, especially when only hand tools or simple animal-operated equipment is used. This factor is important in the dominantly clay paddy fields of Asia.

- Simplified weed control by wetland preparation and flooding. Only a limited number of weed species can grow and compete with rice under flooding. Weed control is a major problem on nonflooded rice lands, e.g. on the phreatic rice lands in West Africa.

- Greater availability of plant nutrients. Under flooding more nitrogen is supplied to the soil, mainly because of biological nitrogen fixation. This is the main reason that rice grows year after year in paddy fields without application of fertilizer nitrogen. Phosphorus becomes more available after a soil is flooded as do several minor elements with the noticeable exception of zinc. While this enhanced availability of plant nutrients is generally an advantage, other phenomena in flooded and reduced soils may negate the positive effects of an aquatic milieu in this respect.

The Asian technique of bunding and leveling land for rice cultivation increases the capacity of the land to retain water by limiting runoff and by storing surface water. An artificially induced aquatic regime on pluvial and phreatic rice lands can be indicated by the addition of the word anthraquic to the terms pluvial and phreatic. This term is a contraction of anthropic indicating the man-made aspect, and aquic related to aqua, the Latin word for water. Adding anthraquic to the term fluxial makes it redundant because fluxial rice lands are by definition aquatic for part or most of the growing season.

Bunding of rice lands, and its collateral leveling of sloping land, bring about a considerable change in the water regime of that land (De Datta, 1981). The overall effect is that runoff water is diminished and more water, whether from a natural source or from irrigation, or both, is retained on or in the soil. Bunding and leveling of land for rice make a near perfect measure of water conservation. In areas of marginal rainfall, with soils that have a moderate or even low water-holding capacity, rice can grow on rainfed bunded paddy lands. The practice of bunding and leveling to create an aquatic environment in rice fields in Asia has permitted rice growing in areas beyond the crop's natural ecological boundaries. In most wetland rice soils only a 0.10 to 0.30 m thick surface layer is saturated during the growing season. However, hydrologic conditions often vary within a single paddy field. Flooding or inundation (shallow ponding of water) easily occurs in soils with a slow natural hydraulic conductivity (e.g., in many clayey soils), in soils with a low porosity, and in soils with an impervious layer at a shallow depth. Of even greater importance, however, is the diminished permeability of the surface and subsurface horizons due to the soil and crop management under wet conditions. Therefore, puddling is practiced so that the loss by percolation is slower than the accumulation of water from whatever source in the paddy fields. The expectation from a puddling practice is the formation of a less permeable subsurface horizon, plough pan, which reduces percolation and makes the ponding of water possible, even on soils that are naturally well-drained and permeable.

Fluvisols, Gleysols, and Cambisols are the most common pedological members belonging to paddy cultivation around the world, but some other members such as Acrisols and Luvisols, to some lesser extent, are also under paddy farming on older land surfaces (Kyuma, 2005). Eswaran et al., (2001) has mentioned Inceptisols and Ultisols as the commonly used ones for aquatic rice cultivation. Irrespective of their pedological nature, all paddy soils are submerged for at least a few months a year, either naturally or artificially. As cultivated rice (*O. sativa*) originated from a semi-aquatic ancestor, it is very sensitive to water shortage (Kögel-Knabner et al., 2010). Managing paddy soils under water is entirely different from managing other soils used for upland crops, and this produces important differences, particularly in chemical and biochemical or microbiological processes. However, paddy soils are also kept dry or flood-fallowed during the turnaround period between two crops or for the rest of the year, again naturally or artificially. This cyclic change in micro-environmental conditions exhibits properties not encountered in other soils and differentiates paddy soils from most other soil systems.

2.4.2 Description of the study site

The study was conducted in Bangladesh and the soils are termed 'floodplain soils' covering 80 % of the country. These floodplain soils are highly suitable for paddy rice cultivation. They are formed by alluvial sediments carried by huge discharges from the Himalayas through a strong network of rivers. The sediments have been deposited under different geomorphological conditions in different areas: piedmont plains near the foot of hill (the Himalayas), river meander floodplains, estuarine floodplain and tidal floodplain. The floodplain sediments generally have a high silt content. The site under investigation belongs to meander floodplain soil commonly known as the Brahmaputra floodplain (Fig. 3.5). This floodplain soil mostly overlies a sandy substratum at moderately shallow depth (Brammer, 1996). The Brahmaputra floodplain is the most extensive soils in Bangladesh under paddy cultivation comprising 1 599 645 ha which is 13 % of the total floodplain area (Brammer, 1996).

The Brahmaputra floodplain soil is imperfectly to poorly drained seasonally flooded and the flooding is predominantly through within field bunds by ponded monsoon rainwater or irrigation water. In the USDA Soil Taxonomy, the soil belongs to order - Inceptisol and subgroup - Aeric Haplaquept (in FAO system the major soil group is Fluvisol which correspond to the soil order in USDA classification). These soils correlate to Hydragic Anthrosol in WRB (World Reference Base for Soil Resources). Paddy rice is cultivated in the ploughed (puddled) top soil overlying a plough pan. The ploughed layer is silt loam and silt clay loam in texture and is slightly acidic in reaction (when not submerged). The original alluvial stratification within 30 cm from the surface has been subjected to biological mixing, the subsoil shows developed structure and oxidised mottles in dry seasons (Brammer, 2002).

Three paddy fields namely, Field 1 (F1), Field 2 (F2) and Field 3 (F) were investigated (Fig. 3.5). The map co-ordinates conform to the Bangladesh Transverse Mercator projection with datum Gulshan 303. The fields belong to Bangladesh Agricultural University in Mymensingh, Bangladesh. The soil was developed on alluvial deposits (Brammer, 1996). Paddy rice fields of the Brahmaputra floodplain are not saline.

Field 1 is 1.4 ha and has the central co-ordinates 24.718708°N and 90.429306°E. The soil mainly consists of fine sand to silt with a clay content of approximately 15 % This field has a continuous paddy cultivation history of more than 35 years. Crop symptom and yield

information from the same field also confirms the non-saline growing condition due to the fact that rice varieties recommended for the field are sensitive to soil salinity. An intensive paddy cultivation practice in this field usually results in three paddy harvests each year.

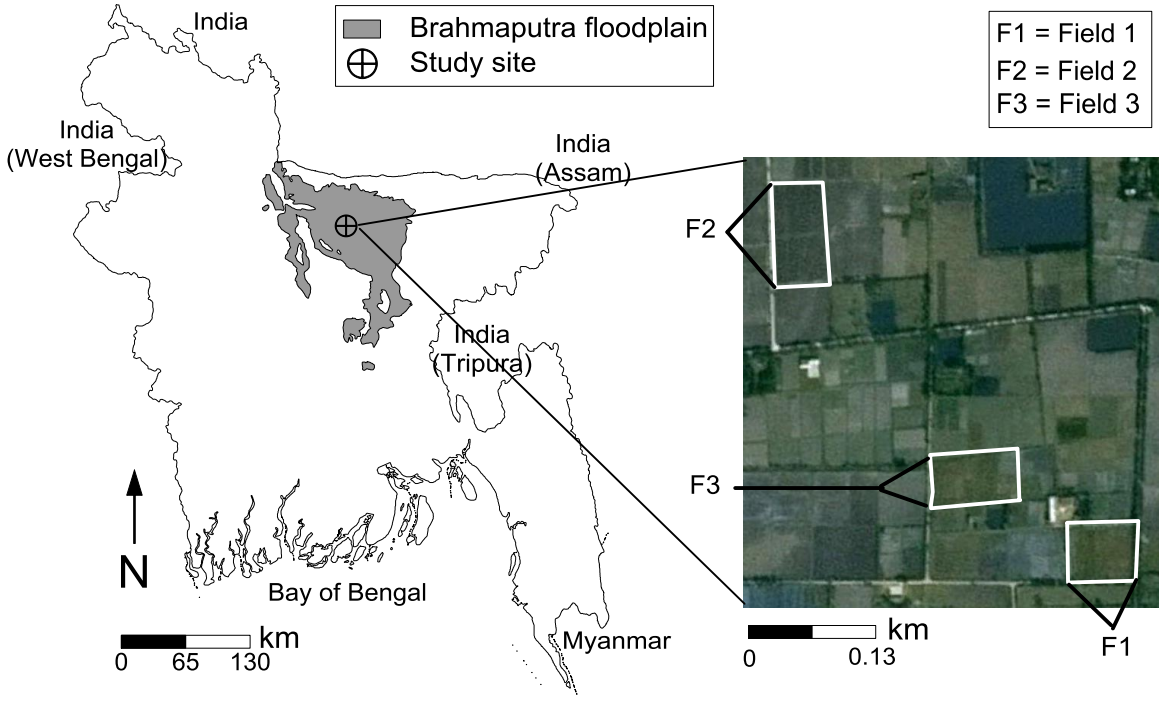

Figure 2.4 The Brahmaputra floodplain of Bangladesh and locations of the three fields: F1, F2 and F3 in the floodplain shown as white rectangles in the right picture.

Field 2 is 2.7 ha and also has been under continuous paddy cultivation for more than 35 years. The field with central co-ordinates 24.72450°N and 90.42317°E has alluvial deposited soil material and consists mainly of fine sand to silt. The soil in the area of the experimental field has a silt texture with less than 5 % clay. Paddy cultivation practice in this field usually results in two paddy harvests each year (one fallow season).

Field 3 is a 1.6 ha paddy field located with central co-ordinates 24.720038°N and 90.427007°E. This field has a paddy cultivation history of more than four decades and usually gives three paddy harvests per year. The soil of the field generally consists of fine silty material.

2.5 The management zone approach

In site specific soil management (SSSM), a zone is defined as "a sub-region of a field that expresses a fairly homogeneous combination of factors for which a single management scheme is appropriate." Thus, the delineation of management zones is a way of classifying the spatial variability within a field. Typical spatial data with which to start developing a management zone strategy include grower knowledge, bare soil photos, first order soil survey maps, field topography and soil electrical conductivity maps (Corwin and Lesch, 2005a). Over time, information that further describes the patterns of yield variation within a field can be added to delineate zones that are expected to be more stable. This includes grid or targeted soil sampling results plus geo-referenced crop yield reports (Adamchuk et al., 2011). Management zone strategies maximize economic return by optimizing rates of yield-limiting inputs and controlling the adverse effects of weeds and other crop pests.

Traditionally, researchers have attempted to evaluate the accuracy of a management zone either in economic term from the crop output or by conducting field experiments on the delineated zones. Historical comparison of yield records attained with a previous uniform rate input strategy can be used to evaluate the betterment of the zones (Dobermann et al., 2003). Scientists have also conducted research in various locations to evaluate the effect of certain site characteristics on crop yield. Using sophisticated multiple-variable regression analysis, the effect of many factors contributing to zonal variability can be estimated (Green et al., 2007). From a soil management point of view, any soil factor(s) that is highly correlated with yield can be assumed to be an important soil characteristic that should be included in a management zone delineation strategy (Artherton et al., 1999). However, it is difficult to generalize about the expected zone delineation process, because SSSM is a suite of technologies and practices used to improve decision making rather than a single technology (Mzuku et al., 2005). Because soil is heterogeneous, zone delineation process may vary across crops, geography, and farming systems. Further, understanding of the key variables for a particular agro-ecosystem is likely to predominate on the zone delineation strategy for SSSM.

SSSM is an integrated multidisciplinary management strategy that uses information technologies to bring data from multiple sources to bear on decisions associated with crop production (Whelan et al., 1997; Corwin and Lesch, 2005b). A key difference between conventional management and SSSM is the application of modern information technologies

to provide, process, and analyze multisource data of high spatial resolution for decision making (Lark, 1998). SSSM has three components: capture of data at an appropriate scale and frequency, interpretation and analysis of that data and implementation of a management response at an appropriate scale and time. Research and development of many technologies used in SSSM have occurred outside the agricultural community. The most widely used technologies in SSSM today, such as the global positioning system (GPS), geographic information systems (GIS), and remote sensing have their core constituencies outside agriculture. Crop and soil sensors operating on farm machinery, variable-rate fertilizer applicators, and yield mapping systems are technologies that have been developed within the agriculture sector. Retrospectively, SSSM involves the integration of these technologies with soil and agronomic knowledge.

2.6 Georeferenced information

Georeferencing refers to data based by their geographic locations. This spatial emphasis implies a new way of looking at agricultural information and site variability (Stafford, 2000). Although spatial variability has now been recognized, data comparisons have often been made without specific information on site location, yielding qualitative results. The value of a quantitative database for SSSM practices increases when the data layers are spatially referenced to each other (Hummel et al., 1996). Co-registration of data becomes critically important as management units get smaller and as more precise field data (location precision from sub-meter to a few centimeters) become available. Data referenced to physical location allow different types of information to be compared and quantitatively analyzed at multiple locations (Gibbons, 2000). Georeferenced soil core samples collected from a field can be compared with other spatially explicit available data for decision making, such as characteristics of the mapped topography, apparent electrical conductivity, yield monitor data, nutrient status of delineated zones etc. Georeferencing of collected information is accomplished by the use of GPS technology.

2.6.1 Global positioning system

The GPS is a system of satellites emitting electronic signals that can be received by mobile field instruments sensitive to the transmitting frequency. Positioning is achieved through the use of simultaneously received satellite transmissions from four or more satellites above the horizon (Casady and Adamchuk, 2003). With a constellation of 24 satellites, any

location on earth can have four or more satellites in view for 24 hours each day. By referencing the satellite's exact location and the time the signal takes to travel between the transmitter and the receiver, the location of the receiver can be determined by triangulation.

Use of the GPS receiver allows latitude and longitude coordinate information to be associated with data obtained from a specific site on the field traversing by a proximal sensor. The GPS can also be used to provide navigational guidance, enabling a vehicle operator to revisit a spot in the field and check the data quality (Kevin and Pocknee, 2000). The GPS is an essential field component for most quantitative mapping based soil management practices (Zhang et al., 2002). Once the information is recorded and duly georeferenced, the data can be included in the database to construct maps of soil spatial variability.

2.6.2 Geographic information system and mapping software

Digital geographic data that can be stored, analyzed, integrated, and displayed in different representations, form the core of precision agriculture (Zhang et al., 2002). The software packages used to handle such data are available with a wide range of capabilities and are able to graphically display georeferenced data. Although a single data layer can be mapped with the use of less-sophisticated software, high resolution sensor data, more complex relationships and multivariate comparisons are best performed with full function GIS packages. The data layers derived from combinations of raw data can generate information about spatial variability among soil properties. Adequately co-registered data can be quantitatively analyzed through the use of geostatistical and multivariate classification procedures (Pena-Yewtukhiw et al., 2000). As such, GIS and geostatistics form the core in analyzing sensor data. Processed data from a sensor can be fused with a spatially distributed process model for subsequent decision making in SSSM.

2.6.3 Apparent electrical conductivity mapping

Computer generated maps are an alternative method for displaying soil information. They provide quantitative interpretations of EC_a data, which can improve understanding of soil distributions and landscape relationships (Doolittle et al., 1994; Corwin and Lesch, 2003). Mapping EC_a is aided by global positioning technologies (Mueller et al., 2003; Jaynes et al., 2005).

Maps of soil EC_a can be useful in site-specific management, to characterize soil parameters such soil salinity (Rhoades and Ingvalson, 1971), CEC (McBride et al., 1997), clay content (Williams and Hoey, 1987), topsoil thickness (Doolittle et al., 1994), permafrost layers (Kawasaki and Osterkamp, 1988), and geologic strata (Zalasiewicz et al., 1985). Interpolation procedures are necessary to create maps quantifying EC_a values over continuous soil surfaces. Interpolation quality depends on measurement errors, EC_a variability, and the procedures used to measure and interpolate EC_a (Mueller et al., 2004).

3

Obtaining and analyzing sensor data

3.1 The EM38 and the EM38-MK2 sensors

Both the EM38 and the EM38-MK2 (Fig. 3.1) are developed by Geonics Ltd. (Ontario, Canada). The EM38 comprises two electrical coils: one a transmitter and the other a receiver, placed 1 m apart on either end of the instrument; the EM38-MK2 comprises three electrical coils: one a transmitter and the two other receivers, placed 0.5 m and 1 m apart from the transmitter.

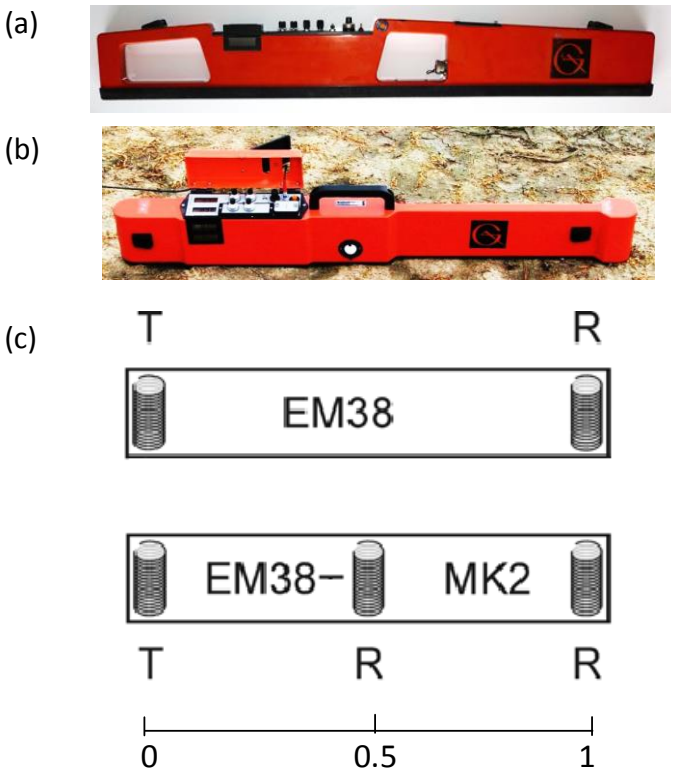

Figure 3.1(a) The EM38 and (b) the EM38-MK2 sensors, (c) coil configurations of the two sensors in a vertical orientation. T and R refer to the transmitter and receiver coils. The horizontal distance is on scale.

When powered on, the transmitter coil is excited with a sinusoidal current at a frequency of 14.6 kHz. This creates a time-varying primary magnetic field (Hp) in the vicinity of the coil. It induces eddy currents which are approximated as circular electrical current loops in the soil. The magnitude of the eddy currents is proportional to the electrical conductivity of that layer of the soil. Each current loop generates a secondary magnetic field (Hs) proportional to the value of the current flowing within the loop. A fraction of the secondary magnetic field from each loop is intercepted by the receiver coil of the instrument; the sum of

these signals is amplified and formed into an output voltage. The exact amplitude and phase of the secondary field will differ from those of the primary field as a result of soil property differences.

The configuration of the EM38 sensor, and resulting primary magnetic field lines, shown in Fig. 3.2, is referred to as the vertical dipole mode of operation as this is defined by the axis of cylindrical-symmetry of the primary magnetic field lines. When the sensor is placed on its side, where the axis of symmetry of primary field lines is horizontal, produces a configuration known as horizontal dipole mode. Each orientation has its own depth-response profile. A key assumption in understanding the surface measurement of the two sensors is that individual 'current loops' are not influenced by other parallel loops (McNeill 1980a). Therefore, the net secondary magnetic field at the receiver becomes the sum of the independent secondary magnetic fields from each of the individual current loops.

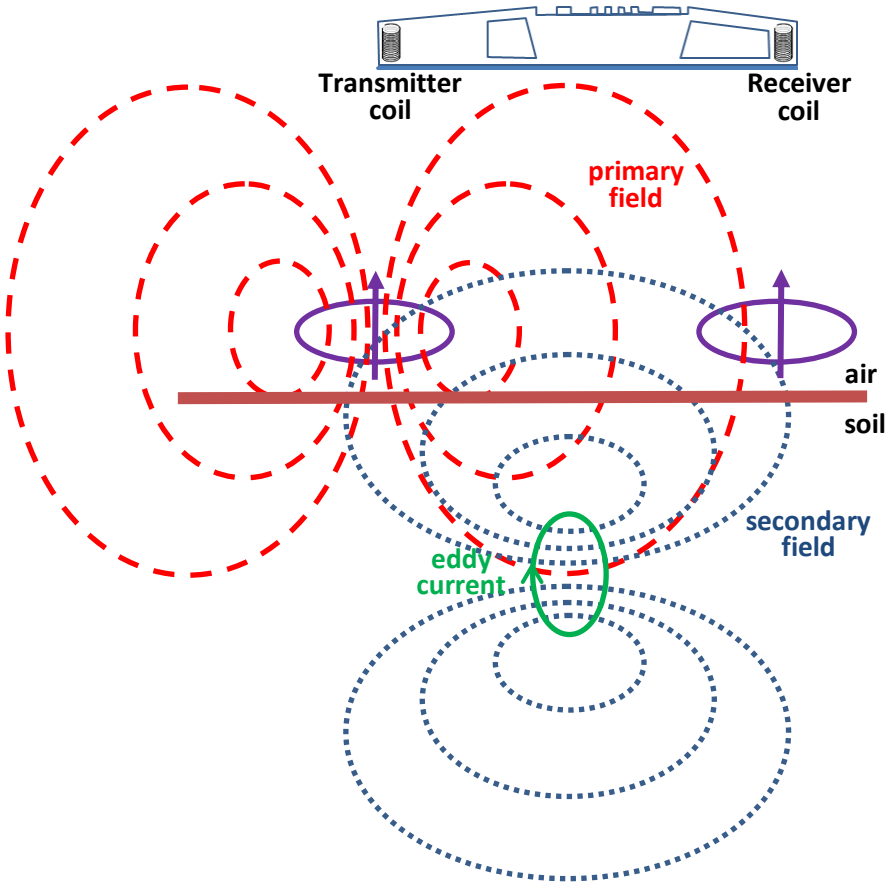

Figure 3.2 Schematic diagram of the EM38 in vertical orientation showing the principle of electromagnetic induction and the induced magnetic dipoles (straight arrows).

The relative response curves [Fig. 3.3(a)] describe the relative contribution to the secondary magnetic field arising from a thin horizontal layer at any normalized depth z (depth divided by inter-coil spacing) (McNeill, 1980a). For the vertical orientation (EC_a-V), while the surface soil only makes a very small contribution to the secondary field. The response in the horizontal orientation (EC_a-H) shows a completely different behavior as the largest contribution now comes from the near surface soil material.

The equations governing the relative response (z) of the EM38 are (McNeill, 1980b):

$$\varphi_H(z) = 2 - \frac{4z}{\left(4z^2+1\right)^{\frac{1}{2}}} \tag{3.1}$$

$$\varphi_v(z) = \frac{4z}{\left(4z^2+1\right)^{\frac{3}{2}}} \tag{3.2}$$

Integration of the relative response gives the cumulative response *R*(*z*) from the soil volume below a depth z (McNeill, 1980a):

$$R_v(z) = 1 - \frac{1}{\left(4z^2+1\right)^{\frac{1}{2}}} \tag{3.3}$$

$$R_H(z) = 1 - \left(4z^2+1\right)^{\frac{1}{2}} + 2z \tag{3.4}$$

The cumulative response (expressed as % of the measured signal) is defined as the relative contribution to the secondary magnetic field from all material below a certain depth z. Fig. 3.3(b) shows that for the vertical coil orientation all material below a depth of 2 m still contributes 25% to the secondary magnetic field, while in the horizontal orientation this contribution is only 12%. The effective depth of influence (DOI) is defined as the depth from which 70% of the response comes (or the depth below which the contribution is only 30%) and for the vertical and horizontal orientation respectively the DOI is 1.5 m and 0.75 m (Abdu et al., 2007; Corwin and Lesch, 2005b).

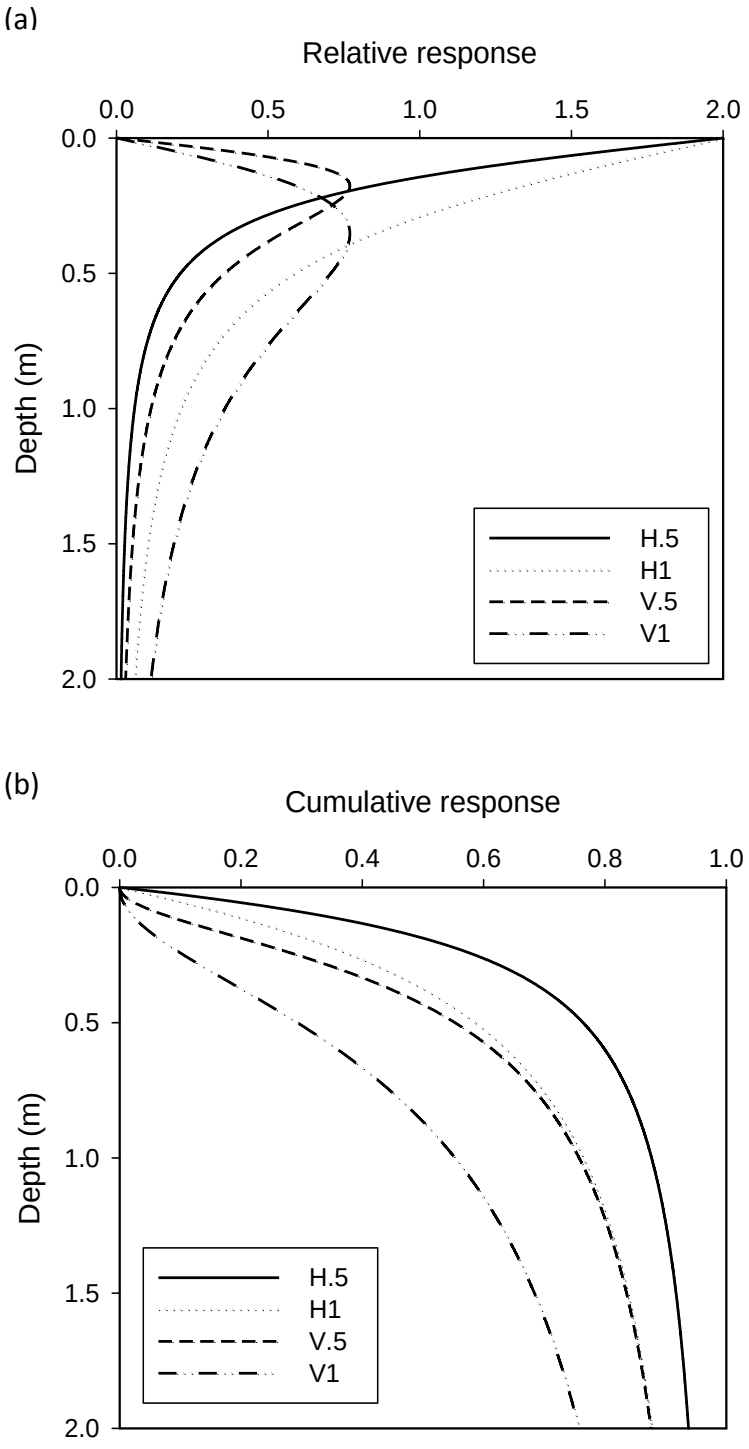

Figure 3.3(a) The response curves as a function of depth for the two orientation of the EM38 and EM38-MK2: the relative response and (b) the cumulative response. H = horizontal orientation, V = vertical orientation, 0.5 = 0.5 m intercoil distance, 1 = 1 m intercoil distance.

If the earth is *n*-layered, the reading of the EM38 sensor in vertical (EM_v) and horizontal (EM_H) orientation can be calculated as (Slavich, 1990):

$$EM_v = \sum_{i-1}^{n_v} EC_{a\,i}(R_{v(i-1)} - R_{v\,i}) \tag{3.5}$$

$$EM_H = \sum_{i-1}^{n_h} EC_{a\,i}(R_{H(i-1)} - R_{H\,i}) \tag{3.6}$$

where $EC_{a\,i}$ is the mean EC_a of the *i*th layer, $R_{v\,i}$ and $R_{H\,i}$ are the cumulative response from the ith layer for the horizontal and vertical orientation respectively, n_v is the number of layers for the vertical depth of measurement and n_h the number of layers for the horizontal depth of measurement. Since the EC_a readings represent the average conductivity of the different layers within the depth of investigation, the measurements are referred to as depth-weighted or bulk EC_a, weighted according to the depth response curves using equations (3.1) and (3.2).

The operation of the EM38 is illustrated in Fig. 3.4 for two cases with a difference in topsoil depth, given the constraint that the topsoil has a lower clay content than the subsoil.

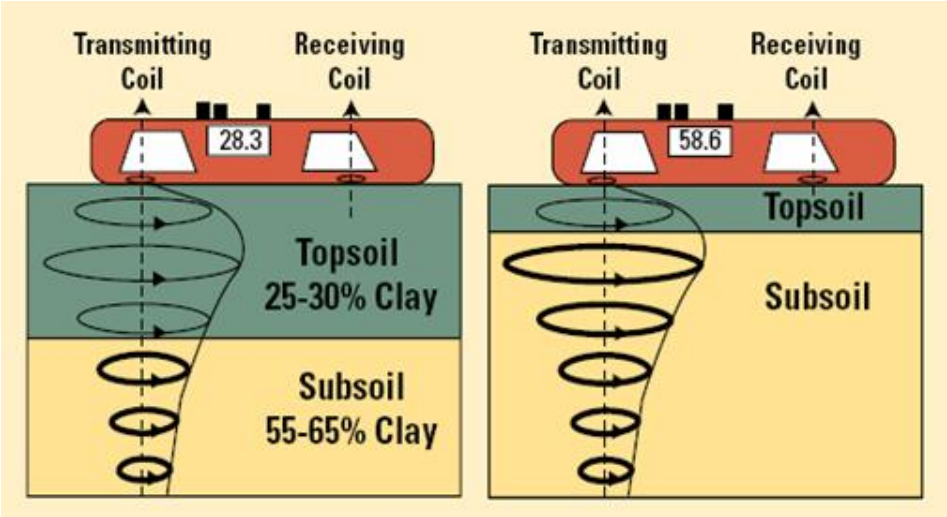

Figure 3.4 Principle of operation of EM38 in soils. The thicker circles (current loops) indicate soils that are better conductors of electrical current (left) deeper clayey topsoil giving less response (right) shallow clayey topsoil giving higher response (Davis et al., 1997).

The EM38 induces horizontal electric current loops in the soil and the current in each loop is proportional to the electrical conductivity of the soil which is in Fig. 3.4. shown by the thick ellipses. The individual currents are weighted as a function of the depth and summed to generate the instrument response. The response is larger when a larger part of the soil profile has a high conductivity like in the right case of Fig. 3.4.

Sensor calibration

Before starting a field survey the EM38 needs to be adjusted to the survey environment and a calibration is required. As the instrument is a sensitive indicator of electrically conductive materials all metal objects, small or large, must be taken away from the vicinity and operators body. The calibration is done according to the manufacturer instructions described in the EM38 Operating Manual (Geonics limited, 2003):

a. Initial nulling

When the sensor is turned on, the transmitter coil is used to generate a time-varying primary magnetic field which induces eddy currents into the soil. The receiver coil measures both this strong primary magnetic field and the much smaller secondary field arising from the eddy currents. An internally generated signal is then used to cancel or 'null' the large primary signal so that it does not overload the electronic circuit. This facilitates the measurement of the signal coming from the eddy currents. Therefore, the sensor is lifted to a height of 1.5 m so that it no longer responds to the soil electrical conductivity. With the instrument in its horizontal orientation, the I/P mode is nulled first by adjusting manually the I/P control knob so that the meter reading is zero. Then the mode is switched to the Q/P mode and this mode is nulled too so that the instrument reads zero. The instrument is successfully nulled at this stage when both modes read zero.

b. Instrument zeroing

This adjustment is used to set the sensor to zero so that the instrument meter would read zero if the unit were taken to a greater height above the earth. With the instrument at the height of 1.5 m and the master unit still in the horizontal orientation, the Q/P mode is adjusted manually by the Q/P control knob so that the sensor reading (H) is approximately 50 mS m^{-1}.

Then the sensor is rotated on it axis and placed in its vertical orientation and the Q/P reading (V) is noted. Then the difference between the two Q/P readings as H and V is taken (H′ = V – H). The instrument is brought back to horizontal position (H) and the Q/P knob is adjusted so that the meter reading becomes H′. Next, the instrument is rotated back to vertical orientation and the meter reading becomes 2H′. This step is complete when in vertical orientation the reading is twice the value of the horizontal orientation.

The above mentioned steps are also applicable for calibrating the EM38-MK2 except that the procedure should be carried out twice: for 1 m intercoil separation and also for 0.5 m intercoil separation.

Besides, during a field survey drift of the EM38 reading can occur and should be accounted for. To compensate for this drift effect, a calibration transect should be used to monitor the drift during the field survey. Also putting the sensor in a well isolated sled can lower the effect of temperature changes on the sensor reading.

The EC_a measurements in this research were post-corrected for instrumental drift according to the deviation from an initial diagonal measurement (calibration line) across the field and standardized to a reference temperature of 25°C by the method of Sheets and Hendrickx (1995):

$$EC_{a\,25} = EC_{a\,obs}\left(0.4470 + 1.4034.e^{-T/26.815}\right) \qquad (3.7)$$

with $EC_{a_{25}}$ is the standardized EC_a value at 25°C and $EC_{a_{obs}}$ the observed EC_a value at soil temperature T (°C). During all field surveys, soil temperature was recorded every hour by a bi-metal sensor pushed into the soil to a depth of 0.25 m below soil surface. The temperature remained stable at about 30°C. In this thesis, all EC_a measurement values refer to EC_a values at 25°C.

3.2 Geostatistics

Proximal soil sensors provide high resolution information that can be used to account for soil variability. However, these point measurements do not provide a continuous coverage. Spatial prediction is required to estimate the values at unvisited locations so that the gaps can be filled in. Geostatistics is a collection of statistical tools that enable us to spatially characterize a phenomenon by generating predictions at unsampled locations. Predictions are made based on inferences made about the behaviour of the variable in question at different sampling locations. These inferences use a random function model that considers unknown values to be spatially dependent random variables (Isaaks and Srivastava, 1989; Webster and Oliver, 2007). A random variable, $Z(\mathbf{x})$, is a variable whose values are randomly generated from a probability distribution (Webster and Oliver, 2007). The observed value of a soil variable at location **x** is considered as a random variable due to the incomplete knowledge we have about the interactions of the underlying factors that determine the value of the soil variable at a location. At every location **x**, the value of a soil property is therefore considered as one realization of a distribution with mean, variance and cumulative distribution function. In order to construct the distribution function, assumptions of stationarity are required. The important assumption for the characterization of the spatial variability of a soil variable is the assumption of intrinsic hypothesis. This hypothesis states:

The mathematical expected difference between two values of a random variable taken at two different locations depends only on the distance vector **h** (lag distance) between their locations and not on the location **x**.

$$\mathrm{E}[Z(\mathbf{x}) - Z(\mathbf{x}+\mathbf{h})] = 0 \tag{3.8}$$

For all vectors **h** the increment $Z(\mathbf{x}+\mathbf{h}) - Z(\mathbf{x})$ has a finite variance which does not depend on **x**,

$$\mathrm{Var}[\{Z(\mathbf{x}) - Z(\mathbf{x}+\mathbf{h})\}] = \mathrm{E}[\{Z(\mathbf{x}) - Z(\mathbf{x}+\mathbf{h})\}^2] = 2\gamma(\mathbf{h}) \tag{3.9}$$

where the quantity $\gamma(\mathbf{h})$ is known as the variogram at lag h.

3.2.1 Variography

The variogram is the key to geostatistics as it describes the scale and pattern of the spatial variation among measured values. It considers the squared difference between two measured values (Matheron, 1962) (Eq. 3.8).

$$\gamma(\mathbf{h}) = \frac{1}{2N(\mathbf{h})} \sum_{\alpha=1}^{N(\mathbf{h})} \{ z(\mathbf{x}_\alpha) - z(\mathbf{x}_\alpha + \mathbf{h}) \}^2 \tag{3.10}$$

where $z(\mathbf{x}_\alpha)$ and $z(\mathbf{x}_\alpha + \mathbf{h})$ are observations of a random variable Z separated by a distance vector **h**, known as a lag. $N(\mathbf{h})$ is the number of pairs of $\{ z(\mathbf{x}_\alpha), z(\mathbf{x}_\alpha + \mathbf{h}) \}$.

A plot of $\gamma(\mathbf{h})$ versus **h** is called the experimental variogram. The spatial dependency between measurements assumes observations closer to one another have more similar values than the ones further apart. Accordingly, the variogram between observations increases with increasing separation distance, **h**, until it reaches to maximum at a distance beyond which observations are no more spatially correlated. This maximum semivariance is called the sill variance, *C*. The lag **h** at which the variogram reaches the sill represents the range of spatial dependency (correlation), a. Theoretically, the variogram at **h** = 0 is zero. However, due to errors in data measurement (error variance) and spatial variation within distances closer than the smallest sampling interval (micro variance), the variogram can have a value greater than zero at **h** = 0. This variance is called the nugget variance, c_0. It is often found that as the lag distance approaches zero, the semivariance remains a positive value. The nugget is the intercept of the variogram with the Y-axis and represents unexplained spatially dependent variation or purely random variance. The ratio of the nugget effect to the sill, referred as the relative nugget effect, (RNE, expressed in %) describes the proportion of spatially unstructured variation in relation to the total variance.

In order to describe the $\gamma(\mathbf{h})$ relationship fully and to meet the requirement of the positive definite function property of the variogram, a variogram model needs to be fitted for the experimental variogram. There are different theoretical models to fit the variogram of which the spherical (Eq. 3.11) and the exponential models (Eq. 3.12) are the most commonly used models with soil data (Webster and Oliver, 2007).

Spherical model:

$$\gamma(\mathbf{h}) = c_0 + c_1.\left(\frac{3\mathbf{h}}{2a} - \frac{1}{2}\left(\frac{\mathbf{h}}{a}\right)^3\right) \qquad if\ 0 < \mathbf{h} \le a$$
$$\gamma(\mathbf{h}) = c_0 + c_1 \qquad if\ \mathbf{h} > a \qquad (3.11)$$
$$\gamma(0) = 0$$

Exponential model:

$$\gamma(\mathbf{h}) = c_0 + c_1.\left(1 - \exp\left(-\frac{3\mathbf{h}}{a}\right)\right) \qquad \forall\ 0 < \mathbf{h} \qquad (3.12)$$
$$\gamma(0) = 0$$

where $c_0 + c_1$ being the sill, c_1 the structured variance, c_0 the nugget variance, a the range.

Fig. 3.6 shows the two commonly used theoretical models.

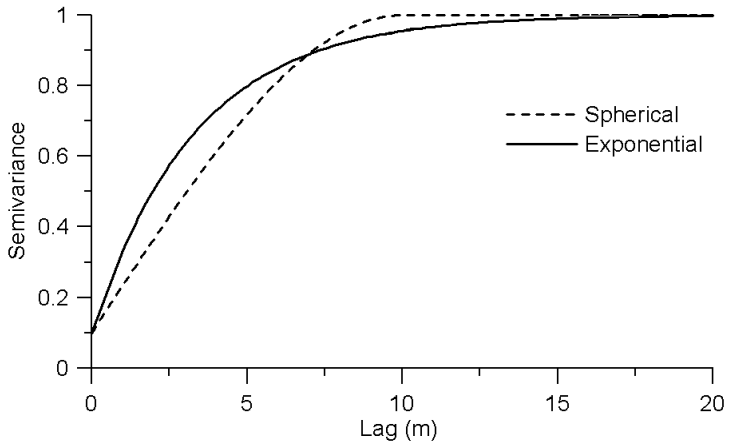

Figure 3.5 Spherical and exponential models with same nugget effect, sill and range (c_0 = 0.1, c_1 = 0.9, a = 10).

A spherical model has a linear structure up to about 2/3 of the range, beyond which it levels off. Spherical models describe variables with abrupt boundaries at discrete and regular spacing but without a well defined distance between the abrupt changes. Variables characterized by abrupt changes at all distances are described by an exponential model. Exponential models have a linear start up to 1/3 of the range, but they start steeper than a spherical model. Since the sill is reached only asymptotically there is no finite range. For

practical purposes, an effective range is defined as the **h** value at which 95% of the sill is reached.

In this research selection of the most appropriate theoretical model was done visually where the model fitting is judged graphically (Goovaerts, 1997). The variogram model is used to build the covariance matrices by converting the distance matrices between (i) measured points and (ii) between measured point and point of estimation. The covariance matrices are then used to calculate weight for measurements used for prediction. Variogram modeling was conducted with the software program Surfer (Golden Software Inc., Golden, U.S.A.)

3.2.2 Kriging

Kriging refers to a set of geostatistical prediction methods that aim at generating unbiased estimations with a minimum estimation variance (Webster and Oliver, 2007). The estimates are calculated as weighted linear combinations of neighbouring measurements where the weights are obtained as a function of distance and clustering through minimizing the squared difference between the true and the estimated values. Considering a random variable Z that has been measured at n locations, $Z(\mathbf{x}_\alpha)$, α = 1,…,n, the kriging estimator at an unsampled location $\mathbf{x}_0$ can be written as:

$$Z^*(\mathbf{x}_0) - m(\mathbf{x}_0) = \sum_{\alpha=1}^{n(\mathbf{x}_0)} \lambda_\alpha \cdot [Z(\mathbf{x}_\alpha) - m(\mathbf{x}_\alpha)] \tag{3.13}$$

where $Z^*(\mathbf{x}_0)$ is an estimated value at $\mathbf{x}_0$ using the neighbouring measurements $Z(\mathbf{x}_\alpha)$, the number of neighbourhood measurements used for the estimation is $n(\mathbf{x}_0)$, λ_α are the weights assigned to data $Z(\mathbf{x}_\alpha)$, and the expected values (or means) at locations $\mathbf{x}_0$ and $\mathbf{x}_\alpha$ are $m(\mathbf{x}_0)$ and $m(\mathbf{x}_\alpha)$, respectively.

The weights are calculated by minimizing the estimation variance, $\sigma^2(\mathbf{x}_0)$:

$$\sigma^2(\mathbf{x}_0) = \mathrm{E}[\{Z^*(\mathbf{x}_0) - Z(\mathbf{x}_0)\}]^2 \tag{3.14}$$

under the constraint of unbiasness:

$$E[Z^*(\mathbf{x}_0) - Z(\mathbf{x}_0)] = 0 \tag{3.15}$$

There are several variants of kriging algorithms differing based on how the deterministic mean is considered, the kind of data transformation and wheatear a secondary variable is involved or not. The most common type of kriging is ordinary kriging (OK). This section gives an introduction to ordinary kriging and other methods are discussed together with the related studies.

Ordinary kriging

OK assumes the mean of observations to be unknown but stationary within the local neighbourhood. Accordingly, the ordinary kriging estimator $Z^*_{\mathrm{OK}}(\mathbf{x}_0)$ is written as:

$$Z^*_{\mathrm{OK}}(\mathbf{x}_0) = \sum_{\alpha=1}^{n(\mathbf{x}_0)} \lambda_\alpha Z(\mathbf{x}_\alpha) \qquad \text{with} \qquad \sum_{\alpha=1}^{n(\mathbf{x}_0)} \lambda_\alpha = 1 \tag{3.16}$$

where $n(\mathbf{x}_0)$ is the number of observations in the local neighbourhood around $(\mathbf{x}_0)$ and λ_α are the weights assigned to each of the observations. The appropriate weights are found using the variogram model with its associated parameters. The weights need to sum to one to ensure the estimate is unbiased and they can be obtained by solving:

$$\begin{cases} \sum_{\beta=1}^{n(\mathbf{x}_0)} \lambda_\beta \gamma(\mathbf{x}_\alpha - \mathbf{x}_\beta) + \psi = \gamma(\mathbf{x}_\alpha - \mathbf{x}_0); & \alpha = 1,\ldots,n(\mathbf{x}_0) \\ \sum_{\beta=1}^{n(\mathbf{x}_0)} \lambda_\beta = 1 \end{cases} \tag{3.17}$$

where $\gamma(\mathbf{x}_\alpha - \mathbf{x}_\beta)$ is the variogram between the sampling locations $\mathbf{x}_\alpha$ and $\mathbf{x}_\beta$, and $\gamma(\mathbf{x}_\alpha - \mathbf{x}_0)$ is the variogram between sampling locations $\mathbf{x}_\alpha$ and the unsampled location $\mathbf{x}_0$. The Lagrange multiplier, ψ, is introduced to minimize the ordinary kriging variance under the constraint of unbiasness that the sum of weights must equal one.

The most straightforward method to solve the ordinary kriging system is through matrix algebra. The kriging system consists of (n+1) linear equations an (n+1) unknowns: one Lagrange multiplier ψ and weights $n(\mathbf{x}_0)$. The variogram model provides the variogram values. In matrix form the OK system is:

$$[\lambda] = [\mathrm{A}]^{-1}[\mathrm{B}] \tag{3.18}$$

where $[\lambda]$ is matrix of unknown weights and the Lagrange multiplier, $[\mathrm{A}]$ is the matrix of variograms between observation points and $[\mathrm{B}]$ is the average variogram between observation points and $\mathbf{x}_0$.

$$[\boldsymbol{\lambda}] = \begin{bmatrix} \lambda_1 \\ \lambda_2 \\ . \\ . \\ \lambda_{n(\mathbf{x}_0)} \\ \psi \end{bmatrix} \tag{3.19}$$

$$[\mathrm{A}] = \begin{bmatrix} \gamma(\mathbf{x}_1 - \mathbf{x}_1) & \gamma(\mathbf{x}_1 - \mathbf{x}_2) & . & . & \gamma(\mathbf{x}_1 - \mathbf{x}_{n(\mathbf{x}_0)}) & 1 \\ \gamma(\mathbf{x}_2 - \mathbf{x}_1) & \gamma(\mathbf{x}_2 - \mathbf{x}_2) & . & . & \gamma(\mathbf{x}_2 - \mathbf{x}_{n(\mathbf{x}_0)}) & 1 \\ . & . & . & . & . & . \\ . & . & . & . & . & . \\ \gamma(\mathbf{x}_{n(\mathbf{x}_0)} - \mathbf{x}_1) & \gamma(\mathbf{x}_{n(\mathbf{x}_0)} - \mathbf{x}_2) & . & . & \gamma(\mathbf{x}_{n(\mathbf{x}_0)} - \mathbf{x}_{n(\mathbf{x}_0)}) & 1 \\ 1 & 1 & . & . & 1 & 0 \end{bmatrix} \tag{3.20}$$

$$[\mathrm{B}] = \begin{bmatrix} \gamma(\mathbf{x}_1 - \mathbf{x}_0) \\ \gamma(\mathbf{x}_2 - \mathbf{x}_0) \\ . \\ . \\ \gamma(\mathbf{x}_{n(\mathbf{x}_0)} - \mathbf{x}_0) \\ 1 \end{bmatrix} \tag{3.21}$$

Ordinary kriging provides the error variance (kriging variance) computed as:

$$\sigma^2_{\mathrm{OK}}(\mathbf{x}_0) = \sum_{\alpha=1}^{n(\mathbf{x}_0)} \{\lambda_\alpha \gamma(\mathbf{x}_\alpha - \mathbf{x}_0)\} + \psi \quad . \tag{3.22}$$

This procedure solves the weights λ_β and the Lagrange multiplier from which the estimator $Z^*_{\mathrm{OK}}(\mathbf{x}_0)$ is found. The same procedure is then repeated for every location which provides the continuous raster map of a soil variable under investigation.

In this study, OK was conducted with the software program Surfer (Golden Software Inc., Golden, U.S.A.)

3.3 Classification

Classification techniques are methods that can be used to organize data into classes or groups based on similarities among the data (Cline, 1949). Most classification algorithms do not rely on assumptions common to conventional statistical methods, such as the underlying statistical distribution of data, and therefore they are useful in situations where little prior knowledge exists. The potential of classification algorithms to reveal the underlying classes or groups in data can be exploited in a wide variety of applications, including soil property classification, EC_a pattern recognition, modeling and identification. This section is intended to present the fuzzy classification algorithms based on the *k*-means functional. However, a general overview of classification methods including crisp classification is given to highlight the rationale behind fuzzy or soft classification.

The main purpose of classification in a geographical context such as a soil survey is to enable a concise description of the spatial variation of soil as a three-dimensional multivariate system. In this field of application, classification rather than ordination is generally preferred for data reduction because the relationships between the properties are often nonlinear. However, where spatial variation is gradual instead of abrupt, such as often with EC_a, disjoint classes poorly fit the reality to be described. Therefore an approach with fuzzy classes seems more appropriate. In the type of soil management applications we are dealing with, description is not the only purpose. Class memberships as, for instance, presented on EC_a maps are used for prediction of soil and crop properties. Ideally, the classification system is

designed in such a way that it provides an optimal basis for spatial interpolation as well as prediction of properties from class memberships. An optimal classification aims at reducing information loss while identifying groups of individuals sharing common values.

3.3.1 Data matrix

Classification techniques can be applied to data that are quantitative (numerical), qualitative (categorical), or a mixture of both. In this section, the classification of quantitative data is considered. The data, for instance EC_a values are typically observations from a survey. Each observation consists of n measured variables, grouped into an n-dimensional vector $\mathbf{z}_k = [z_{1k},...,z_{nk}]^T$, $\mathbf{z}_k \in \mathbb{R}^n$. A set of N observations is denoted by $\mathbf{Z} = \{\mathbf{z}_k | = 1,2,...,N\}$, and is represented as an $n \times N$ matrix:

$$\mathbf{Z} = \begin{bmatrix} z_{11} & z_{12} & \cdots & z_{1N} \\ z_{21} & z_{22} & \cdots & z_{2N} \\ \vdots & \vdots & \vdots & \vdots \\ z_{n1} & z_{n2} & \cdots & z_{nN} \end{bmatrix} \tag{3.23}$$

In the classification terminology, the columns of this matrix are called objects, the rows are called the attributes (or features), and $\mathbf{Z}$ is called the data matrix. The meaning of the columns and rows of $\mathbf{Z}$ depends on the context. In geo-referenced EC_a survey, for instance, the columns of $\mathbf{Z}$ may represent EC_a-H or EC_a-V, and the rows are then EC_a values (variables) observed in each location (position).

3.3.2 Classes and centroids

Various definitions of a class can be formulated, depending on the objective of classification. Generally, one may accept the view that a class is a group of objects that are more similar to one another than to members of other classes (Bezdek, 1981; Jain and Dubes, 1988). The term ‘similarity’ is considered as mathematical similarity, measured in some well-defined sense. In metric spaces, similarity is often defined by means of a distance norm. Distance can be measured among the data vectors themselves, or as a distance from a data vector to some centre of the class, the centroid, which is the average of all the points in a class. The centroids are usually not known beforehand, and are sought by the classification

algorithms simultaneously with the partitioning of the data. The centroids may be vectors of the same dimension as the data objects, but they can also be defined as geometrical objects, such as linear or nonlinear subspaces or functions. The performance of most classification algorithms is influenced not only by the geometrical shapes and densities of the individual class, but also by the spatial relations and distances among the classes. Classes can be well-separated, continuously connected to each other, or overlapping.

3.3.3 Classification methods

Many classification algorithms have been introduced in the literature. Since classes can formally be seen as subsets of the data set, one possible method of classification can be according to whether the subsets are fuzzy (soft) or crisp (hard).

3.3.3.1 Hard classification

Hard classification methods are based on classical set theory, and require that each object belongs only to one class. Hard classification means partitioning the data into a specified number of mutually exclusive subsets. The objective is to separate the data set $\mathbf{Z}$ into c classes (groups, clusters). For the time being, assume that c is known, based on prior knowledge, for instance. Using classical sets, a hard classification of $\mathbf{Z}$ can be defined as a family of subsets $\{A_i | 1 \le i \le c\} \subset P(\mathbf{Z})$[1] with the following properties (Bezdek, 1981):

$$\bigcup_{i=1}^{c} A_i = \mathbf{Z}, \tag{3.24a}$$

$$A_i \cap A_j = \emptyset, \quad 1 \le i \ne j \le c, \tag{3.24b}$$

$$\emptyset \subset A_i \subset \mathbf{Z}, \quad 1 \le i \le c. \tag{3.24c}$$

Equation 3.24-a means that the union subsets A_i contains all the data. The subsets must be disjoint, as stated by equation 3.24-b, and none of them is empty nor contains all the data in $\mathbf{Z}$ (equation 3.24-c). In other words, it means that the classes are mutually exclusive, jointly exhaustive and non-empty. In terms of membership (characteristic) functions, a partition can be conveniently represented by the partition matrix $\mathbf{U} = [\mu_{ik}] c \times N$. The ith row of this

matrix contains values of the membership function μ_i of the ith subset A_i of $\mathbf{Z}$. It follows from (3.24) that the elements of $\mathbf{U}$ must satisfy the following conditions:

$$\mu_{ik} \in \{0,1\}, \quad 1 \le i \le c \quad 1 \le k \le N, \tag{3.25a}$$

$$\sum_{i=1}^{c} \mu_{ik} = 1, \quad 1 \le k \le N, \tag{3.25b}$$

$$0 < \sum_{k=1}^{N} \mu_{ik} < N, \quad 1 \le i \le c. \tag{3.25c}$$

The space of all possible hard partition matrices for $\mathbf{Z}$, called the hard partitioning space (Bezdek, 1981), is thus defined by

$$M_{hc} = \left\{ \mathbf{U} \in \mathbb{R}^{c \times N} \middle| \mu_{ik} \in \{0,1\}, \forall_i, k; \sum_{i=1}^{c} \mu_{ik} = 1, \forall k; 0 < \sum_{k=1}^{N} \mu_{ik} < N, \forall_i \right\}. \tag{3.26}$$

A hard classification may not give a realistic picture of the underlying data. Boundary data points may represent patterns with a mixture of properties of data, and therefore cannot be fully assigned to either of these classes, or do they constitute a separate class. This shortcoming can be alleviated by using fuzzy classification as shown in the following sections.

3.3.3.2 Fuzzy classification

In the theory of fuzzy sets, $\mu_{ik} \in \{0,1\}$ in equation 3.25a is relaxed, so that memberships are allowed to be partial, i.e. to take any value between and including 0 and 1. Therefore, the generalization of the hard classification to a soft classification such as the fuzzy case, follows directly by allowing μ_{ik} to attain real values in $[0, 1]$. Conditions for a fuzzy partition matrix, analogous to equations in 3.25 are given as:

$$\mu_{ik} \in [0,1], \quad 1 \le i \le c \quad 1 \le k \le N, \tag{3.27a}$$

$$\sum_{i=1}^{c} \mu_{ik} = 1, \quad 1 \le k \le N, \tag{3.27b}$$

$$0 < \sum_{k=1}^{N} \mu_{ik} < N, \quad 1 \le i \le c. \tag{3.27c}$$

The ith row of the fuzzy partition matrix $\mathbf{U}$ contains values of the ith membership function of the fuzzy subset A_i of $\mathbf{Z}$. Equation 3.23-b constrains the sum of each column to 1, and thus the total membership of each $\mathbf{z}_k$ in $\mathbf{Z}$ equals one. The fuzzy partitioning space for $\mathbf{Z}$ is the set

$$M_{fc} = \left\{ \mathbf{U} \in \mathbb{R}^{c \times N} \middle| \mu_{ik} \in \{0,1\}, \forall_i, k; \sum_{i=1}^{c} \mu_{ik} = 1, \forall k; 0 < \sum_{k=1}^{N} \mu_{ik} < N, \forall_i \right\}. \tag{3.28}$$

Fuzzy *k*-means classification

One approach to fuzzy classification is the fuzzy *k*-means. Fuzzy *k*-means (De Gruijter and McBratney, 1988) [or, fuzzy *c*-means (Bezdek, 1981)] is a direct generalization of hard *k*-means. Most analytical fuzzy classification algorithms are based on the optimization of the basic *k*-means objective function, or some modification of it. Therefore it is good to start with the fuzzy *k*-means functional. It minimises the within-class sum square errors functional J under the above three conditions in equation 3.27 and is defined by the following objective function:

$$J = \sum_{i=1}^{n} \sum_{k=1}^{c} m_{ik}^{\varphi} d^2(\mathbf{x}_i \mathbf{c}_k) \tag{3.29}$$

where is n the number of data, c is the number of classes, $\mathbf{c}_k$ is the vector representing the centroid of class k, $\mathbf{x}_i$ is the vector representing individual data i and $d^2(\mathbf{x}_i \mathbf{c}_k)$ is the squared distance between $\mathbf{x}_i$ and $\mathbf{c}_k$ according to a chosen definition of distance, which for simplicity further denoted by d_{ik}^2. φ is the fuzzy exponent and ranges from 1 to ∞. It determines the degree of fuzziness of the final solution that is the degree of overlap between groups. With $\varphi = 1$ (the lowest meaningful value of φ is 1), the solution is a hard partition. As φ approaches infinity, the solution approaches its highest degree of fuzziness. Many practitioners use φ=2. The value of the cost function J can be seen as a measure of the total variance of $\mathbf{x}_i$ from $\mathbf{c}_k$.

The minimisation of the objective function J provide the solution for the membership function (Bezdek,1981):

$$m_{ik} = \frac{d_{ik}^{2/(\varphi-1)}}{\sum_{j=1}^{c} d_{ij}^{2/(\varphi-1)}} \qquad i = 1,2,.....,n; \qquad k = 1,2,.....,c \tag{3.30}$$

$$\mathbf{C}_k = \frac{\sum_{i=1}^{n} m_{ik}^{\varphi} x_i}{\sum_{i=1}^{n} m_{ik}^{\varphi}} \qquad k = 1,2,.....,c \tag{3.31}$$

The Fuzzy *k*-means algorithm is as follows:

i. Choose a number of classes k, with $1 < k < n$
ii. Choose a value for the fuzziness exponent φ, with $\varphi > 1$
iii. Choose a definition of distance on the variable space.
iv. Choose a value for the stopping criterion ε (ε = 0.001 gives reasonable convergence).
v. Initialize membership matrix {**M** = **M**$^{(0)}$}, e.g. with random memberships or with memberships from a hard *k*-means partition.
vi. At iteration (it=1,2,3) calculate (re- calculate) **C** = **C**$^{(it)}$ using equation $\mathbf{C}_k = \ldots\ldots$ and **M**$^{(it-1)}$
vii. Re-calculate **M** = **M**$^{(it)}$ using equation $m_{ik} = \ldots..$ and **C**$^{(it)}$.
viii. Compare **M**$^{(it)}$ to **M**$^{(it-1)}$ in a convenient matrix norm. If $\|\mathbf{M}^{(it)} - \mathbf{M}^{(it-1)}\| < \varepsilon$, then stop; otherwise return to step vi.

Fuzzy *k*-means with extragrades

By their nature, continuous classes should provide better representations of outliers or atypical individuals than discontinuous classes. This is especially the case with outliers located between classes (groups or clusters) in property space. We can refer to this type of individuals as intragrades. Fuzzy *k*-means, for instance, will indeed give intermediate memberships to intragrades. However, outliers outside the main body of data points, referred to as extragrades, are still not suitably represented by fuzzy *k*-means.

Therefore, De Gruijter and McBratney (1988) modified the objective function J to account for extragrades (or, outliers). This improvement makes the memberships directly

depend upon the distances to the class centroids as:

$$J = \alpha \sum_{i=1}^{n} \sum_{k=1}^{c} m_{ik}^{\varphi} d_{ik}^{2} + (1+\alpha) \sum_{i=1}^{n} m^{*\varphi} \sum_{k=1}^{c} d_{ik}^{-2} \tag{3.32}$$

where m^* denotes the membership to a fuzzy class of outliers and α is a parameter that determines the mean value of m^*. The aim is to accommodate the outliers in a special class to decrease the effect of them on classification. The members of this particular class are not concentrated in a fuzzy hypersphere around a defined class centre, as with regular classes. Instead, they are spread across and over regions of larger distances between an individual and the class centres.

Minimisation of this objective is similar to that used in fuzzy *k*-means. The solution for the membership is as follows:

$$m_{ik} = \frac{d_{ik}^{-2/(\varphi-1)}}{\sum_{j=1}^{c} d_{ij}^{-2/(\varphi-1)} + \left(\frac{1-\alpha}{\alpha} \sum_{j=1}^{c} d_{ij}^{-2} \right)^{-1/(\phi-1)}} \qquad i = 1,2,\ldots\ldots,n; \quad k = 1,2,\ldots\ldots,c \tag{3.33}$$

$$m^* = \frac{\left(\frac{1+\alpha}{\alpha} \sum_{j=1}^{k} d_{ij}^{-2} \right)^{-1/(\phi-1)}}{\sum_{j=1}^{c} d_{ij}^{-2/(\varphi-1)} + \left(\frac{1+\alpha}{\alpha} \sum_{j=1}^{c} d_{ij}^{-2} \right)^{-1/(\phi-1)}} \qquad i = 1,2,\ldots\ldots,n \tag{3.34}$$

$$\mathbf{C}_k = \frac{\sum_{i=1}^{n} \left\{ m_{ic}^{\varphi} - (1-\alpha)\alpha^{-1} d_{ik}^{-4} m^{*\varphi} \right\} x_i}{\sum_{i=1}^{n} \left\{ m_{ic}^{\varphi} - (1-\alpha)\alpha^{-1} d_{ik}^{-4} m^{*\varphi} \right\}} \qquad k = 1,2,\ldots\ldots,c \tag{3.35}$$

The algorithm for solving the above equations can be found in deGruijter and McBratney (1988) and is implemented in the software programme FuzME (Minasny and McBratney, 2002).

Performance measure

In order to determine the optimal number of classes, validity functions can be used.

The Fuzziness Performance Index (FPI) estimates the degree of fuzziness generated by a specified number of classes and is defined as (Roubens, 1982):

$$\mathrm{FPI} = 1 - \frac{kF - 1}{k - 1} \tag{3.36}$$

where, F is the partition coefficient defined as:

$$\mathrm{F} = \frac{1}{n}\sum_{i=1}^{n}\sum_{k=1}^{c} m_{ik}^2 \tag{3.37}$$

The Normalized Classification Entropy (NCE) or the Modified Partition Entropy (MPE) estimates the degree of disorganization created by a specified number of classes and is defined as:

$$\mathrm{NCE} = \frac{H}{\log k} \tag{3.38}$$

where, H is the entropy function defined as:

$$\mathrm{H} = -\frac{1}{n}\sum_{i=1}^{n}\sum_{k=1}^{c} m_{ik} \times \log\left(m_{ik}\right) \tag{3.39}$$

The optimum number of classes is established on the basis of minimising these two measures (FPI and MPE or NCE). FPI ($0 \leq \mathrm{FPI} \leq 1$) is a measure of the degree of membership sharing among classes, where a value close to 1 indicates a strong sharing of membership and 0 represents distinct classes with no membership sharing. The NCE ($0 \leq \mathrm{NCE} \leq 1$) estimates the degree of disorganization in the classification and a value close to 1 indicates strong disorganization and 0 reflects superior organization. As a result, this method minimises the within class variance, and consequently, individuals classified into the same class have similar attributes.

Compactness and Separation validity function (*S*) (Xie and Beni, 1991) is defined as compactness over separation as:

$$S = \frac{J_2}{n \times d_{\min}^2} \tag{3.40}$$

where J_2 is:

$$J_2 = \sum_{i=1}^{n} \sum_{k=1}^{c} m_{ik}^2 d_{ik}^2 \tag{3.41}$$

and $d_{\min}$ is the separation measurement, the minimum distance between the class centroids; *n* is the number of data, *c* is the number of classes and *m* is the membership.

The fuzzy *k*-means classification software FuzMe (Minasny and McBratney, 2002) was used in this research.

4

FloSSy: A floating soil sensing system for paddy rice fields

The content of this paper was published as:

Islam, M.M. and Van Meirvenne, M., 2011. FloSSy: A floating sensing system to evaluate soil variability of flooded paddy fields. In: Stafford, J.V. (Ed.), Precision Agriculture 2011, Czech Centre for Science and Society, Prague, Czech Republic, pp. 60-66.

4.1 Introduction

Soils of flooded fields like those under continuous paddy cultivation pose severe practical limitations to the collection of high-resolution soil information. An efficient system for measuring the within-field variation of soil properties is a prerequisite to introducing precision agriculture (PA) to such a type of land use. PA as an alternative to traditional uniform management of paddy fields is sought to increase the profitability of crop production since production inputs are regulated according to local needs. Therefore, high-resolution soil information as an indicator of the spatial soil variability offers potential for PA applications also under flooded conditions. Thus, the exploration of within-field soil variability using an appropriate sensing system is very important to investigate the possibilities of adopting PA in paddy soils. Yet, no appropriate sensing technology to identify the soil spatial variability within these fields has been reported so far.

In order to acquire high-resolution soil spatial information, several sensors and sensing systems have been introduced and evaluated for PA (Sudduth et al., 1997). Among the proximal soil sensors, the ones based on EMI are commonly used to furnish exhaustive information, even at a spatial resolution of less than one meter (Simpson et al., 2009). EMI sensors measure the soil EC_a which can be interpreted in terms of spatially variable soil parameters like salinity (Triantafilis et al., 2000), texture (Saey et al., 2009), organic carbon fraction (Martinez et al., 2009), moisture (Brevik et al., 2006) and depth to a clay layer (Saey et al., 2008a). The efficiency of field measurements of EC_a increases if more area can be covered in less time by using a mobile sensing system. Rhoades (1992) introduced the concept of a mobile EMI sensing system which has been intensively used worldwide, for instance, by Carter et al. (1993), Cannon et al. (1994), Triantafilis et al. (2002) and Cockx et al. (2005). In these systems, a motor vehicle usually pulls the sensor on a carrying platform over the study field and as such soil information is captured on-the-go. A GPS receiver provides the location of respective measurements. Under flooded field conditions, however, the use of such a system is limited due to several practical problems arising from the inundated situation. Examples are the non-suitability of the usual motor vehicle to operate in a flooded field, accidental turning over of the entire sensor carrying platform in water, proneness of electronics to moisture damage etc. Until now, all reported mobile sensing systems have been applied to fields with dry and unsaturated soil conditions. In a flooded field situation, invasive proximal soil sensors would fail in sensing the soil beneath standing

water, and remote sensing sensors would be incapable of providing soil-related results. Moreover, flooded soils like paddy fields are not easily accessible for soil sampling due to the almost permanent inundated condition. Despite these limitations, on-the-go sensor measurement of soil variability under flooded conditions is essential to implement PA practices in wetland crop cultivation systems. Consequently, a soil sensing system is needed to acquire information about the spatial variability of inundated paddy soils.

Therefore, the objective of this study was to develop, operate and evaluate a floating sensing system capable of providing relevant soil information to support PA under flooded paddy field conditions.

4.2 Materials and methods

4.2.1 The Floating Soil Sensing System (FloSSy)

Low-land paddy cultivation is typical for a flood prone country like Bangladesh. Extensive soil information from these regularly flooded paddy soils is limited due to water logging. To acquire high resolution soil data efficiently in wet field conditions, a Floating Soil Sensing System (FloSSy) was developed. The FloSSy was designed so that it can be used in flooded fields even under seasonal rainy conditions. Therefore, the housing for all electronics and communication cables was made waterproof. To provide the geographic locations of the recorded soil measurements, the system was equipped with a GPS receiver. Moreover, the FloSSy simultaneously processed real-time raw EC_a and GPS information and converted those to the format required by the user. This required a software component, the FloSSy logger, to function in fully automated on-the-go mode. The graphical user interface (GUI) of the logger displayed the traversing path of the sensor in real-time otherwise it would be impossible, in a flooded field, to track the previously measured path in order to keep a constant distance between measured lines. A last condition that was fulfilled was related to the weight of the sensor carrying platform: light weight material that could float on water was used for the construction of the platform. At the same time, it was made stable enough against water waves to prevent accidental turning over.

As such, the FloSSy consists of an EMI soil sensing instrument, a GPS, a field laptop, a real time sensor data processing and path guidance software, a waterproof housing for the soil

sensor, a floating platform for the sensor and the GPS and a wetland cultivation vehicle to pull the entire sensing platform on water (Fig. 4.1).

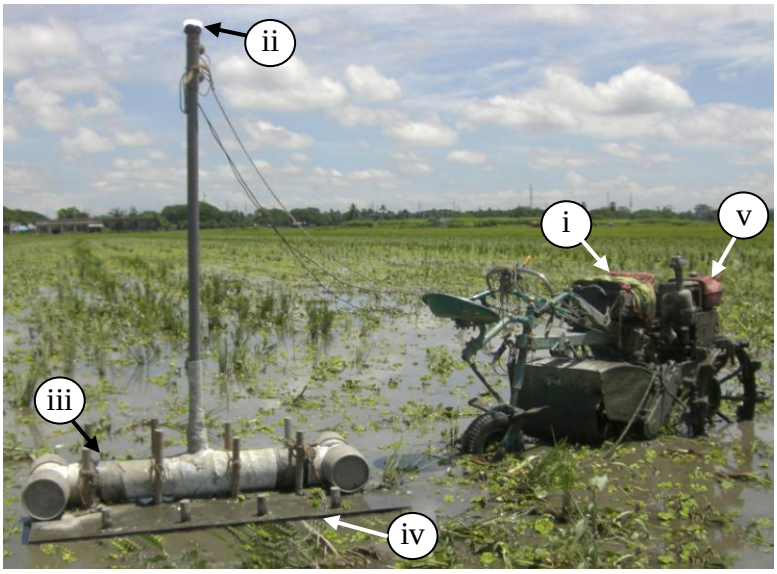

Figure 4.1 FloSSy with: (i) laptop (protected by a plastic sheet), (ii) GPS antenna, (iii) waterproof sensor housing with an EM38 inside, (iv) floating platform and (v) power tiller.

The EM38 soil sensor (Geonics Limited, Ontario, Canada) was used because of its non-invasive nature, structural simplicity, light weight and small physical dimension: all characteristics important for a floating sensor platform. Technical details and working principle of the EM38 can be found in McNeill (1980b). The sensor signal is a function of soil parameters like soil salinity, organic matter content, soil moisture content, bulk density, clay content and the amount of charge on the clay particles (Rhoades et al., 1999; Triantafilis et al., 2002). If one or more parameters are reasonably homogeneous, the influence of a more variable parameter becomes more important. For instance, for a given salinity, EC_a increases as the volumetric water content at field capacity, gravimetric water content of a saturated soil and soil bulk density increase (Rhoades et al., 1999). Such correlated soil properties can be expected to be determined from the EC_a measurements. The EM38 sensor can be operated in two orientations each having a different depth response profile. The horizontal orientation receives its major influence from the near-surface (0 - 0.3 m) soil layers while the vertical dipole orientation receives a dominant influence from the deeper (0.3 - 0.6 m) soil layers (Saey et al., 2008a).

The GPS receiver NL-422MP (the NAVILOCK®, Berlin-Zehlendorf, Germany) was used to georeference the sensor-collected EC_a information. Both the EM38 and the GPS were connected to an all-terrain grade laptop (Dell ATG 600 model), resistant against harsh environmental hazards. Separate USB 2.0 cables were used to transmit ASCII data streams to separate communication ports of the computer.

The floating platform was sufficiently lightweight to be trailed by a 12 HP vehicle operating on a muddy inundated field. First, a watertight housing was made according to the dimensions of the EM38 sensor from a cylindrical PVC (polyvinyl chloride) tube. The ends of the tube were closed with T-shaped PVC socket caps. The socket joints between the caps and the cylinder allowed opening and closing the hollow chamber whenever needed. The EM38 was placed inside the PVC cylinder and removable foam packing was used on either sides of the sensor to ensure safety against vibration. Another 1.8 m long PVC pipe was joined vertically to the sensor carrying pipe which enabled the data communication cables to be connected to the sensor. On top of this vertical pipe the GPS receiver was attached. Therefore, the position indicated by the GPS corresponds to the centre of the EM38 sensor on the ground. A custom designed wooden sled was made to carry the sensor-bearing PVC tube. One rectangular shaped wooden board (1.5 m by 0.60 m by 0.05 m) resting on top of two wooden planks was attached with 8 wooden screws to produce the platform structure. The platform can be attached to the back of a vehicle with a rope. In order to have noise free signals a distance of 1.8 m between the sensor head position and the closest metal part of the vehicle was ensured. A special type of motor vehicle called a ‘power tiller’ that is operated in wetland paddy cultivation systems was used to pull the sensor-carrying platform.

4.2.2 Software development

The computer language G from LabVIEW (National Instruments, 2003) was used to design and implement the FloSSy logger, software for EC_a and GPS data logging and processing. The software architecture was designed for real-time soil sensor and GPS communication, data acquisition, decoding of the information byte, processing and display of acquired EC_a data.

The processed data are written to a text file with headers and tab delimited values at a frequency of 4 times per second. The logged file contains the data on geographic location co-

ordinates in WGS 84 datum format along with the time-stamped EC_a values and respective serial number for each entry.

The communication port settings on both the GPS and the EM38 are configurable from the GUI of the FloSSy logger. These settings need to be adjusted at the beginning of each survey after connecting the instruments and the computer. The GUI displays the raw and the processed data from both the EM38 and GPS. The traversing path of the FloSSy was displayed on a computer screen in real time to guide the distance between measured parallel lines. For this, the laptop was secured inside a box and covered with a polyethylene jacket to guard against the splashes of field mud and raindrops. The laptop screen was visible to the vehicle driver.

4.3 Results and Discussion

The developed FloSSy was tested to measure in detail the soil EC_a of field 1 (Chapter 2.4.2) which is not easily accessible for soil sampling due to the almost permanently inundated condition. During the survey in October 2009, seasonal land preparation for the paddy crop had already been completed. This practice commonly involves puddling and incorporation of crop residues and organic matter. The water height of the field was approximately 18 - 20 cm; more than the usual height of 10 - 12 cm because of the rainy monsoon season. The horizontal orientation of the EM38 was used. This results in a depth of influence of about 0.75 m below the sensor (which includes a water layer and the saturated soil) and represents 70 % of the accumulated depth response (under the condition of soil homogeneity). The sensor is more sensitive to near surface materials when it is operated in horizontal orientation. It can be deduced from the relative response functions of the sensor that the horizontal orientation receives its major influence from up to 0.4 m depth below the sensor. Hence, makes the sensor suitable for investigating shallow soil depths.

With a traversing speed of approximately 3.6 km h^{-1} and a measurement frequency of 4 Hz, the spatial resolution obtained along each traversed line was about 0.25 m. Parallel spaced lines were separated by 1 m. With such a configuration, the FloSSy produced 56 319 EC_a measurements that ranged from 10 mS m^{-1} to 38 mS m^{-1} with a standard deviation of 3.6 mS m^{-1}. To estimate the soil EC_a at unmeasured locations in the field, OK was used as the interpolation method (Chapter 3.3.2). Hence, the spatial structure of the EC_a measurements was captured by variogram modeling (Chapter 3.3.1) and used to assign weights to the

unsampled neighbours during OK (Goovaerts, 1997). A theoretical spherical variogram model was manually fitted to the experimental EC_a variogram using the surface mapping program Surfer (Golden Software Inc., Golden, CO, U.S.A.). An EC_a map with a pixel resolution of 1 by 1 m was obtained (Fig. 4.2).

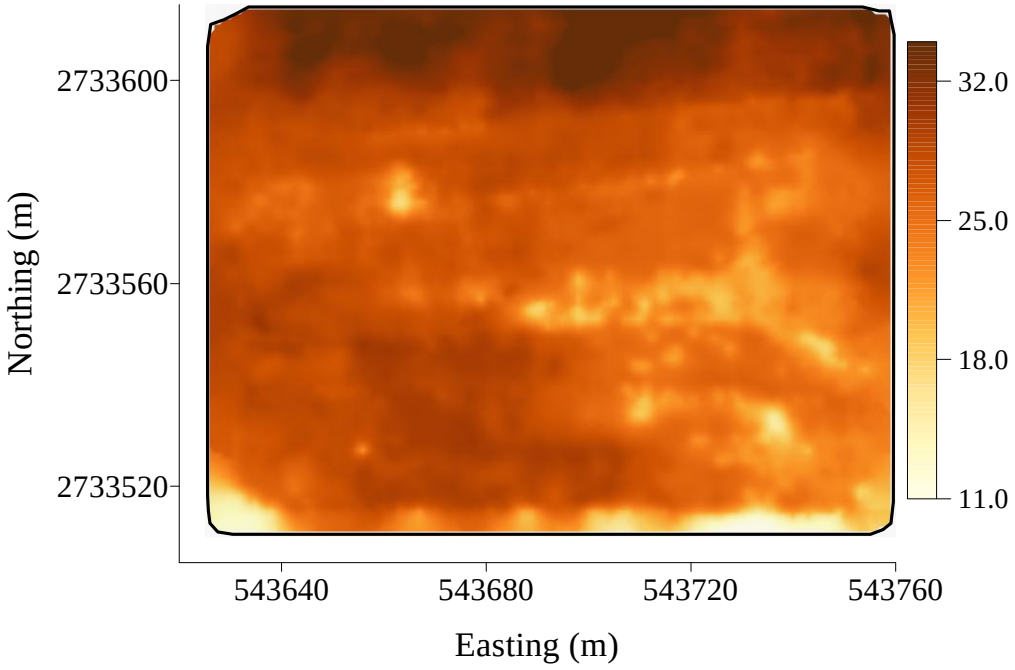

Figure 4.2 The EC_a (mS m^{-1}) of paddy field 1.

The kriged EC_a map clearly shows the spatial variation of EC_a across field 1. In paddy fields with water standing on top of the soil surface, the influence of soil moisture dynamics as a source of variation in EC_a remains homogeneous throughout the entire field which promotes the detection of soil variation with greater accuracy. This increases the reliability of EC_a to interpret the variation in soil properties. Details on this aspect of investigations is given in chapter 5.

Soil EC_a can be used to infer specific soil properties when the contributions of other soil properties affecting the EC_a measurement are known. Soil survey reported that the ploughed layer of the silty Brahmaputra floodplain soils is fairly homogenous in terms of texture and it is not saline (Brammer, 1996). In these light textured soils having low clay content, variation in EC_a of the ploughed top-soil layer could be primarily related to organic carbon (OC) variation. To verify this, 48 soil samples were collected according to a grid of 15 by 15 m between a depth of 0 to 0.15 m within the wet field and OC analysis was performed following

the conventional Walkley and Black method. Only the top (up to 0.15 m) soil was considered for sampling because the incorporation of organic matter and crop residues are usually limited to the ploughing depth (about 0.16 m). Besides this, the fibrous rooting pattern of the paddy crop is concentrated within this depth and rarely penetrates through a plough pan beneath. Another consideration was the sensitivity of the EM38 to shallow depths for the used orientation. The average OC content of the field was 21 g kg^{-1} with a coefficient of variation (CV) of 12 %. This OC variation was high considering the small size of the field receiving uniform crop management practices. The Pearson correlation coefficient was used to investigate the link between EC_a and OC. It was 0.72 which indicates a relatively strong relationship.

Soil EC_a is likely to be influenced by a number of factors as well like variation in the depth and thickness of the plough pan and the ploughed layer, textural variation of the top and subsoil layers etc. The following chapters of this thesis focus on these top soil and sub soil properties and their influence on EC_a using the different orientations of the EM38.

4.4 Conclusions

For the first time FloSSy allows to acquire and store detailed geo-referenced soil information within flooded fields. The results of the field study imply the adjustment of soil management according to the soil variability at a within-field scale for adopting precision agriculture in wet fields. By incorporating a non-invasive and non-contact proximal soil sensor information about the soil beneath the standing water was acquired. Measuring a wet field with this system has additional advantages. First, the effect of dynamic soil moisture behavior on the actual source of EC_a variation can be excluded. Hence, the soil EC_a response can be attributed primarily to the variations in soil properties other than soil moisture, like texture and organic material. Second, a water surface offers a smooth plane for the sensor carrying platform. This ensures EC_a measurements which are more stable due to the absence of irregular movements of the sensing platform as is usually caused in measuring on dry arable fields. In specific situations variability of a soil property (e.g. OC) can be detected with increased accuracy when the within-field variations in EC_a are due to a predominate influence of one soil property.

It was concluded that FloSSy is useful in collecting EC_a data to evaluate relevant soil properties, as needed to allow the within-field management for precision agriculture in flooded crop fields.

5

Comparing apparent electrical conductivity measurements on a paddy filed under flooded and drained conditions

The content of this paper was published as:

Islam, M.M., Meerschman, E., Saey, T., De Smedt, P., Van De Vijver, E. and Van Meirvenne, M., 2012. Comparing apparent electrical conductivity measurements on a paddy field under flooded and drained conditions. Precision Agriculture, 13: 384-392.

5.1 Introduction

Wetland paddy cultivation in floodplain ecosystems is one of the major agricultural land use systems in all rice growing countries. In Bangladesh, floodplain alluvial soils occupy nearly 80 % of the land area (Brammer, 1981). Every growing season, paddy fields are flooded to a water height ranging between 0.10 m and 0.25 m during land preparation and early crop development, respectively. This water is deliberately reduced by draining the fields during crop maturity and harvesting. The fields are under water for approximately eight months a year. Due to the sequence of flooding and draining, the physico-chemical behavior of these soils is different than under constant aerated soil conditions (IRRI, 1987). For practical reasons, these soils are mostly sampled under dry conditions. How representative the results are when applied to wet growing conditions is questionable. Therefore, the extent of obtaining high resolution soil information under both wet and dry conditions that can serve as a basis to guide precision paddy soil management was investigated.

Management of soil resources with the aid of proximal soil sensing has already been introduced for PA (Sudduth et al., 1997). Among the sensing techniques, the ones based on EMI are the most common (Simpson et al., 2009). Measured output of an EMI sensor translated in terms of soil EC_a can be interpreted to explain the within-field variability of soil properties (Rhoades et al., 1999; Saey et al., 2009). However, effects of dynamic soil moisture behavior can obscure the actual source of variation in the measured EC_a (Brevik et al., 2006). Therefore, Triantafilis et al. (2000) suggested conducting an EC_a survey when the field moisture content is about the field capacity level. Still, this strategy is difficult to apply in practice because of the spatial heterogeneity of moisture content across a field related to soil texture variation, micro-topography, fluctuating ground water levels, etc.

Because paddy fields are water saturated during the largest part of the year, it is possible to measure EC_a without the masking effect of moisture dynamics. For this purpose, a proximal soil sensing system able to operate on flooded fields as well as on dry fields was developed. It is worth mentioning that only non-invasive and non-contact proximal soil sensors are suitable for this purpose. Invasive soil sensors would fail to obtain acceptable results under flooded conditions and remote sensors would be incapable of acquiring information of the soil beneath the standing water.

The main objectives of this study were to (1) characterize the within-field spatial variability of a paddy field under flooded and drained conditions, (2) compare the results of both surveys, and (3) interpret the differences in terms of stable soil properties like texture.

5.2 Materials and methods

5.2.1 Study site

The study was conducted on a paddy field 1 of the Bangladesh Agricultural University in Mymensingh (chapter 2.4.2).

5.2.2 The Floating Soil Sensing System (FloSSy)

To acquire high resolution soil data on both drained and flooded fields, a mobile soil sensing system: the Floating Soil Sensing System (FloSSy) as described in chapter 4 was used (Islam et al., 2011a). In the FloSSy, the EM38 as proximal EMI soil sensor was selected primarily because of its light weight (about 3.5 kg) and small physical dimension (1.05 m by 0.16 m by 0.05 m). More technical details and operating principles of the EMI technique and the EM38 sensor can be found in chapter 3.1.

Operating the sensor in the horizontal orientation, as was the case in this study, results in a depth of influence (representing 70 % of its accumulated depth response under the condition of soil homogeneity) of about 0.75 m. Hence, with a water depth between 0.10 m and 0.25 m, sufficient influence of the near-surface soil beneath the water layer could be measured with a floating sensor.

5.2.3 EC_a survey and data processing

The EC_a survey under dry conditions (EC_a-d), i.e. without water inundation, was conducted in July 2009 immediately after the rice harvest. In order to avoid damaging the paddy stubbles a wooden support was attached on two edges beneath the sensor platform so that is was raised 0.12 m from the ground during the dry survey. One month later, EC_a was measured under wet conditions (EC_a-w) before the seasonal land preparation for planting of rice seedlings, with a water height between 0.16 and 0.18 m. The traversing speed was approximately 3.6 km h^{-1}, parallel measurement lines were 1 m apart with in-line

measurements every 0.25 m. Next, the EC_a-measurements were averaged to one value per m^2; they were post-corrected for instrumental and temperature drift according to chapter 3.1.

5.2.4 Variogram analysis and kriging

Information on the structure of the spatial variance of the EC_a measurements was obtained through variogram analysis. Omni-directional standardized variograms were computed for EC_a-d and EC_a-w. Both experimental variograms $\gamma(\mathbf{h})$ were best fitted with a spherical model (Chapter 3.3.1). Next, the EC_a data were interpolated to a regular grid with a resolution of 1 m by 1 m using OK (Goovaerts, 1997). For both variogram analysis and kriging, the mapping software Surfer (Golden Software Inc., U.S.A.) was used.

5.2.5 Soil sampling and analysis

The field was sampled twice and each time a total of 65 soil samples were collected. A random sampling scheme was used for 30 samples while the other samples were collected according to a fixed grid spacing of 7 by 5 m to ensure an even field coverage. After both EC_a surveys, three replicated soil samples were taken within 1 m^2 at each sampling location 0-0.15 m depth and pooled per location. For bulk density analysis soil samples of known volume (100 cm^3) were collected using Kopecky rings after the dry survey. Textural fraction analysis was performed following the sieve-pipette method while organic carbon (OC) was determined for samples collected after both surveys by the conventional Walkley and Black method. The oven-dry method was used for the moisture determination after the dry survey. During the wet EC_a survey, at each of these sampling locations, the water height was also measured using a graduated measuring scale.

5.3 Results and discussion

5.3.1 EC_a data

The 56 319 EC_a sensor measurements ranged from 11 mS m^{-1} to 39 mS m^{-1} for EC_a-d and from 12 mS m^{-1} to 41 mS m^{-1} for EC_a-w. Thus the mean EC_a-w (27.5 mS m^{-1}) was slightly higher than the mean EC_a-d (23.6 mS m^{-1}), which can be explained by the increased conductivity due to the water layer and the saturated soil. A standard deviation of 4.4 mS m^{-1} for EC_a-d and 3.6 mS m^{-1} for EC_a-w indicated an overall higher variability within the EC_a-d data. This difference indicated spatially variable moisture dynamics within the field under

drained conditions, whereas the moisture content can be considered to have a minimal and fairly homogeneous influence under flooded conditions.

5.3.2 Variogram analysis and kriging

Fig. 5.1 shows the standardized experimental variograms and their spherical variogram models for EC_a-d and EC_a-w.

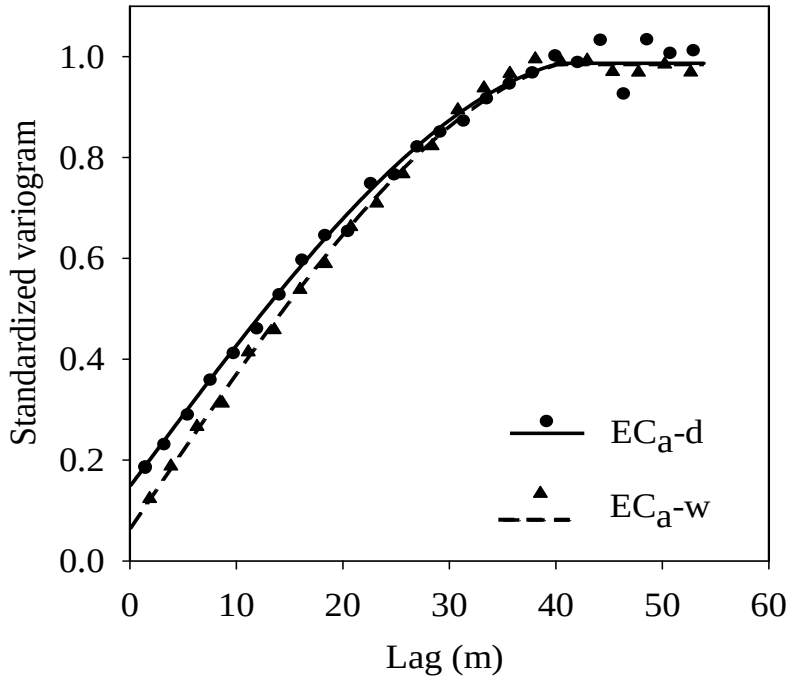

Figure 5.1 The standardized experimental variograms and their spherical variogram models (curves) for EC_a-w (triangles) and EC_a-d (dots).

As can be seen in Table 5.1, both variograms had the same range and a very similar behaviour of their structured part. However, the nugget variance was considerably higher for EC_a-d (16 %) than for EC_a-w (6 %).

Table 5.1 Parameters of the standardized spherical variogram models for EC_a-w and EC_a d; C_0 the nugget variance, C_1 the structured variance and a the range.

Variable	C_0	C_1	a (m)
EC_a-d	0.16	0.83	41
EC_a-w	0.06	0.93	41

Since the measurements were conducted by the same instrument and operator, this difference was mainly related to differences in the measurement conditions. Under dry conditions, the sensor platform was pulled over the soil surface, so the uneven micro-topography created more micro-scale variability in the measurements (e.g. less stability and more vibration of the sensing platform because of uneven soil surface) than the smooth water surface under flooded conditions. Besides this, under dry condition, the near surface material beneath the sensor platform is actually a combination of air (non-conductive) and soil (conductive). This common field condition often makes the sensor readings obtained in the horizontal orientation noisy. On the other hand, the wet field provided a perfect measurement condition and the homogeneous EC of the standing water layer might also have played a role in reducing the nugget variance.

Visual comparison of the EC_a-d and EC_a-w maps obtained by OK (Chapter 3.3.2) showed similar patterns (Fig. 5.2). The highest EC_a values were found in the north of the field while the lowest were measured in the south and south-east of the field. To assess the spatial distribution of this shift, EC_a-Δ = EC_a-w - EC_a-d of 5209 wet and dry paired measurements co-located within a radius of 0.25 m was calculated which were uniformly distributed over the field. The resulting points were interpolated with OK (Fig. 5.3). The EC_a-Δ map shows that the shift of EC_a between wet and dry conditions was not homogeneous over the field. The largest EC_a-Δ values were found in those parts where EC_a-d and EC_a-w were the lowest. These EC_a-Δ differences must not have been caused by the difference in the height of the sensor above the ground for the two surveys but indicate to have a link with soil properties causing conductivity variation. Therefore the link between EC_a and some selected soil properties were considered for investigation.

5.3.3 Relation between EC_a and soil properties

Summary statistics of measured soil properties across the 65 sampling locations are presented in Table 5.2. According to the USDA soil texture classification the average soil texture of the field is sandy loam (average sand, silt and clay contents are 54.5, 39.6 and 5.9 %, respectively). However, large variation in the coarse textural fractions (a standard deviation of 4.7 % for the sand data) indicated the non-homogeneous condition of the field.

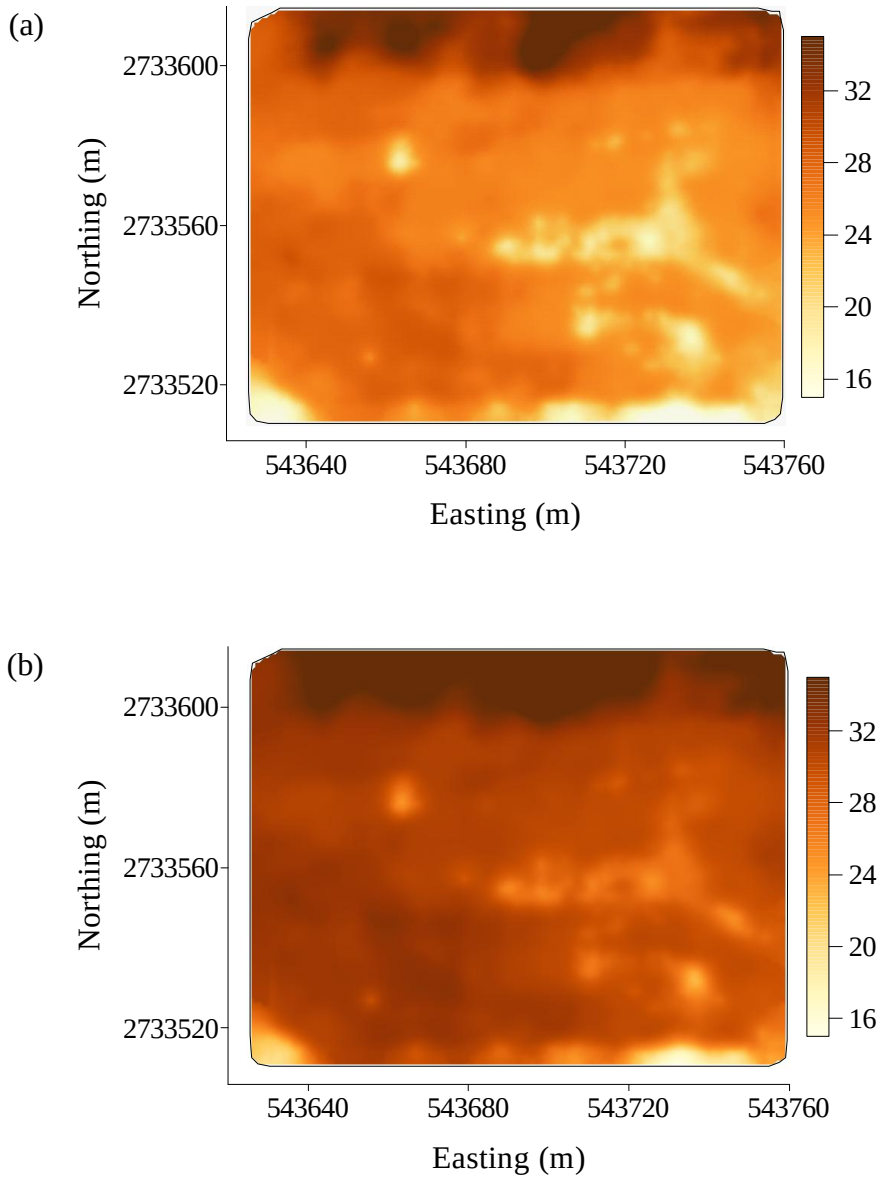

Figure 5.2 Interpolated EC_a-d (a) and EC_a-w (b) measurements (mS m^{-1}) of field 1.

Consequently, moisture content measured under dry conditions was variable. The average OC content was higher (1.7 g kg^{-1}) in wet condition than that of dry condition (1.2 g kg^{-1}) probably because of the decomposed paddy roots and stubbles. Small difference in water height (between 0.15 and 0.17 m, above the saturated soil surface) under flooded condition indicated a rather limited difference in surface elevation within this field.

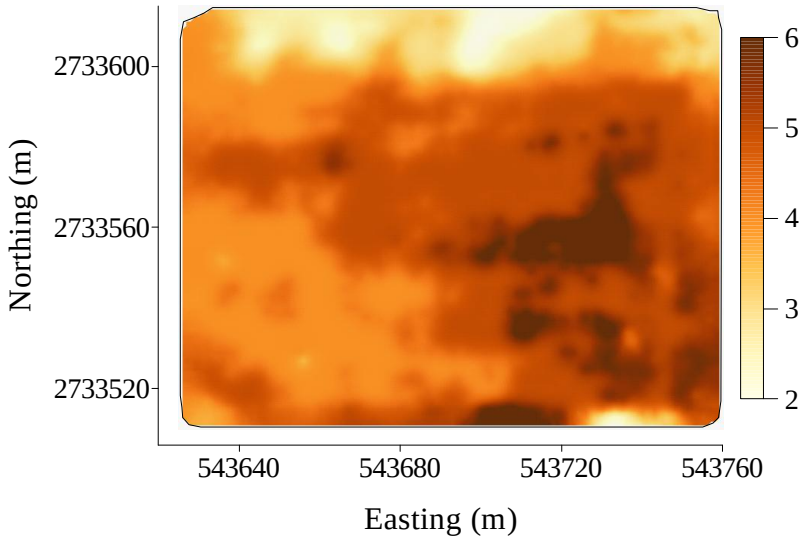

Figure 5.3 Interpolated EC_a-Δ values (mS m^{-1}) of field 1..

Table 5.2 Population parameters of EC_a, soil textural fractions and other measured soil properties; OC-d and OC-w = organic carbon in dry and wet field conditions and OC-Δ as the numerical difference, s^2 = variance; number of samples (n) = 65.

Variable	**Minimum**	**Maximum**	**Mean**	s^2
Sand (%)	43	66	54.5	22.2
Silt (%)	30	51	39.6	20.7
Clay (%)	3	9	5.9	1.2
Volumetric moisture (%)	24.9	31.9	28.7	2.2
Water height (m)	0.16	0.18	0.17	0.0
OC-d (g kg^{-1})	0.8	1.6	1.2	0.1
OC-w (g kg^{-1})	1.2	2.0	1.7	0.3

Next to soil moisture, it is well documented that soil texture (especially the clay fraction) is a key soil property influencing EC_a measurements under non-saline conditions (Rhoades et al., 1999; Saey et al., 2009). Although soil texture can be considered as a stable property which obviously would not have changed between the two surveys, the spatial distribution of EC_a-Δ can still be explained by soil texture. Fig. 5.4 shows the relation between sand and EC_a-Δ at the 65 locations where soil samples were taken.

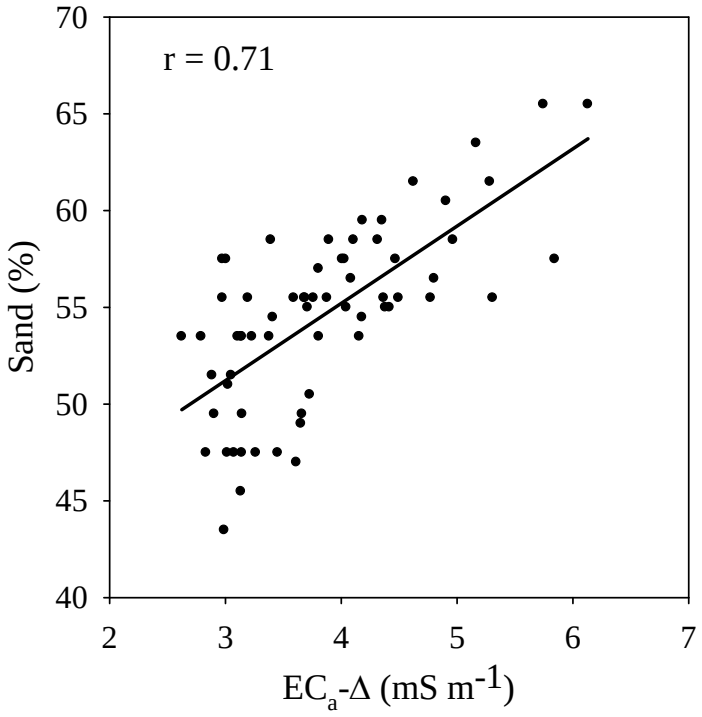

Figure 5.4 Relationship between EC_a-Δ (mS m^{-1}) and sand fraction (%) at 65 locations.

Table 5.3 Pearson correlation coefficient (r) between EC_a-d, EC_a-w, EC_a-Δ and relevant soil properties (n = 65).

Variable	Clay	Silt	Sand	Volumetric moisture	Water height	OC-w	OC-d	OC-Δ
EC_a-d	0.42	0.58	-0.64	0.37	-	-	0.26	-
EC_a-w	0.46	0.62	-0.69	-	0.34	0.36	-	-
EC_a-Δ	-0.53	-0.63	0.71	-	-	-	-	0.49

The Pearson correlation coefficient (r) between EC_a-d, EC_a-w, EC_a-Δ and the measured soil properties are shown in Table 5.3. The correlation coefficients between EC_a and soil texture were stronger than between EC_a and other soil properties. EC_a-w and soil texture had better correlation coefficients than those with EC_a-d which can be explained by the increased moisture differences in a spatial context. Actually, the range of volumetric soil moisture content within a field narrows in wet condition compared to the dried condition. This finding

strongly points to a relationship between soil texture, i.e. mainly the sand content variation, and the soil moisture dynamics. Soil organic matter did not show a strong relationship probably because of low OC content under natural undisturbed field condition. However, this relationship could be different when a paddy field undergoes a series of seasonal puddling operations (artificially disturbed) following incorporation of crop residues and organic substances. The depth of the water layer above the ground for the wet survey was not a major cause driving the changes noticed in the EC_a-Δ map because the water height difference across the field was approximately 0.02 m only.

5.4 Conclusions

Although the patterns in the EC_a maps obtained by measuring a paddy field under both drained and flooded conditions did not differ very much, measuring a paddy field under flooded conditions offers several advantages. First, the nugget variance is considerably lower (10 % in the test case). Furthermore, because variation in moisture content can be considered as negligible under flooded conditions, the soil EC_a response can be attributed more directly to variations in soil texture. Consequently, the relationships between soil textural fractions and EC_a are improved in flooded soil conditions.

Measuring EC_a under two contrasting moisture conditions provides additional information concerning the relationship between moisture dynamics and soil texture. This can support the evaluation of soil processes, such as leaching, allowing within-field management.

Finally, the accessibility of paddy fields for proximal soil sensing increases dramatically when measuring under flooded conditions becomes possible with equipment like FloSSy.

6

A floating sensing system to evaluate soil and crop variability within flooded paddy rice fields

The content of this paper was published as:

Islam, M.M., Cockx, L., Meerschman, E., De Smedt, P., Meeuws, F., Van Meirvenne, M., 2011. A floating sensing system to evaluate soil and crop variability within flooded paddy rice fields. Precision Agriculture. 12(6), 850-859.

6.1 Introduction

Floodplain alluvial soils are a valuable natural resource for agricultural crop production in countries like Bangladesh where they occupy almost 80 % of the country's area (Brammer 1996). The most frequent land use of these soils is paddy rice cultivation whereby the fields remain inundated for most of the year. As a consequence, direct methods for the acquisition of information on soil properties are problematic as well as common indirect methods, like air- or space-borne remote sensing. Therefore, these alluvial soils are usually mapped as being fairly homogenous (Alam et al., 1993) and PA, which aims at adjusting soil management according to the soil variability at a within-field scale, has not been considered. However, at present, technological advances in proximal soil sensing allow high resolution soil information to be obtained under flooded conditions which can serve as a basis to investigate the possibilities of adopting PA in paddy soils.

Several proximal soil sensors have been introduced for PA under dry land conditions (Sudduth et al., 1997). Among these, the ones based on EMI are the most commonly used, even at a sub-meter resolution (Simpson et al., 2009). EMI sensors measure the soil EC_a which can be interpreted in terms of soil properties like salinity (Triantafilis et al., 2000), texture (Saey et al., 2009), bulk density or pore volume (Rhoades et al., 1999) and depth to a clay layer (Saey et al., 2008a). Soil EC_a is also linked to the soil moisture status (Brevik et al., 2006), but the spatial variation of soil moisture is limited under water-saturated conditions because the range of moisture content decreases when a field becomes wet. Thus, in a flooded environment, variations in EC_a reflect changes in soil properties except soil moisture. EC_a data have also been used to define management classes which could be linked to variations in crop yield (e.g. Li et al., 2007; Vitharana et al., 2008). However, research relating EC_a and paddy rice yield is rare. One exception is Ezrin et al. (2010), but these authors used soil resistivity measurements (requiring soil contact) under dry land conditions. Yet, they reported a significant positive relation between EC_a and paddy rice yield. Currently, no report is available on the non-invasive use of a proximal soil sensor to analyze the within-field spatial variability of soil properties in paddy fields under flooded conditions.

The main objective of this study was to develop, operate and evaluate a mobile proximal soil sensing system capable of providing relevant information to support PA under flooded paddy field conditions, as in Bangladesh. The within-field variability of rice yield was used to evaluate the relevance of this system.

6.2 Materials and methods

6.2.1 The floating sensing system

To acquire high resolution soil data under wet field conditions (including monsoon rains), the FloSSy was used. It consists of an EMI soil sensor which was put in a waterproof housing on a raft. More details on EMI are given by Corwin et al. (2008). Preference was given to the EM38 because of its robustness, structural simplicity, light weight and small physical dimension. A more technical detail on the EM38 sensor and a description of the FloSSy are given in chapter 3.1 and chapter 4, respectively. The vertical orientation to ensure a major influence of the soil beneath the water layer (maximum 0.25 m) and the ploughed layer (about 0.16 m) was used in this study. This orientation has a relatively high sensitivity to material between 0.30 to 0.60 m depth below the sensor. However, the EM38 can also be operated in a horizontal orientation which receives its relatively major sensitivity from the near-surface soil (Saey et al., 2008b).

6.2.2 Study site

Field 2 of the Bangladesh Agricultural University in Mymensingh (chapter 2.4.2) was selected as a study area to evaluate the soil spatial variability of the field. To reduce the loss of water and dissolved nutrients, paddy fields of the area are puddled during land preparation. During puddling, the topsoil is inundated and the subsoil is compacted by repeated ploughing at the same depth (approximately at a depth of 0.16-0.20 m). An additional advantage of puddling is the effective control of weeds during the growing period.

6.2.3 EC_a survey and data processing

The EC_a survey with FloSSy was conducted in July 2009, after the usual field preparation by puddling and before the seasonal plantation of rice seedlings. At the time of measurements, the water height on the field was approximately 0.18-0.20 m. The traversing speed was approximately 3.6 km h^{-1} and the measurement frequency was 4 Hz. Measurement lines were about 1 m apart and care was taken to orient them as much as possible parallel. The measurements were averaged to one value per square meter, so the processed data resolution was 1 observation per m^2. EC_a measurements were post-corrected for instrumental

drift and standardized to a reference temperature of 25°C by the method of Sheets and Hendrickx (1995) as mentioned in chapter 3.1.

Since field measurements could not be conducted exactly on a grid basis, the soil EC_a data were interpolated to a fixed resolution using OK (Chapter 3.3.2) and the final EC_a map had a pixel resolution of 1 by 1 m.

The interpolated EC_a data were classified using the fuzzy *k*-means classification procedure (Chapter 3.4). The FPI and the MPE as described in chapter 3.4 were used to guide the classification. The optimum number of classes was determined when these two measures were minimal.

6.2.4 Soil and crop sampling

Within the field, 50 soil samples were collected according to a fixed spacing of 20 by 20 m. At each sampling location, three replicate samples were taken within 1 m^2 at three depths (0 - 0.15 m, 0.15 - 0.30 m and 0.30 - 0.45 m). Given the flooded conditions of the land, a custom-built hand-operated paddy field sampler was designed (Fig. 6.1). It contains a metal tube attached to the top of the soil-sampling core which has three holes to drain water out of the drill when the sampler is pushed into the flooded muddy soil. To avoid loss of soil during withdrawal, pneumatic pressure was maintained inside the core with a one-way gate valve attached to the top of the sampling core. During insertion of the sampler, opening of the valve allowed reduction of air pressure inside the core. A pulley controlled shutter gate was provided to open and close the bottom during insertion and removal from the soil, respectively. The oven dried (105°C) weight of the soil samples allowed calculation of its bulk density given the known volume of the sampler (0.75 L).

At each of the 50 sampling locations, the paddy grain yield was determined by harvesting manually 1 m^2. The weight of the unhusked fresh grains was measured, adjusted to a moisture content of 14 %, and expressed as t ha^{-1}.

6.3 Results and discussion

6.3.1 Electrical conductivity (EC_a)

The 30 396 EC_a measurements ranged between 22 mS m^{-1} and 49 mS m^{-1} with a mean of 34.7 mS m^{-1} and a variance of 21.4 (mS m^{-1})^2, so the coefficient of variation was 13 %. The distribution was close to Gaussian with coefficients of skewness (0.16) and kurtosis (2.8) approaching normal values (0 and 3, respectively). The variogram was best described by a spherical model (Chapter 3.3.1) with $\gamma(\mathbf{h})$ the variogram at lag distances **h**, the nugget variance C_0 = 1.2 (mS m^{-1})^2, the sill $C_0 + C_1$ = 14.3 (mS m^{-1})^2 and the range a = 38 m.

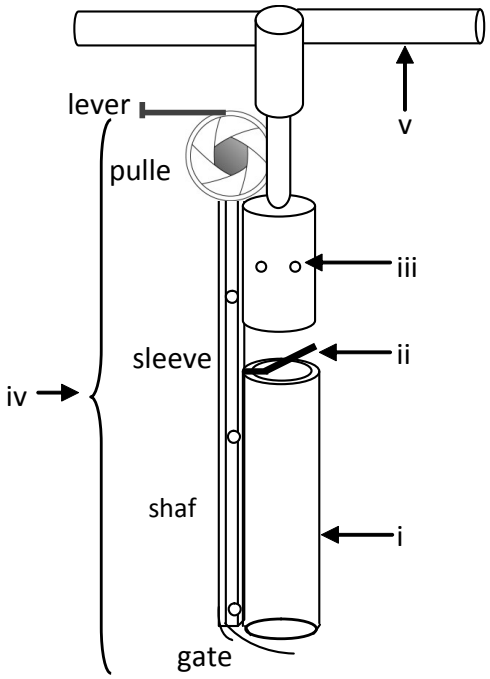

Figure 6.1 Schematic overview of the paddy field soil sampler: i. 150 mm x 80 mm soil core, ii. One-way gate valve, iii. excess water draining holes, iv. shutter with lever, pulley, sleeve, shaft and gate; v. handle rod.

Thus, the EC_a data were characterized by a strong spatial structure with a very low noise component as indicated by a nugget to sill ratio of 8.4 %. The EC_a map interpolated with OK is shown in Fig. 6.2(a). The EC_a map shows patterns of fluctuating EC_a values across the field, however, without a systematic trend. Therefore, the field was classified in zones to delineate management classes using the fuzzy *k*-means algorithm. The optimal number of EC_a classes was identified as three since the FPI and NCE were minimum at this number.

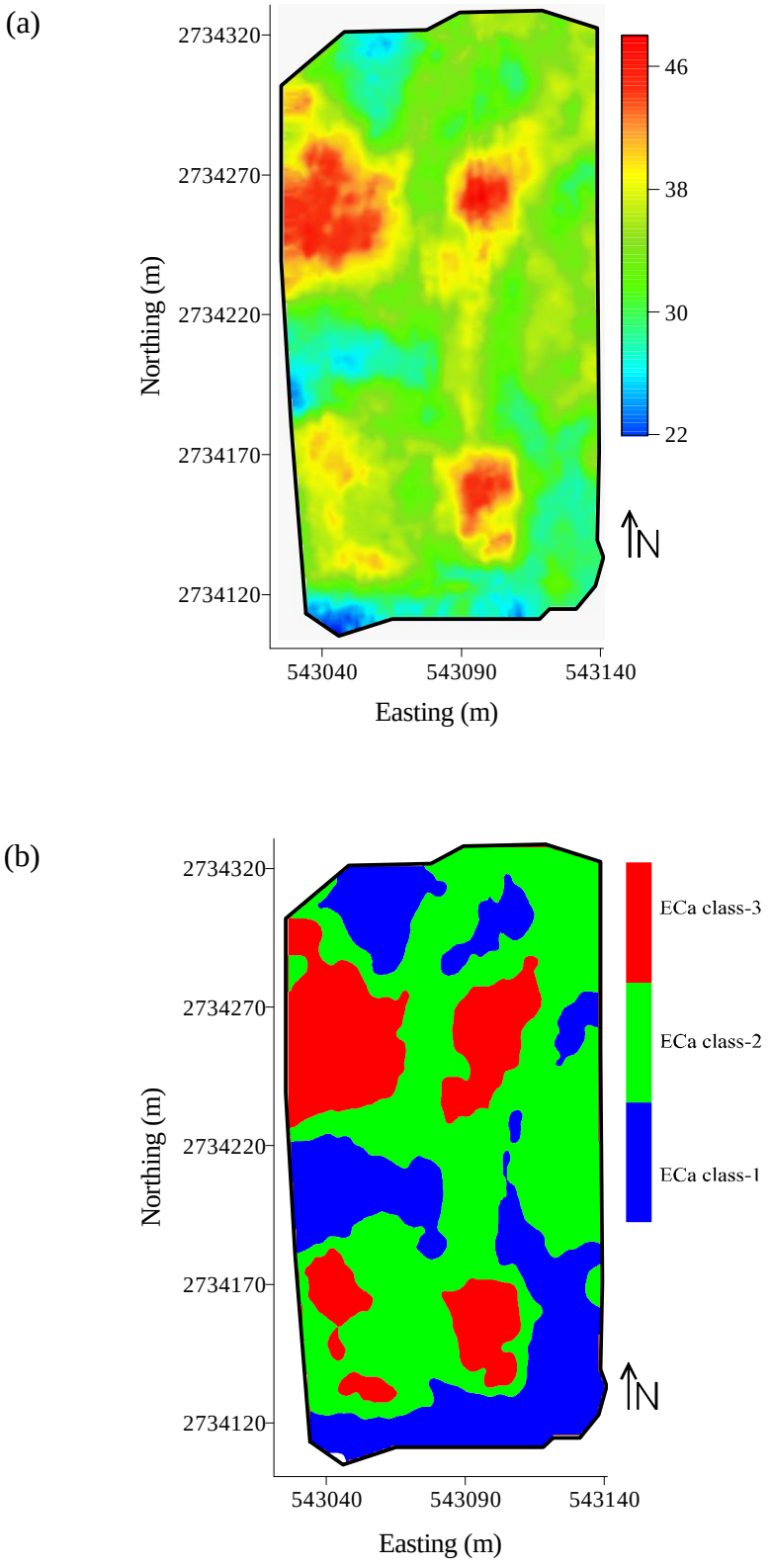

Figure 6.2 (a) The interpolated ECa (mS m-1) map of the paddy field 2 and (b) Delineated ECa classes of the field.

Fig. 6.2(b) shows a map of these three classes: EC_a class-1 grouped low EC_a values around a centroid value of 29.2 mS m^{-1}, EC_a class-2 represented intermediate EC_a values with a centroid value of 35.0 mS m^{-1} and EC_a class-3 combined the high EC_a values with a centroid value of 41.3 mS m^{-1} (areas less than 15 m^2 were merged with the surrounding class for practical reasons). These classes represented 28 %, 60 % and 12 % of the area, respectively, but only class-2 consisted of one contiguous zone. Class-1 and -3 contained several zones (map polygons) which occurred over the entire field.

6.3.2 Bulk density

To interpret the observed variation of EC_a in the flooded paddy field, it was not feasible to turn to published information. The reconnaissance soil survey reported that these floodplain soils are not saline and fairly homogenous in terms of texture and drainage class (Brammer, 1981), but no information on the detailed scale of the study is available, so this general statement should be considered with some caution. Nevertheless, as a first approximation, the alluvial parent material, soil genesis processes and general land use activities of the studied field were assumed to be fairly uniform resulting in a limited variability in clay and organic matter. Therefore, bulk density as a soil property influencing EC_a was considered (Rhoades, et al., 1999). Besides, bulk density is a key soil parameter for wetland paddy cultivation. Low bulk density of the ploughed topsoil facilitates paddy root growth whereas high bulk density of the subsoil restricts leaching of nutrients. Bulk density values are also used to indicate the degree of ploughed soil softness and subsoil compaction. In light textured soils, as is the case for the studied field, a high bulk density value indicates a well-formed plough pan.

To investigate the relationship between EC_a and bulk density, the 50 observations of bulk density at the three depth intervals were grouped according to the EC_a classes. Table 6.1 gives the summary statistics together with a statistical comparison of the mean values. For all three depth intervals, the significantly smallest mean bulk density values were found in EC_a class-1, i.e. the class with the smallest EC_a values. For EC_a classes -2 and -3 the differences were also significant for the first two depth intervals, but not for the 0.30 - 0.45 m interval. So, in general, soil bulk density followed the same trend as the EC_a values, i.e. the higher the EC_a, the higher the bulk density. However, it should be taken into account that variation in EC_a is not be only influenced by bulk density because other soil properties like texture, organic matter etc also influence EC_a variation and may complicate the identification of the

Table 6.1 Descriptive statistics and mean comparison of soil bulk density (Mg m^{-3}) among the EC_a classes; SD = standard deviation.

	Soil bulk density (Mg m^{-3})				
Soil depth (m)	**EC_a class**	**Mean***	**Minimum**	**Maximum**	**SD**
0 - 0.15	class-1	1.26[a]	1.17	1.33	0.05
	class-2	1.32[b]	1.28	1.36	0.02
	class-3	1.37[c]	1.32	1.41	0.03
0.15 - 0.30	class-1	1.44[a]	1.42	1.45	0.01
	class-2	1.63[b]	1.42	1.76	0.11
	class-3	1.76[c]	1.65	1.79	0.05
0.30 - 0.45	class-1	1.43[a]	1.42	1.44	0.01
	class-2	1.46[b]	1.43	1.53	0.04
	class-3	1.46[b]	1.37	1.51	0.04

*Within a soil depth, means followed by the same letter do not differ significantly (p = 0.05) according to Fisher's least significant difference test; number of samples per ECa class = 16, 25 and 9 for class-1, class-2 and class-3 respectively; SD = Standard deviation.

major driving variable. Although the aim of this paper was not to find a cause for this relationship, it seems to indicate that the finer the saturated soil pores are, the larger their electrical conductivity becomes.

Within each EC_a class, the soil bulk density increased from 0 - 0.15 m to 0.15 - 0.30 m and decreased in the deeper layer (0.30 - 0.45 m). Low bulk density values in the topsoil indicated topsoil softness, while the high bulk density of the 0.15 - 0.30 m layer represents compaction by puddling and the formation of a plough pan. Both topsoil softness and subsoil compaction are required for a high paddy rice yield. However, the large variation in the 0.15 - 0.30 m layer of bulk density (between 1.42 and 1.79 Mg m^{-3}) indicated that soil compaction was not uniform within this field.

6.3.3 Paddy rice yield

Table 6.2 provides the summary statistics of the rice yield data. A difference of 2.0 t ha^{-1} was found between the lowest and highest yield, which is considerable given an average yield of 4.9 t ha^{-1}. To evaluate the link between EC_a and rice productivity, the yield data were also

grouped according to the EC_a classes and the significance of the differences between the classes were analyzed statistically. The average rice yield was the lowest (4.4 t ha^{-1}) for EC_a class-1, increased significantly in class-2 (5.2 t ha^{-1}) and stabilized in class-3 (mean = 5.4 t ha^{-1}, not significantly different from the mean of class-2).

Table 6.2 Descriptive statistics and mean comparison of the paddy yield observations (t ha^{-1}) for the whole field and stratified per EC_a class; *n* = number of samples, SD = standard deviaiton.

	Yield observations (t ha^{-1})				
	n	**Mean***	**Minimum**	**Maximum**	**SD**
Whole field	50	4.9	3.6	5.6	0.5
ECa class-1	16	4.4[a]	3.5	5.0	0.4
ECa class-2	25	5.2[b]	4.6	5.6	0.2
ECa class-3	9	5.4[b]	4.7	5.5	0.3

*Means followed by the same letter do not differ significantly (p = 0.05) according to Fisher's least significant difference test; *n* = number of samples, SD = Standard deviation.

The general relationship between EC_a and rice yield was best modeled by a second order polynomial (the adjusted R^2 of a linear model was 0.68 and of a second order polynomial 0.80):

$$Yield = -8.295 + (0.672*EC_a) - (0.00821*EC_a^2) \qquad R^2 = 0.80 \qquad (6.1)$$

with yield in t ha^{-1} at a moisture content of 14 % and EC_a in mS m^{-1} at 25 °C (dashed curve in Fig. 6.3).

Since the yield statistics of EC_a class-1 were different from those of EC_a classes -2 and -3 (Table 6.2), this relationship was investigated separately within class-1 and within the grouped classes -2 and -3. For both groups of data, a linear regression was found to be a better fit than a second order polynomial on the basis of the adjusted R^2 (full curves in Fig. 6.3). For class-1 the regression was:

$$Yield = -7.437 + (0.402*EC_a) \qquad R^2 = 0.83 \qquad (6.2)$$

and for the combined class-2 and class-3 data:

$$Yield = 3.309 + (0.052*EC_a) \qquad R^2 = 0.46\ . \qquad (6.3)$$

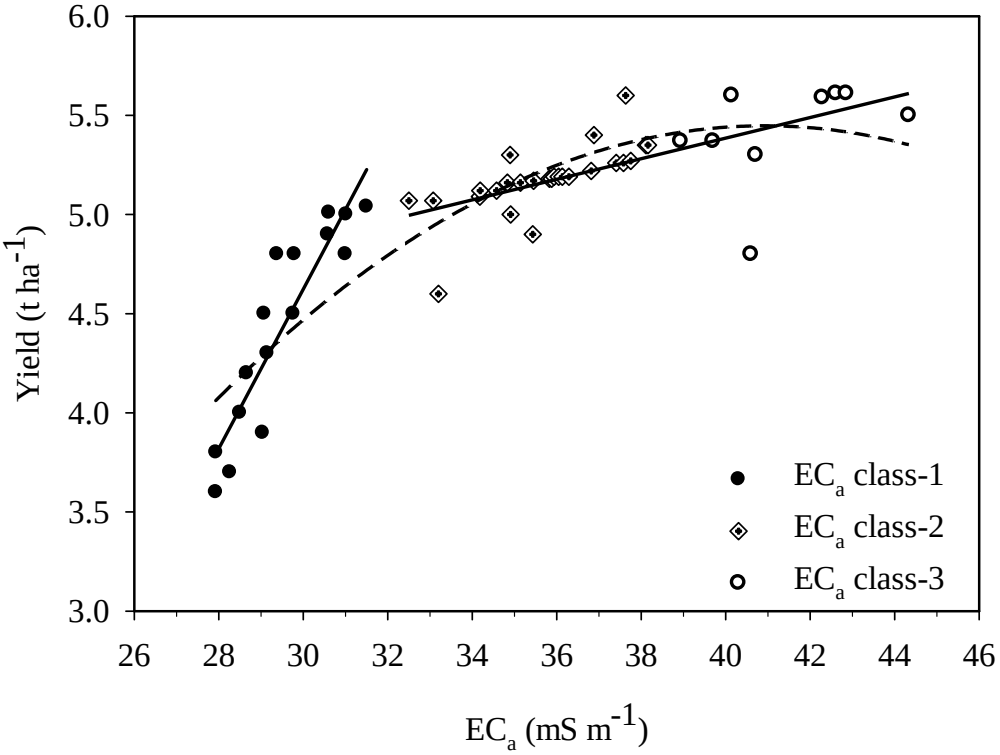

Figure 6.3 Relation between EC_a and paddy yield for field 2 as a whole (dashed curve) and per EC_a zone (full curves). One EC_a zone consisted of EC_a class-1, while the other zone grouped EC_a class-2 and-3. Points were symbolized according to the EC_a class.

The difference in slope of both regressions clearly indicate a difference in soil-yield relationship within both EC_a zones (class-1 versus class-2 and class-3). This implies that a small increase in EC_a for class-1 is likely to bring about a greater yield increase within this class compared to the same EC_a increase for class-2 and -3.

Since EC_a class-1 had both the lowest soil bulk density values within the 0.15 - 0.30 m layer and the lowest rice yield, it would be reasonable to assume that both are related. After all, under flooded conditions, a less compacted subsoil will result in an increased leaching of nutrients, although more research is needed to confirm this statement.

6.4 Conclusions

An efficient system for measuring the within-field variation of soil properties of flooded fields is a prerequisite to introduce precision agriculture in such a type of land use. EMI was chosen for this purpose and implemented in a FloSSy which was successfully used to measure in detail the soil EC_a of a field which is not easily accessible for soil sampling due to the almost permanent inundation, as in the intensively cropped paddy areas of Bangladesh. The EC_a measurements showed a clear spatial pattern of varying values. These data were optimally classified in three EC_a classes. The differences among these classes showed significant differences in soil bulk density in the first two depth intervals and were the largest in the puddled subsoil (0.15 - 0.30 m below surface). In general, the larger the EC_a, the higher the bulk density.

The first EC_a class had a significantly lower paddy rice yield compared to the yield of the other two classes with a clearly different linear relationship between EC_a and yield. This indicated a different soil-yield relationship among the delineated EC_a zones. Since the yield was the lowest in the EC_a class with lowest subsoil bulk density, it was postulated that a poorly compacted plough pan might have facilitated the leaching of nutrients reducing its crop yield potential.

It can be concluded that an EMI-based floating sensing system is useful in collecting EC_a data which can support the evaluation of relevant soil and crop properties allowing the within-field management of flooded paddy rice fields.

7

Delineating water management zones in a paddy rice field using a floating soil sensing system

The content of this paper was published as:

Islam, M.M., Saey, T., Meerschman, E., De Smedt, P., Meeuws, F., Van De Vijver, E. and Van Meirvenne, M., 2011. Delineating water management zones in a paddy rice field using a floating soil sensing system. Agricultural Water Management, 102, 8-12.

7.1 Introduction

The most frequent cultivation system of rice is paddy rice where the fields remain flooded for most of the cropping season. Maintenance of standing water at a recommended depth is crucial to ensure sufficient water availability to the crop. Water losses from a flooded paddy field on a plain landscape like in Bangladesh occur either by evapotranspiration (ET) or by percolation below the rooting zone. Since ET is directly linked to crop production, the most efficient reduction of water loss and dissolved nutrients in paddy fields is to reduce the downward flux (Bouman and Tuong, 2001). Therefore, these fields are typically puddled during land preparation. While the soil is kept saturated, it is ploughed repeatedly to reduce porosity. An extra advantage of puddling is the effective control of weed growth as standing water in the paddy rice fields strongly reduces weed emergence (Yoshida, 1983). However, preventing water losses by drainage from paddy fields remains a challenge for the rice growers. The problem persists as the formation of a homogenously puddled and relatively impermeable layer with an underlying continuous plough pan is complicated by the spatial variability of soil properties, in particular soil texture. A sandy zone within a generally clayey field might create locally less impermeable conditions resulting in unexpectedly large water losses affecting the entire field. If lost water is not refilled, dry zones form inside the field where weeds start to flourish immediately, competing for nutrients. These surface expressions become evident only after the land preparation when paddy rice has already been planted. As a consequence, direct methods for the acquisition of detailed information on soil-water properties before land preparation would be welcome. Therefore PA which aims at adjusting soil management according to the within field soil variability, needs to be considered. Recent technological advances in proximal soil sensing allow the acquisition of high resolution soil information under flooded conditions that can be interpreted to detect the within field variability and serve as a basis for precision soil-water management.

Soil EC_a measured with an EMI based proximal soil sensor can be interpreted to explain variation in soil properties (Sudduth et al., 1997), like texture (Saey et al., 2009), salinity, bulk density or pore volume (Rhoades et al., 1999) and depth to a clay layer (Saey et al., 2008a). However, often the influence of dynamic moisture variation on the measured EC_a (Brevik et al., 2006) obscures the actual source of variation and complicates the detection of soil variation. This masking effect of moisture is eliminated in a flooded environment where variations in EC_a directly reflect changes in soil properties other than soil moisture (Islam et

al., 2011c). For paddy fields, the traditionally used dry EC_a survey is also not practical because the surveyor has to wait until the fields are drained. To overcome these limitations, a proximal soil sensing system suited to operate on flooded fields was designed.

The main objective was to assess the applicability of the sensing system to delineate zones related to water percolation losses at a within field scale. Hence, the characterization of a paddy field under wet and drained conditions and the comparison of both surveys were followed by interpretation of the differences in terms of soil texture and water percolation.

7.2 Materials and methods

7.2.1 Study site

Field 1 of the Bangladesh Agricultural University in Mymensingh was selected to conduct the study (chapter 2.4.2). Rice varieties suitable for non-saline soil conditions are used on these soils and the field has a wet paddy cultivation history of more than three decades. Puddling of wet soil is the usual practice of land preparation before crop planting.

7.2.2 The soil sensing system

To acquire high resolution soil data on both dry (drained) and flooded field conditions, we used the FloSSy (Islam et al., 2011a). More technical details and operating principles of the EMI technique can be found in chapter 3.1 and an elaborated description of the FloSSy is given in Chapter 4. The EM38 sensor was used in the vertical orientation. Hence, with a standing water depth of 0.10 m to 0.25 m, influence of the shallow soil material beneath the water layer could be measured.

7.2.3 EC_a survey and data processing

The EC_a survey under dry conditions (EC_a-d) was conducted in July 2009 immediately after the rice harvest. The sensing platform was at 0.12 m above the soil surface to ensure minimal damage to the rice stubbles (commonly used for soil organic matter during land preparation for the next crop). One and a half month later, before the seasonal land preparation for the planting of rice seedlings, EC_a was measured again under flooded conditions (EC_a-w) with 0.10 to 0.12 m water standing on the soil surface. Thus the distance above the soil surface was similar in both surveys. Measurements were taken along parallel

lines 1 m apart. With a ground speed of approx. 3.6 km h^{-1}, the logging frequency of the system was 4 Hz. Soil temperature was recorded every hour using a bimetal soil temperature sensor pushed into the ground at a depth of 0.25 m below the surface. During both surveys, the soil temperature remained stable at 30°C. The obtained EC_a measurements were averaged to one value per m² and post-corrected for instrumental drift and soil temperature changes according to the method described in Chapter 3.

7.2.4 Variogram analysis and kriging

The structure of the spatial variance of the EC_a measurements was examined through variogram analysis. Omni-directional standardized variograms were computed for EC_a-d and EC_a-w. Both experimental variograms $\gamma(\mathbf{h})$ were best fit with a spherical model (Chapter 3.3.1). Afterwards the EC_a data were interpolated to a regular grid with 1 m by 1 m resolution using OK (Goovaerts, 1997) as described in chapter 3.3.2. The interpolated EC_a-w values were classified into groups using a fuzzy *k*-means classification procedure of chapter 3.4 and the optimum number of classes was chosen where FPI and MPE were minimal.

7.2.5 Water percolation measurement and soil texture analysis

After land preparation and EC_a-w measurements, the soil was characterized at 65 locations: 30 locations were selected according to a grid to ensure equal coverage and the rest were randomly located.

At every location, the steady state infiltration (final infiltration rate) was measured three times within 1 m^2 with a double ring infiltrometer (0.30 m inner ring diameter and 0.45 m outer ring) by measuring the decrease in water level in the inner ring as a function of time. The insertion depth of the rings was about 0.16 m (depth of the soft ploughed layer), the field was flooded and the water level outside and inside the rings was similar. The final infiltration rate would actually refer to the flux percolation rate (which indeed equals the hydraulic conductivity). Measurements continued for two days to check the hydraulic gradient which became unity (dH = 1). Under water saturated paddy field conditions, these measurements indicate the spatial variability of permeability of the least conductive layer, the plough pan (Moormann and van Breemen, 1978).

After the percolation measurements soil samples were taken at the same locations at a 0 - 0.30 m depth interval and the three replications obtained within each 1 m^2 were mixed. The three major textural fractions (clay: 0 - 2 μm, silt: 2 - 50 μm and sand: 50 - 2000 μm) were analyzed following the conventional sieve-pipette method.

7.3 Results and discussion

7.3.1 EC_a-data

Table 7.1 shows the population statistics of the EC_a measurements for both surveys. The mean EC_a-w (39.4 mS m^{-1}) was higher than that of EC_a-d (35.7 mS m^{-1}), which can be explained by the general increase in conductivity due to the water saturated conditions.

Table 7.1 Population parameters of EC_a, soil textural fractions and water percolation; *n* = number of samples, s^2 = variance.

Variable	*n*	Minimum	Maximum	Mean	s^2
EC_a-d (mS m^{-1})	14 125	27	43	35.7	19.1
EC_a-w (mS m^{-1})	14 125	36	44	39.4	9.4
Sand (%)	65	12	65	43	24.2
Silt (%)	65	30	69	47	12.8
Clay (%)	65	4	20	11	5.7
Percolation rate (mm day^{-1})	65	15	33	23	15.0

Also a clear decrease in the variance was observed: 19.1 (mS m^{-1})^2 for EC_a-d and 9.4 (mS m^{-1})^2 for EC_a-w, indicating a twice as large variability within the EC_a-d data. So inundating the field resulted in less variable EC_a measurements with a larger signal-noise ratio. This clearly indicates the added value of mobile EC_a measurements in water saturated fields.

7.3.2 Variogram analysis and kriging

Fig. 7.1 shows the standardized experimental variograms and the fitted spherical models for EC_a-d and EC_a-w and Table 7.2 gives the parameters of fitted models. It can be observed that both variograms display a very similar behaviour in their structured part: the same model with almost identical ranges. However, the nugget variance was considerably higher for

EC_a-d (32 %) than for EC_a-w (10 %), expressing more micro-variability or noise. Since the measurements were conducted with the same sensing system, this difference should be related to differences in the measurement conditions.

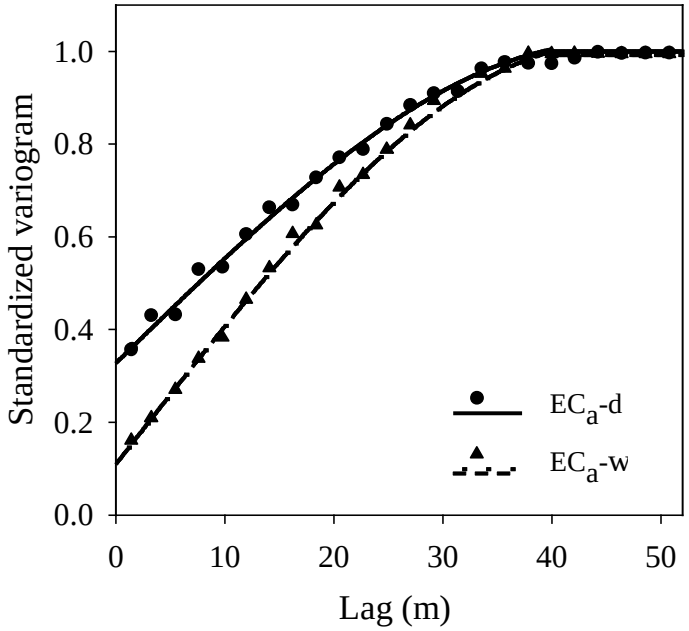

Figure 7.1 Standardized experimental variograms (dots and triangles) and their spherical models (curves) of the EC_a-d and EC_a-w data.

Under dry conditions, the sensor platform was pulled over an uneven land surface with soil clods and crop stubbles, while under flooded condition the floating device experienced almost no shaking. Furthermore, the homogenous EC_a of the standing water layer under the flooded conditions might have contributed also in reducing the measurement variability and the nugget variance.

Table 7.2 Parameters of the standardized spherical variogram models for EC_a-d and EC_a-w.; c_1 the structured variance, c_0 the nugget variance, a the range.

Variable	C_0	C_1	a **(m)**
EC_a-d	0.32	0.68	41
EC_a-w	0.10	0.90	42

The interpolated maps of EC_a-d and EC_a-w showed similar patterns (Fig. 7.2, (a) & (b)). The highest EC_a values were located in the north of the field while the lowest were found near the south-east and south-west corners. In general, both maps show patterns of fluctuating EC_a values with a similar trend.

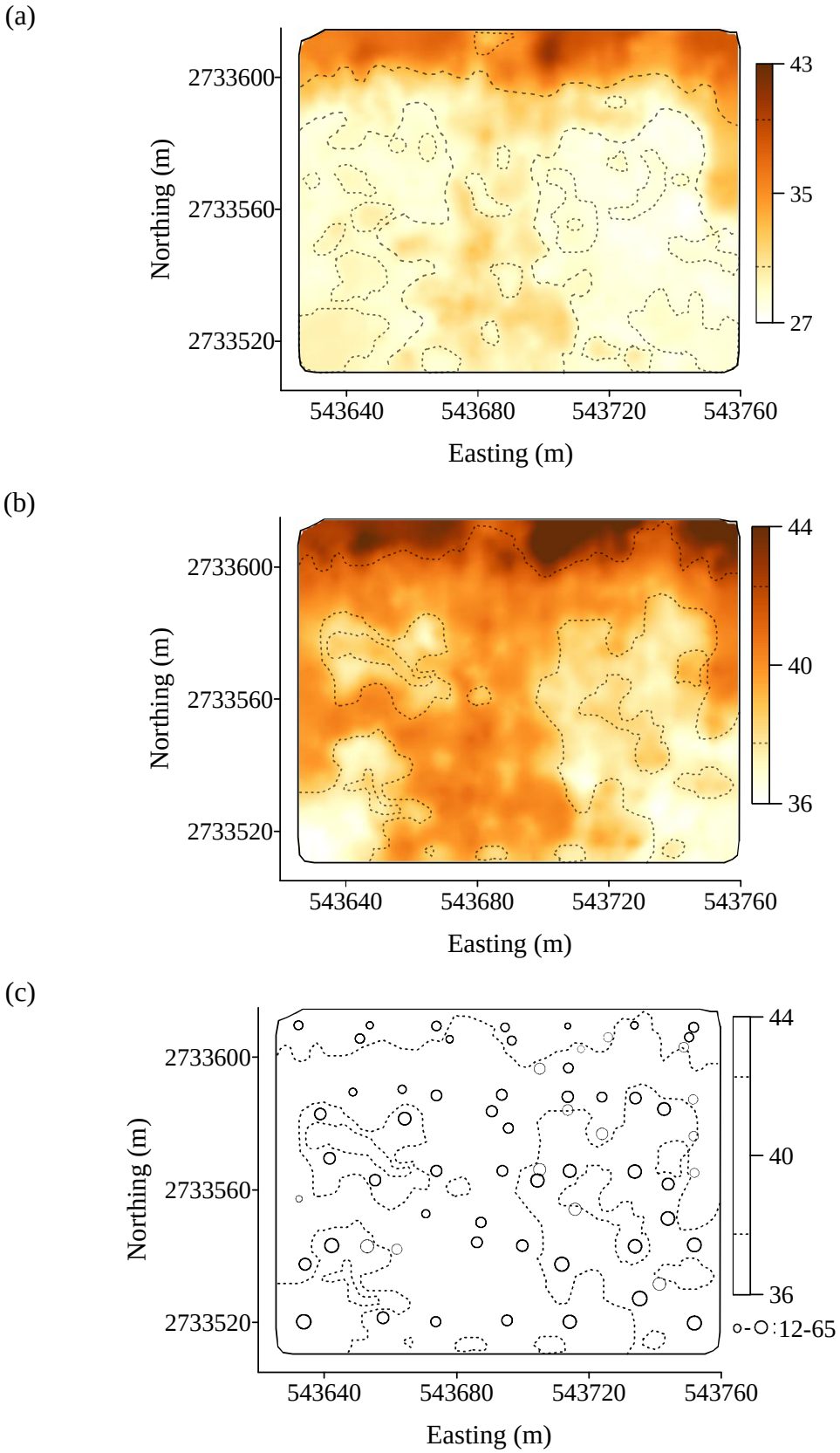

Figure 7.2 The interpolated (a) EC_a-d (mS m^{-1}), (b) EC_a-w (mS m^{-1}) maps of paddy field 1; the dashed lines indicate the upper and lower quartiles of EC_a data and (c) sand content (%) at the 65 locations, expressed as proportionate circles and plotted with the EC_a-w quartile lines.

7.3.3 EC_a and soil texture

Besides soil moisture, soil texture and organic matter (OM) play key roles in influencing EC_a measurements under non-saline conditions (Rhoades et al., 1999; Saey et al., 2009). Considering the shallow plough layer (approx 0.15 m) of the paddy field and fibrous root growth pattern of paddy plants, soil beneath the ploughed layer is assumed to be poor in OM (Alam et al., 1993). Given that texture is a stable soil property, the spatial distribution of EC_a of both surveys was explained by the spatial variation of soil texture. Table 7.1 provides the statistics of the textural analysis of the 65 soil samples. On average the topsoil has a loamy texture, but there is some variation and two more textural classes were encountered: sandy loam and silt loam (Fig. 7.3).

Table 7.3 gives the correlation coefficients (*r*) between the soil textural fractions of the top 0.30 m and the EC_a measured under dry and flooded conditions of the 65 soil samples. The largest absolute *r* was found for the sand fraction, although the silt fraction showed a similar value.

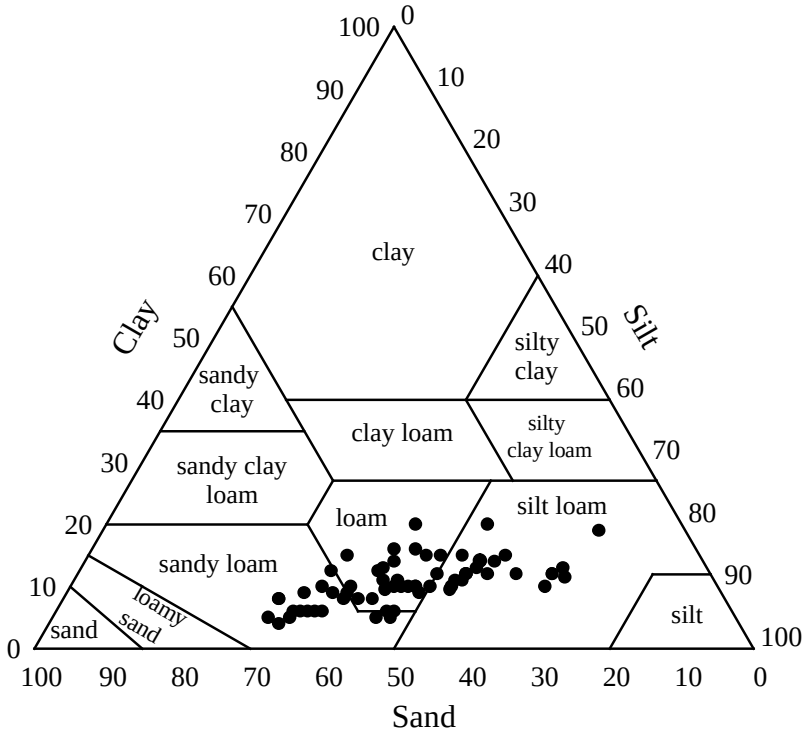

Figure 7.3 Soil texture analysis of 65 locations plotted on the USDA soil texture triangle.

The correlation coefficients between all soil textural fractions and EC_a-w were stronger than with EC_a-d, which can be explained by the increased moisture variability under drained conditions. The moisture content variation remains rather limited in fine textured locations compared to coarse textured locations when the soil becomes wet. Fig. 7.3(c) shows a plot of the sand fraction projected on two contour lines of the EC_a-w map [Fig. 7.3(b)]. The general relationship is clear: more sand was found where the EC_a-w is the smallest. So, the relationship between soil texture and EC_a was observed more accurately under flooded conditions because of the more homogeneous moisture conditions and the increased stability of the sensing platform.

Table 7.3 Pearson correlation coefficient (r) between EC_a-d and EC_a-w, and the textural fractions (n = 65).

Variable	Clay	Silt	Sand
EC_a-d	0.55	0.81	-0.83
EC_a-w	0.56	0.84	-0.86

Considering the stronger relation between EC_a-w measurements and soil texture, the EC_a-w data were classified to delineate EC_a classes using the fuzzy *k*-means algorithm. During classification, both FPI and MPE decreased until an optimum combination was found which was identified as two. Fig. 7.4 shows these two classes.

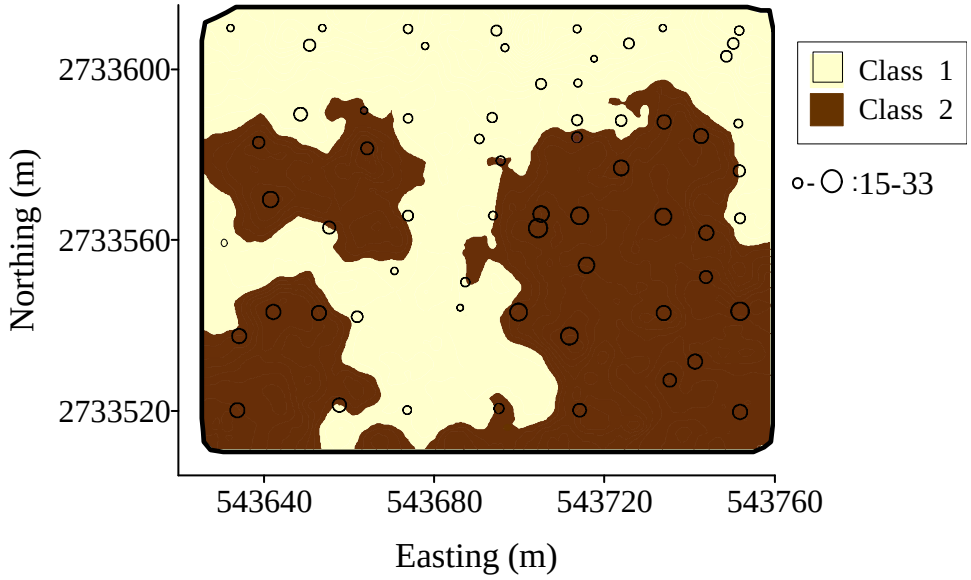

Figure 7.4 Map of the EC_a classes obtained by fuzzy *k*-means classification; percolation rates (mm day^{-1}) at the 65 locations are expressed as proportionate circles.

In Fig. 7.4 class-1 grouped high EC_a values with a centroid value of 42.1 mS m^{-1} and class-2 the low EC_a values with a centroid value of 38.3 mS m^{-1} (areas less than 10 m^2 were merged with the surrounding class for practical reasons). These delineated EC_a classes were considered as different entity having significance for soil-water percolation behaviour of the field.

7.3.4 Water percolation

The statistics of the 65 percolation measurements are given in Table 7.1. The mean percolation rate was 23 mm day^{-1}, which is very low. Yet at some locations a value of 15 mm day^{-1} was found where at another it increased to 33 mm day^{-1}. Vertical movement of water depends on several soil properties among which variation in soil texture and soil compaction are important for paddy field conditions. Under natural conditions (after crop harvest) when the field has not been subjected to land preparation yet, soil texture can be more important than compaction. In a sandy loam soil in northern India, one year after paddy cultivation, percolation rate was found to be 20 mm day^{-1} (Prihar, 1975). In a more recent study Kukal and Aggarwal (2003) found a percolation rate of 30.1 mm day^{-1} in a sandy loam paddy field which declined to 13.1 mm day^{-1} after a moderated puddling practice. To investigate the link between water percolation and EC_a, the 65 observations of the percolation rate were grouped according to the EC_a classes. Table 7.4 gives the summary statistics together with a statistical comparison of the mean values of these classes.

A significantly lower mean percolation rate was found in EC_a class-1, i.e. the class with the higher EC_a values, while the percolation rate was significantly higher for EC_a class-2, having lower EC_a values. So in general, water percolation rate followed the opposite trend of the EC_a values, i.e. the lower the EC_a, the higher the percolation. This is also illustrated by the percolation values plotted in Fig. 7.4. Since EC_a class-2 had the larger water percolation values and higher sand fraction than class-1, it can be reasonably assumed that both are related. The significant difference of the other two soil textural fractions between the two classes also indicates this relationship. Higher fine textural fractions (silt and clay) in class-1 significantly reduced water percolation and vice-versa. However, a linear relationship between ECa and permeability or ECa and soil textural fractions was not considered for investigation in this study because the focus was on the development of a methodology. Therefore, future studies are suggested to have a focus on this aspect.

Table 7.4 Statistical parameters of the EC_a classes; *n* = number of samples per EC_a class, SD = standard deviation.

Variable	EC_a class	*n*	Mean*	SD
EC_a-w (mS m^{-1})	class-1	7769	41.9	2.1
	class-2	6356	37.7	2.7
Percolation rate (mm day^{-1})	class-1	37	19	2.1
	class-2	28	27	2.7
Sand (%)	class-1	37	34	4.8
	class-2	28	54	5.3
Silt (%)	class-1	37	53	3.8
	class-2	28	38	3.1
Clay (%)	class-1	37	13	1.7
	class-2	28	8	1.3

* Means of classes are significantly different (P = 0.05) according to Fisher's least significant difference test.

7.4 Conclusions

We used successfully an EMI based floating sensing system to measure in detail the soil EC_a variation beneath the standing water of a flooded paddy field. Although both dry and flooded surveys showed a similar spatial structure of the EC_a values, the EC_a-w measurements were less variable with a larger signal-noise ratio because the sensing platform could be operated in a more stable way and the uniform moisture status of the field reduced the effect of moisture variability on EC_a measurements. As a result, the EC_a response from the flooded field condition was stronger correlated to the soil texture fractions (mainly with the sand fraction). The EC_a-w survey values were grouped into two EC_a classes with a significant difference in water percolation: class-1 with higher EC_a values had a significantly lower average water percolation rate than class-2. The delineated zones can be considered as separate units for soil-water management, hence allowing optimization of water resources during land preparation and irrigation. As such, after paddy planting, construction of bunds could be considered to separate the zones by their boundaries to practice a variable irrigation scheduling for the delineated zones.

It can be concluded that an EMI-based floating sensing system is useful in delineating within-filed zones to support the evaluation of soil-water relationship. This can have further significance in floodplains and wet-land agriculture systems where zone based crop irrigation-drainage regimes can be introduced to promote optimization of benefits from site specific soil-water management practices.

8

Identifying compaction variability in a puddled paddy rice field using a non-invasive proximal soil sensing system

The content of this paper has been submitted as:

Islam, M.M., Meerschman, E., Saey, T., De Smedt, P., Van De Vijver, E. and Van Meirvenne, M. Identifying compaction variability in a puddled paddy rice field using a non-invasive proximal soil sensing system. *Submitted to*-Computers and Electronics in Agriculture.

8.1 Introduction

The specialized land preparation practice of puddling requires the paddy rice farmers to work the soil above water saturation. Puddling helps to control weeds, to ease the transplantation of rice seedlings and to maintain a uniform water depth over the field (Mohanty et al., 2004). Effects of puddling include the decrease in total porosity and a marked redistribution of soil pores as a result of rearrangement of soil particles (De Datta, 1981; Gajri, et al., 1999). Most macropores transmitting water are eliminated and the remaining macropores are partially or completely filled by dispersed finer soil particles (Kukal and Aggarwal, 2003). This results in a drastic reduction in water and nutrient losses caused by deep percolation below the rooting zone (McDonald et al., 2006). Limiting percolation losses and maintaining a flooded condition is crucial to wet paddy cultivation (Kukal and Sidhu, 2004). Standing water in paddy fields not only inhibits further weed infestation during crop development but also increases crop-water availability in periods of limited rainfall. Water availability to the plants increases as percolation rate decreases due to reduction in hydraulic conductivity of the puddled soil layer (Sharma and De Datta, 1985). Thus, puddling remains as a unique method of land preparation for irrigated and lowland paddy rice cultivation.

During land preparation the puddled layer gradually becomes stratified into a standing water layer and a loose water saturated soil layer. Beneath these two, a relatively impermeable dense soil layer known as the plough pan is formed. The formation of a paddy field plough pan requires subsoil compaction which involves repeated ploughing at the same depth using typical paddy field cultivators (De Datta, 1981). A paddy field is optimally puddled when the saturated loose soil layer provides a better physical condition for plant root growth, while the plough pan beneath is compacted enough to restrict water and nutrient losses beyond the rooting depth. However, the degree of compaction of the plough pan is mainly influenced by puddling (De Datta, 1981). A poorly compacted plough pan makes a paddy field prone to nutrient losses through leaching and water losses through percolation. On the other hand, too many puddlings may incur unnecessary waste of water and energy inputs and can have severe consequences in water scarce regions.

In the absence of specific guidance, the intensity of a puddling operation by the paddy farmer usually depends on the availability of water resources (Playán et al., 2008). Despite being capital and energy intensive, paddy farmers commonly opt for high intensity puddling

to attain a presumably homogeneous and sufficiently compacted plough pan. This happens because the detection of compaction during a puddling practice is not readily available. First, flooded conditions make the paddy fields inaccessible for direct observations (Islam et al. 2012) and second, difficult for indirect measurements (Hemmat and Adamchuk, 2008). Furthermore, the standing water layer on top of the saturated soil layer obscures the extraction of soil information using technologies like remote sensing systems (Islam et al., 2011c). However, obtaining information on soil compaction during puddling is required to guide the farmers. For this, acquisition of detailed and geo-referenced soil information, aiming at the adjustment of puddling induced soil compaction needs to be considered. In this regard, obtaining high resolution soil information using proximal sensing systems can serve as a basis for identifying compaction variation and managing soil resources.

Proximal soil sensing using an EMI based sensor provides the opportunity to measure the soil EC_a information while avoiding direct physical contact with the measured soil. In case of non-saline soils, interpretation of the EC_a measurements explains the underlying variation in soil physical properties (Sudduth et al., 1997) such as texture (Saey et al., 2009) and compaction (Brevik and Fenton, 2004); moisture (Brevik et al., 2006), bulk density or pore volume (Rhoades et al., 1999) and depth to clay layer (Saey et al., 2008a). Thus, mobile EC_a surveys complemented with a GPS allow spatial monitoring of soil properties which are relevant for crop growth. Because the traditionally used EC_a surveying systems used in unsaturated field conditions are not applicable as such in flooded paddy fields, a proximal floating soil sensing system suited to operate on flooded fields was designed (Islam and Van Meirvenne, 2011). The system offers the advantage of strongly reducing the effect of moisture differences on the EMI signal (Islam et al., 2012). Therefore, the EC_a measurements under flooded condition offer the possibility of reflecting the dynamic soil physical changes during puddling.

The purpose of this paper is to assess the applicability of a proximal sensing system to detect the compaction variability at a field scale. The objective is three-fold: (1) characterization of puddling induced soil compaction in terms of soil attributes, (2) spatial characterization of differentially compacted areas using high resolution soil EC_a measurements and (3) evaluating these areas in terms of water percolation and paddy yield.

8.2 Materials and methods

8.2.1 Study site

Field 3 (chapter 2.4.2) located at the Bangladesh Agricultural University, Mymensingh in Bangladesh was selected for the three years study (2009-2011). The field lies about 8 m above sea level. It has a traditional paddy cultivation history of more than 45 years, including puddling of soil as a land preparation practice before crop planting.

8.2.2 Compaction experiments

The experimental strategy contained different stages. First, the field was brought to an evenly tilled condition. Next, soil compaction development was introduced through gradually increasing the intensity of puddling. Therefore, three experiments were carried out. Fig. 8.1 shows a schematic layout of the field for the three experiments.

Experiment-1 (Exp-1) was initiated in October 2009 and the same treatments were applied on the entire field. First, a dry deep tillage with a 35 HP tractor operated disc plough was used to remove previous tillage influences and to reach an equally tilled condition. Second, harrowing once with a tine cultivator was followed by flooding the entire field (flood irrigation) to a height of 0.11 m (approx.). No puddling (P0) was done before paddy planting.

Experiment-2 (Exp-2) was conducted in September 2010 for which the field was first harrowed twice at weekly intervals. Then it was flooded to approx. 0.11 m water height and made ready for puddling, using repeated passes of a 12 HP power tiller. A power tiller is a semiautomatic manually operated vehicle equipped with L-shaped tilling blades and cage wheels to conduct puddling operation in wet paddy fields. The paddy field was marked into three areas to receive three puddling intensity treatments. Thus, starting from the west and moving towards the east, three consecutive areas of approx. 90 m × 50 m each were fixed. The three puddling intensities applied were one puddling (P1), two puddling (P2) and three puddling (P3) for the three areas, respectively.

Experiment-3 (Exp-3) started in October 2010 and three puddling intensities were applied for the same three areas of Exp-2 having approx. 0.11 m water height. The puddling intensity treatments were two (P2), four (P4) and six (P6), respectively. So, the puddling intensities of Exp-2 were doubled in Exp-3.

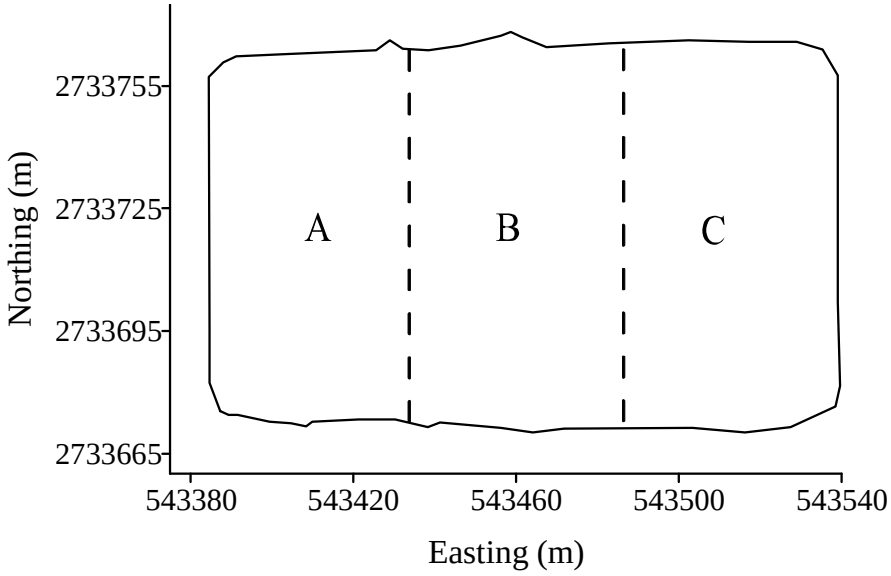

Figure 8.1 Experimental layout of field 3 in three areas indicated as A, B and C. Exp-1 consisted of the P0 (no puddling) treatment in all three areas; Exp-2 consisted of P1 (one puddling), P2 (two puddlings) and P3 (three puddlings) in A, B and C, respectively; Exp-3 consisted of P2 (two puddlings), P4 (four puddlings) and P6 (six puddlings) in A, B and C, respectively; dashed lines indicate treatment boundaries.

8.2.3 Soil sampling and analysis

In September 2009, soil samples were collected at three depth intervals of 0 - 0.15, 0.15 - 0.30 and 0.30 - 0.45 m. Within 1 m^2 at each location, three replicated soil samples were taken and pooled.

After draining the field was sampled again in April 2011 when the soil moisture content was about field capacity. To ensure equal field coverage, 54 locations were identified according to a regular grid of 16 m × 15 m. Three replicates of undisturbed soil samples were collected within 1 m^2 of every location for three depth intervals: 0 - 0.15, 0.15 - 0.30 and 0.30 - 0.45 m. The known volume of the sampling core (0.75 L) and the oven dried (105°C) weight of the soil samples were used to calculate the average soil bulk density at each location. Next, the replicated soil samples were pooled and the three major textural fractions (clay: 0 - 2 μm, silt: 2 - 50 μm and sand: 50 - 2000 μm) were analysed using the conventional sieve-pipette method, while organic carbon (OC) was determined by the Walkley and Black method.

Within 1 m^2 of the 54 sampling locations, soil penetration resistance (PR) was measured by a SC900 soil compaction meter (Spectrum Technologies Inc., Illinois, USA). The meter

has a 30° conical probe with 12.82 mm diameter ASAE standard small tip and takes compaction readings to a depth of 0.45 m at 0.025 m increments using an ultrasonic depth sensor. Penetration resistance was measured by an internal load cell and recorded in a data logger in kPa. At each location three replicated readings were taken and averaged.

8.2.4 The soil sensing system

To acquire high resolution soil data on flooded paddy field conditions, the mobile soil sensing system called the FloSSy as described in Chapter 4 was used. Operating principles, depth weighting functions and technical details of the EM38 sensor can be found in chapter 3.1. Operating the sensor in the vertical orientation, as is done in this study, receives a dominant influence from 0.3 - 0.6 m soil layers. Hence, with a standing water depth of about 0.11 m in the paddy field, influence of the soil material beneath the water layer could be measured.

8.2.5 EC_a survey and data processing

In order to have EC_a information in function of compaction, the inundated field was surveyed three times for the three experiments, in October 2009 (for Exp-1), in September 2010 (for Exp-2), and one month later in October 2010 (for Exp-3). During all surveys, measurements were taken along parallel lines with a spatial resolution of 0.3 m × 0.7 m. A temperature sensor pushed into the ground up to a depth of 0.25 m below the surface recorded the soil temperature during the EC_a surveys. Obtained EC_a measurements were post-corrected for instrumental drift and temperature changes according to the method described in Chapter 3.1.

8.2.6 Geostatistical interpolation

The three EC_a measurement data sets were interpolated to a regular grid with a 0.5 by 0.5 m resolution using kriging. Kriging is a family of geostatistical techniques to estimate the value of a random variable Z at any unsampled location $\mathbf{x}_0$, i.e. $Z^*(\mathbf{x}_0)$, using a weighted linear combination of $n(\mathbf{x}_0)$ observations within a predefined neighbourhood around $\mathbf{x}_0$. The general kriging equation is given in Chapter 3.3.2.

Although all kriging variants are based on the general kriging equation (Equation 3.13) and the variogram model, three variants can be distinguished according to the model considered for $m(\mathbf{x})$: simple kriging (SK), ordinary kriging (OK) and simple kriging with varying local means (SKlm).

SK assumes that $m(\mathbf{x})$ in equation 3.13 is globally stationary, so it simply becomes m, and that is it is known at priori. Therefore, SK works on the residuals and its kriging estimator is

$$Z^*_{SK}(\mathbf{x}_0) = m + \sum_{\alpha=1}^{n(\mathbf{x}_0)} \lambda_\alpha R(\mathbf{x}_\alpha) \tag{8.1}$$

with $R(\mathbf{x}_\alpha) = Z(\mathbf{x}_\alpha) - m$. Hence, SK first subtracts the known global mean m from all observations, then interpolates the residuals using the SK kriging system, and finally adds back m to all estimations. Note that the SK assumptions about $m(\mathbf{x})$ are severe and difficult to verify.

OK is a second kriging type which has more relaxed assumptions about $m(\mathbf{x})$: it assumes that $m(\mathbf{x})$ is locally stationary and that it is unknown. This means that $m(\mathbf{x})$ is constant within the predefined neighbourhood around $\mathbf{x}_0$, implying that $m(\mathbf{x}_0)$ and $m(\mathbf{x}_\alpha)$ are equal. This results in the OK estimator (Equation 3.16).

In the presence of a clear spatial trend, in other words when $m(\mathbf{x})$ is non-stationary, SKlm could be applied. In SKlm the global mean m of SK is replaced by a varying local mean $m(\mathbf{x})$ which is modeled for the entire study area, leading to the following kriging equation

$$Z^*_{SKlm}(\mathbf{x}_0) = m(\mathbf{x}_0) + \sum_{\alpha=1}^{n(\mathbf{x}_0)} \lambda_\alpha R(\mathbf{x}_\alpha) \tag{8.2}$$

with $R(\mathbf{x}_\alpha) = Z(\mathbf{x}_\alpha) - m(\mathbf{x}_\alpha)$, i.e. the residuals at the observed locations. Similar to SK, SKlm first subtracts the varying local mean or spatial trend $m(\mathbf{x})$ from all observations. Since the mean of the residuals $R(\mathbf{x}_\alpha)$ can be considered as globally stationary and it is equal to zero. The residuals are interpolated with the SK kriging system. Finally, $m(\mathbf{x})$ is added back

to all estimations. In SKlm the variogram of the residuals is calculated and modeled. For both variogram analysis and kriging the mapping software Surfer was used (Golden Software Inc., USA).

8.2.7 Water percolation and crop yield measurements

Water percolation (as the method of chapter 7.2.5) was measured in November 2010 for Exp-3 to observe the effect of compaction on water losses. At the 54 soil sampling locations readings were taken periodically three times within 1 m^2 with a double ring infiltrometer (0.30 m inner ring diameter and 0.45 m outer ring). The decrease in water level in the inner ring as a function of time was measured. Measurements continued for three days as the water inside the inner ring approached a stable level. Percolation rates were determined from data on ring water levels and evaporation from an open pan located inside the field and surrounded by paddy rice plants.

At each of the 54 sampling locations the paddy grain yield was determined for Exp-1 and Exp-3. The crops were planted in October 2009 and 2010 and harvested in March 2010 and 2011, respectively. Planting density, intercultural practices, fertilizer and irrigation water inputs were equally applied to the crop over the study years. So, evaluation of crop performance for the two experiments involving no compaction and maximal compaction was made possible. At maturity, the paddy grain of 1 m^2 was manually harvested. The weight of the harvested fresh grains was measured, adjusted to a moisture content of 14 % and expressed in t ha^{-1}.

8.3 Results and discussion

8.3.1 Soil texture, organic carbon, bulk density and penetration resistance

The field was characterized at 54 sampling locations with respect to soil texture, bulk density and penetration resistance. Table 8.1 shows the population parameters of soil texture and OC analysis of the field observed at three depth intervals.

Table 8.1 Population parameters of soil textural fractions and OC (organic carbon) at three soil depths; number of samples (*n*) = 54.

Soil depth (m)		OC (%)	Sand (g kg^{-1})	Silt (g kg^{-1})	Clay (g kg^{-1})	Soil texture class
	Minimum	2.1	240	520	150	
	Maximum	2.5	330	580	190	
0-0.15	Mean	2.3	279	545	176	Silt loam
	SD	0.12	24.7	21.1	15.6	
	Minimum	1.6	230	530	130	
	Maximum	2.4	320	620	180	
0.15-0.30	Mean	1.9	263	580	157	Silt loam
	SD	0.27	29.6	32.0	15.0	
	Minimum	1.9	400	360	100	
	Maximum	2.4	510	490	140	
0.30-0.45	Mean	2.2	442	438	120	Loam
	SD	0.17	28.9	32.2	11.6	

On average the soil (0 - 0.30 m) has a silt loam texture [USDA (United States Department of Agriculture) texture triangle] with a predominant silt fraction (above 50 %). There is a small change in depth (0.30 - 0.45 m), where the texture becomes loamy. Small standard deviation (SD) values for the textural fractions within each depth interval were found. The mean OC content of the field was not very high (2.3 % within 0 - 0.15 m) and also did not differ much with depth increment. With low values of SD (maximum 0.27, within 0.15 - 0.30 m), the OC content exhibited a limited spatial variability in the distribution of soil organic matter.

To investigate the link between compaction and soil bulk density, the 54 observations of bulk density at the three depth intervals were grouped according to P2, P4 and P6 (the three puddling intensities of Exp-3). Table 8.2 gives the descriptive statistics together with a statistical comparison of the mean bulk density values.

Table 8.2 Descriptive statistics and mean comparison of soil bulk density (Mg m-3) between three puddling intensities of Exp-3: P2 = two puddling, P4 = four puddling and P6 = six puddling; *n* = number of samples, SD = standard deviation.

			Soil bulk density (Mg m^{-3})			
Soil depth (m)	**Puddling intensity**	***n***	**Minimum**	**Maximum**	**Mean***	**SD**
0-0.15	P2	18	1.29	1.42	1.37_a	0.05
	P4	18	1.20	1.35	1.26_b	0.04
	P6	18	1.17	1.36	1.26_b	0.05
0.15-0.30	P2	18	1.42	1.76	1.55_a	0.10
	P4	18	1.60	1.78	1.73_b	0.04
	P6	18	1.61	1.79	1.69_b	0.06
0.30-0.45	P2	18	1.43	1.54	1.47	0.04
	P4	18	1.44	1.59	1.49	0.05
	P6	18	1.45	1.60	1.50	0.05

*Within a soil depth interval, means followed by the same letter or without a letter do not differ significantly (P = 0.05) according to Fisher's least significant difference test.

For all three soil depth intervals, the mean bulk density values were small within 0 -0.15 m soil layer (ranged between 1.26 Mg m^{-3} and 1.37 Mg m^{-3}) and large within 0.15 - 0.30 soil layer (ranged between 1.55 Mg m^{-3} and 1.73 Mg m^{-3}). Mean values within 0.30 - 0.45 m soil depth were intermediary (ranged between 1.47 Mg m^{-3} and 1.50 Mg m^{-3}). Within 0 - 0.15 m, P2 had the largest mean bulk density (1.37 Mg m^{-3}). This was significantly different from P4 and P6 where the bulk density values were smaller. The general decrease in bulk density with increasing puddling intensity was caused by the loosening effect of puddling, which implies a compaction reduction. So, bulk density followed the opposite trend of the puddling intensity, i.e. the higher the puddling intensity, the smaller becomes the bulk density. The bulk density values observed for the depth interval 0.15 - 0.30 m were large because the plough pan formation took place at this depth. In other studies, the bulk density of a sandy loam soil layer at 0.15 - 0.20 m depth has also been found to increase with an increase in puddling (e.g. Kukal and Aggarwal, 2003). However, in this study a large variation in bulk density values was observed within 0.15 - 0.45 m soil layer. This was indicated by a larger range of SD

values (0.04 Mg m^{-3} to 0.10 Mg m^{-3}) compared to the other two soil layers. The SD value of 0.10 Mg m^{-3} observed in P2 indicated that this puddling intensity created large variation and therefore was not sufficient to form a plough pan having homogeneous soil compaction. Compaction was increased in P4 and P6. Consequently, soil bulk density increased while SD values decreased, indicating a better compacted plough pan with rather homogeneous field coverage. This indicates the link between increased puddling intensity and plough pan compaction. The deeper soil layer (0.30 - 0.45 m) was probably uninfluenced by puddling and thereby did not show any significant difference for the individual puddling treatments. This is supported by Fig. 8.2 which illustrates the penetration resistance (PR) measurements as a result of increased puddling intensity.

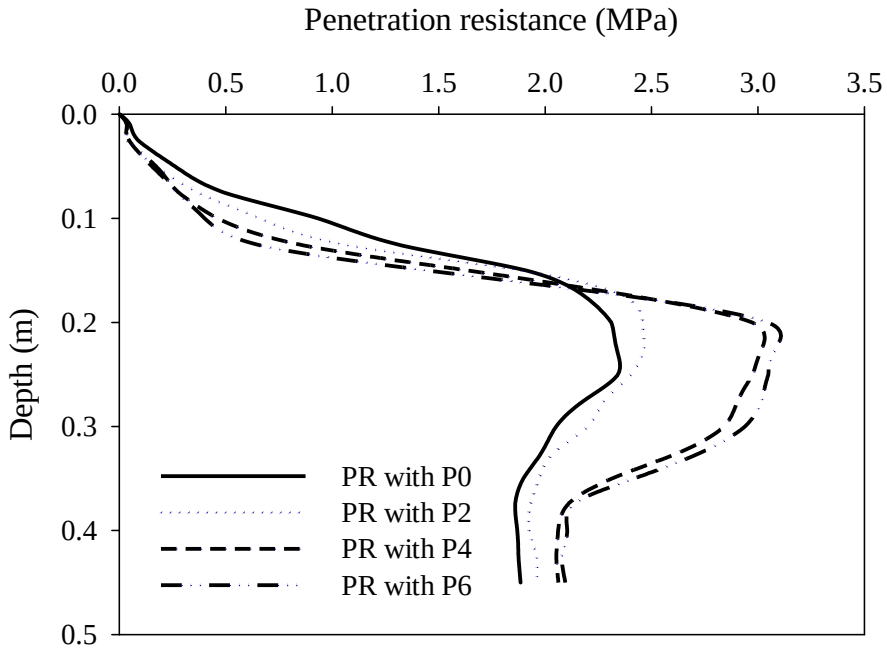

Figure 8.2 Penetration resistance (PR) at different depths as a function of puddling intensity treatments of Exp-1: P0 = no puddling and Exp-3: P2 = two puddling, P4 = four puddling and P6 = six puddling.

Soil resistance to penetration was minimal within the plough layer (0 - 0.15 m) because puddling could loosen the soil up to this depth. The soil of this layer became softer with increased puddling intensity as aggregates were broken down due to the mechanical action, thereby decreasing soil PR. Beneath this layer the resistance increased in P6 over P4 with further increase in puddling intensity and reached to a value above 3.0 MPa. This indicates

the resistance from the compacted plough pan because higher PR values (around 3.0 MPa) were observed within the 0.15 - 0.30 m soil depth; the same depth where bulk density was higher. Kukal and Aggarwal (2003) also reported significantly higher soil PR after puddling, because of increased compaction within the plough pan layer. The deep soil layer (0.30 - 0.45 m) was least influenced by puddling and remained relatively stable to offer an intermediary level of resistance.

8.3.2 EC_a survey

Table 8.3 shows the population parameters of the EC_a measurements for the three surveys. The mean of EC_a of Exp-3 (61.1 mS m^{-1}) was higher than those of Exp-2 (58.6 mS m^{-1}) and Exp-1 (51.4 mS m^{-1}). A difference in the variance was also observed: 3.2 (mS m^{-1})^2 for Exp-1, 13.1 (mS m^{-1})^2 for Exp-2 and 13.7 (mS m^{-1})^2 for Exp-3. This indicated an increase of EC_a variability when the puddling intensity was also increased. As the surveys were conducted by the same sensing system in flooded conditions, the general increase in EC_a for Exp-2 and Exp-3 can be attributed to changes in soil condition.

Fig. 8.3 shows the box plots of EC_a for the puddling intensities for the three experiments. Fig. 8.3a clearly shows that the mean EC_a of Exp-1 was stationary for the three areas of the paddy field receiving the same puddling treatment P0. In Exp-2 (Fig. 8.3b) the expected values started approaching to non-stationarity which became clearly non-stationary in Exp-3 (Fig. 8.3c). So, the three areas with different puddling intensity treatments: P2, P4 and P6 were transformed to have clearly different local means (Exp-3). Thus, the presence of spatial trend caused by soil compaction was evident.

Table 8.3 Population parameters of EC_a measurements of the three surveys; EC_a of Exp-1 with no puddling treatment; EC_a of Exp-2 with one, two and three puddling treatments; EC_a of Exp-3 with two, four and six puddling treatments; *n* = number of samples.

		EC_a (mS m^{-1})			
EC_a survey	***N***	**Minimum**	**Maximum**	**Mean**	**Variance**
Exp-1	54 234	46	56	51.4	3.2
Exp-2	54 204	50	65	58.6	13.1
Exp-3	54 239	53	67	61.1	13.7

(a)

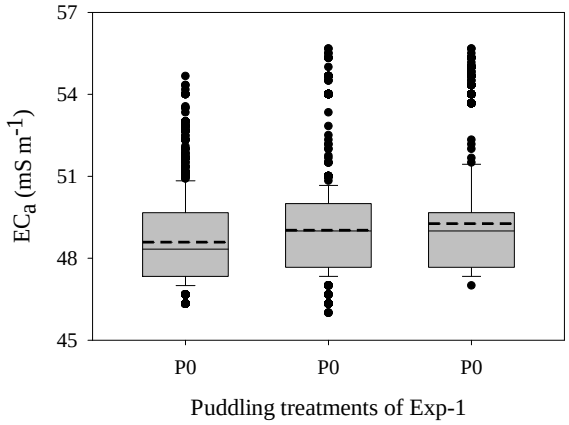

(b)

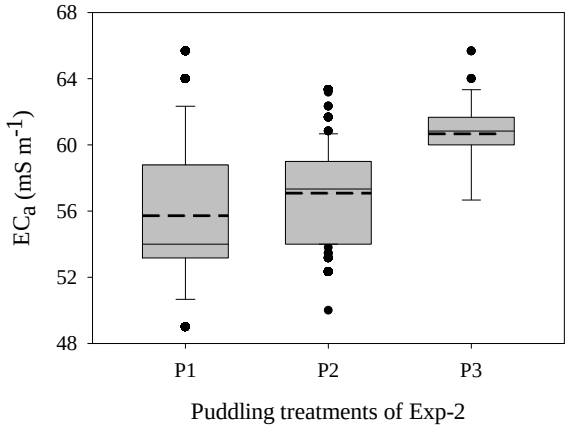

(c)

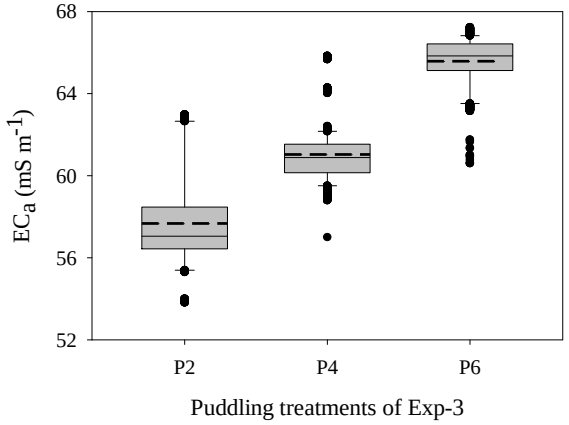

Figure 8.3 Box plots of EC_a (mS m^{-1}) values of paddy field 3 in three areas: (a) EC_a of Exp-1 with no puddling (P0) in all three areas; (b) EC_a of Exp-2 with P1 (one puddling), P2 (two puddling) and P3 (three puddling); and (c) EC_a of Exp-3 with P2 (two puddling), P4 (four puddling) and P6 (six puddling). The top and bottom of the boxes are the first and third quartiles, respectively. The length of the box thus represents the interquartile range. The solid line through the middle of each box represents the median and dashed line the mean. The vertical bars show the extent between the 10th and 90th percentiles and solid circles represent values outside the 10th and 90th percentiles.

We chose OK to interpolate the EC_a data from the Exp-1 and SKlm to interpolate the EC_a data from Exp-2 and Exp-3, because there was a clear spatial trend for the last two. To model the variogram, these two survey data sets were stratified per puddling intensity and the local mean values were subtracted from observations in the respective stratum to obtain residuals.

Fig. 8.4 shows the experimental variograms and the fitted exponential models (Chapter 3.3.1) for the EC_a data set of Exp-1 and pooled residuals of EC_a of Exp-2 and Exp-3. The spatial continuity for the EC_a data set of Exp-1 (Fig. 8.4a) had a range (a) of 29 m which was higher than those of the residual data sets of Exp-2 (Fig. 8.4b) and Exp-3 (Fig. 8.4c). Both the structured part of the spatial variation and the maximal extend of spatial relation decreased as soil compaction increased in P4 and P6. This was indicated by smaller C_1 and a values of the EC_a residuals in P4 and P6.

Fig. 8.5 shows the EC_a measurements of the field: EC_a of Exp-1 interpolated with OK, and EC_a of Exp-2 and Exp-3 interpolated with SKlm. However, stratifying the EC_a data of Exp-2 (according to P1, P2 and P3) and Exp-3 (according to P2, P4 and P6) could result in too few measurements within each stratum for variogram modeling and this technique could induce artifacts along the boundaries (Meul and Van Meirvenne, 2003). With SKlm the effect of the differences in mean was removed and the residuals were pooled yielding sufficient data for variogram calculation and modeling.

The EC_a map of Exp-1 in Fig. 8.5a shows patterns of fluctuating EC_a values across the field. It can be seen that some patchy areas of high EC_a values occurred within the field, especially at the middle of the southern border. Occurrence of these high EC_a values was investigated by field observation and could be attributed to few large soil clods which appeared after disc ploughing. Apart from that, the field did not have a large EC_a variation before puddling for Exp-2. After puddling however, the EC_a map in Fig. 8.5b for Exp-2 shows a trend of increasing EC_a values approaching towards the east from west side of the field. This is the same direction towards which puddling increased in P2 and P3 over P1 (for Exp-2). This spatial trend of increasing EC_a values was even better captured during the EC_a survey of Exp-3 and is mapped in Fig. 8.5c. This map clearly shows the three distinct areas within the field which sequentially received P2, P4 and P6, thereby an increasingly higher puddling intensity. Thus, the connection between EC_a as a representative of plough pan compaction variation caused by puddling was evident.

(a)

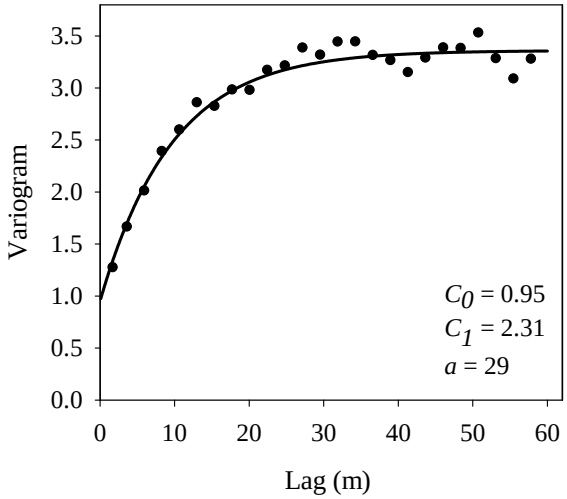

(b)

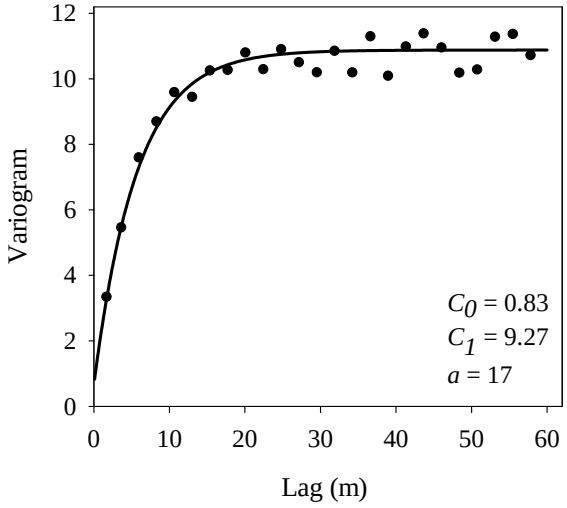

(c)

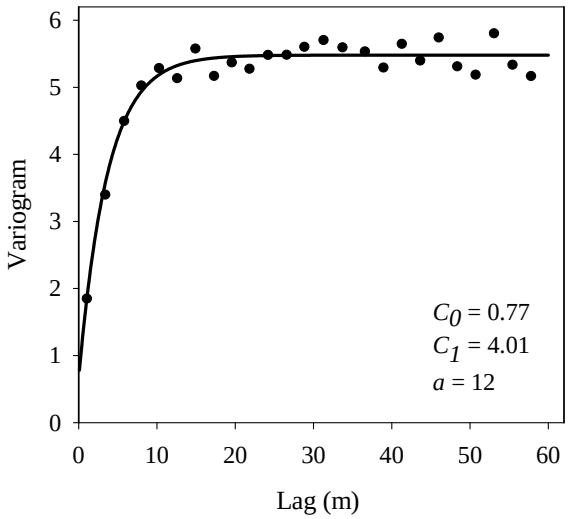

Figure 8.4 The experimental variograms (dots) and the exponential models (line) of three data sets: (a) EC_a of Exp-1, (b) pooled residuals of EC_a of Exp-2, and (c) pooled residuals of EC_a of Exp-3. The parameters of the fitted variogram models are also given: C_0 (nugget), C_1 (sill) and a (range) expressed in m.

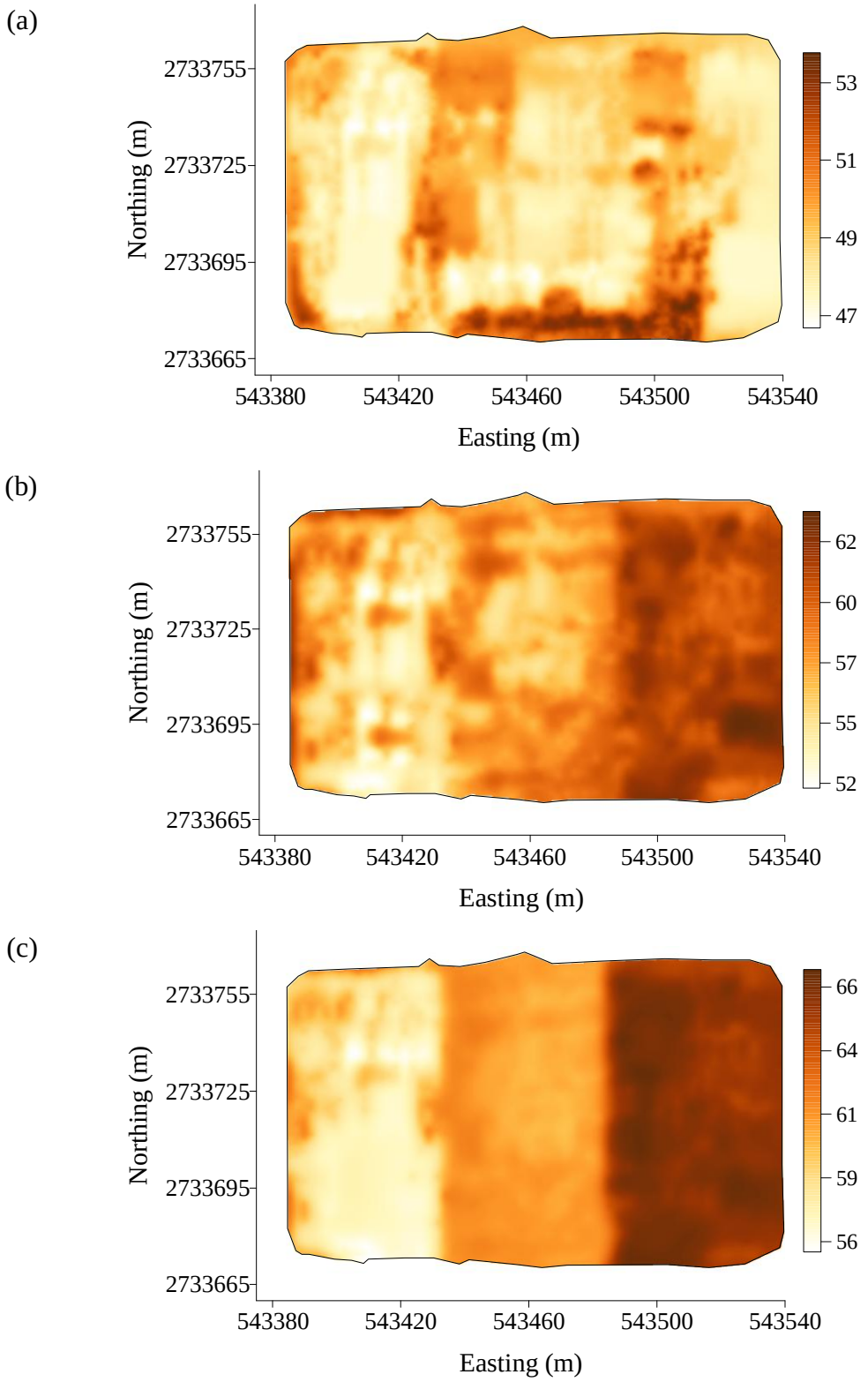

Figure 8.5 The EC_a of paddy field 3: (a) EC_a (mS m^{-1}) of Exp-1 with no puddling (P0); (b) EC_a (mS m^{-1}) of Exp-2 with P1 (one puddling), P2 (two puddling) and P3 (three puddling); and (c) EC_a (mS m^{-1}) of Exp-3 with P2 (two puddling), P4 (four puddling) and P6 (six puddling).

Flooding of non-saline paddy fields provides homogeneous soil water conditions because of water saturation. Under this condition and low values of OM content variation, a key role in influencing EC_a measurements is played by soil texture and bulk density (Rhoades et al., 1999; Saey et al., 2009). Characterization of the field in terms of texture already indicated a limited spatial variability of the field. Besides, given that texture is a stable soil property which does not change laterally by puddling, the spatial distribution of EC_a of the three puddling areas is due to the spatial variation of plough pan compaction linked to soil bulk density variation (McKenzie et al., 2003). Higher bulk density variation of the soil was resulted by puddling variation (different puddling intensity). Thus, more intensive puddling gave rise to higher bulk density values, especially in the compacted soil layer (0.15 - 0.30 m). Puddling of a soil results in redistribution of pore size with a pore geometry which is different than the soil in unpuddled condition. However, explaining the developmental mechanism of compaction and soil pore redistribution was out of the scope of this research and can be found elsewhere (Kukal and Aggarwal, 2003; Kukal and Sidhu, 2004). In the plough pan layer, soil particles come in a better and closer state of contact and the layer is dominated by finer pores. The greater the connectivity and proportion of these fine pores, the larger the electrical conductivity becomes. Finer pore size plays a key role to increase the ion and electrolyte concentration within the pores which further influences the soil electrical conductance pathway.

8.3.3 Water percolation

Puddling is required to maintain a wet growing condition for the paddy crop by decreasing water loss through percolation beyond the rooting zone. Therefore, measurements on water loss were taken to interpret the effectiveness of higher puddling intensities: P2, P4 and P6 in Exp-3. The statistical parameters of the 54 permeability measurements (taken according to the method given in chapter 7.2.5) are given in Table 8.4.

A statistical comparison of the mean values grouped according to P2, P4 and P6 shows that a significantly higher mean percolation rate (27 mm day^{-1}) was found in P2 where the intensity of puddling was relatively low. Increased puddling resulted in a significant decrease of percolation loss in P4 (17 mm day^{-1}) over P2. Further increase in P6 did not significantly decrease the percolation rate (16 mm day^{-1}) of water. Since P2 had the larger mean water percolation value than P4 and P6, it can be reasonably accepted that a well formed plough pan layer was not present in P2 to restrict water losses through percolation. In sandy loam

paddy field soils, Kukal and Aggarwal (2003) observed the percolation rate to be 30.1, 13.6 and 11.6 mm day^{-1} under unpuddled, medium and high puddling intensity respectively, which is similar to the values found in this study. Soil particles in a closer state of contact within the compacted layer results in a sealing and thereby reduces the downward flow of water.

Table 8.4 Statistical parameters and mean comparison of water percolation rate (mm day^{-1}) stratified per puddling intensity treatment of Exp-3: P2 = two puddling, P4 = four puddling and P6 = six puddling; *n* = number of samples per EC_a class, SD = standard deviation.

		Percolation rate (mm day^{-1})			
Puddling intensity	***n***	**Minimum**	**Maximum**	**Mean***	**SD**
P2	18	22	31	27_a	2.6
P4	18	15	22	17_b	1.9
P6	18	14	20	16_b	1.8

*Within a soil depth, means followed by the same letter do not differ significantly (p = 0.05) according to Fisher's least significant difference test.

8.3.4 Paddy rice yield

The ultimate goal of puddling as a land preparation practice is to achieve optimal paddy rice productivity. Therefore, paddy yield data from 54 locations within the field were recorded for Exp-1 and Exp-3. The data were grouped according to the experimental treatments to allow yield comparison. The significance of the differences between the groups was analyzed statistically and is presented in Table 8.5.

The mean paddy yield was the lowest (5.7 t ha^{-1}) in P0 when the field did not receive any puddling. Yield increased with an increase in puddling. The mean paddy yield was 5.8 t ha^{-1} in P2 and increased significantly to 6.9 t ha^{-1} in P4. This yield improvement of 1.1 t ha^{-1} is considerable given the smaller areas of the field receiving the puddling treatments. In P6, no significant increase in paddy yield (mean = 7.0 t ha^{-1}) over P4 was observed. However, the variation in yield was noticeably reduced (SD = 0.35 t ha^{-1} and 0.18 t ha^{-1} for P4 and P6, respectively). This is also indicated by an opposite trend of SD values with increased puddling from P2 to P6. In case of P2, paddy plants suffered from water availability as the

percolation rate was high while in P4, presence of a compacted soil layer ensured enough water for the plant and prevented nutrient leaching. As a consequence, paddy yield was largely increased. Further increase in puddling in P6 had no effect on yield as water and nutrients were not limiting. This indicated the yield stabilization for the given soil and crop type.

Table 8.5 Descriptive statistics and mean comparison of the paddy yield observations (t ha^{-1}) stratified per puddling intensity of Exp-1: P0 = no puddling and Exp-3: P2 = two puddling, P4 = four puddling and P6 = six puddling.

			Yield (t ha^{-1})			
Puddling intensity	**Harvest year**	***n***	**Minimum**	**Maximum**	**Mean***	**SD**
P0 (Whole field)	2010	54	4.4	6.4	5.7_a	0.50
P2	2011	18	4.8	6.5	5.8_a	0.59
P4		18	6.0	7.5	6.9_b	0.35
P6		18	6.7	7.3	7.0_b	0.18

*means followed by the same letter do not differ significantly (p = 0.05) according to Fisher's least significant difference test.

8.4 Conclusions

We puddled an inundated paddy rice field at varying intensities and characterized the puddled areas in terms of soil properties and EC_a. Detailed soil EC_a measured by an EMI based floating sensing system is able to clearly differentiate the variably compacted areas as the measured EC_a values increase with increasing soil compaction. Differences in soil bulk density and penetration resistance represent the compaction variability. The agronomic consequence of compaction can be evaluated using water percolation and paddy rice yield observations. It was concluded that the EMI-based approach supports the evaluation of compaction variation during puddling. The sensing system appears to be a useful tool for precise land preparation and better resource utilization in paddy rice fields.

9

Modeling the within field variation in the depth of the compaction layer in a paddy field using a proximal soil sensing system

The content of this paper has been submitted as:

Islam, M.M., Saey, T., De Smedt, P., Meerschman, E., Van De Vijver, E., Van Meirvenne, M. Modeling the within field variation in the depth of the compaction layer in a paddy field using a proximal soil sensing system. *Submitted to*- Soil Use and Management.

9.1 Introduction

In the intensive paddy rice cultivation system the fields are kept flooded for the greater part of the growing season. During land preparation, the water saturated fields are ploughed or puddled at the same depth. Commonly reported puddling depth used in floodplain paddy fields is about 0.16 m (De Datta, 1981). Repeated puddling creates a physical soil compaction beneath the ploughed top-soil. This compaction forms a distinct high density soil layer known as the plough pan (McDonald et al., 2006) which limits water percolation beyond the rooting zone and keeps the fields under water during the growing season. Soil beneath this plough pan, on the other hand, remains unaffected from tillage induced influences of soil compaction. The soil build-up of a puddled paddy field can thus be presented as a layered system where the plough pan layer has a distinctly different density than the soil below it.

Although puddling is homogeneously practiced within a given paddy field, the vertical extent of the compacted soil layer can vary across the field. As this layer is required to restrict water losses through percolation and nutrient losses through leaching (Kukal and Sidhu, 2004) variation in its thickness can adversely affect the site-specific soil management. The consequences thereof only become clear when dry zones emerge across the field as a result of unexpected water loss. Adjusting soil management practices to correct for the compaction problem is impossible once the crop is already planted. Therefore; the thickness of the compacted layer should be determined prior to paddy planting. This can then allow optimizing the resource use efficiency, yield stability and productivity in the paddy rice cultivation system. Detailed information on the depth of compacted soil layer should be the basis of a more precise management of paddy rice fields.

Soil compaction is indicated by an increase in soil density, but measuring soil bulk density differences consistently with increasing soil depth is difficult. Using typical bulk density samplers with corers or rings, it is not feasible to sample the saturated paddy soils under crop growing conditions. Since a penetrometer measures soil resistance caused by an increase in soil density (Perumpral, 1987) it allows to measure soil compaction in a saturated field. However, penetrometer measurements can only be taken at point locations. This limits the possibility to obtain continuous information about soil compaction. Therefore, non-invasive proximal soil sensing techniques allowing acquisition of high-resolution soil information offer an alternative. A mobile proximal sensing system employing electromagnetic induction (EMI) can measure the apparent electrical conductivity (EC_a) of

the soil without having a direct physical contact with the soil (McNeill, 1980b). The high resolution information obtained from a non-invasive EMI sensor can be interpreted to explain the variation of soil properties (Sudduth et al., 1997) such as salinity (Slavich and Petterson, 1990), texture (Saey et al., 2009), compaction (Brevik and Fenton, 2004) and organic carbon (Martinez et al., 2009). Under non-saline and wet soil conditions, the influence of salinity and moisture variations on the sensor signal is eliminated (Islam et al., 2012). Thus in soils having a low variation in clay content, it is mainly the soil compaction or pore volume variation (Rhoades et al., 1999), and depth to contrasting soil layers (Saey et al., 2008a) that contribute to the EC_a variability. Thus in a puddled paddy field environment, variations in EC_a can reflect changes in soil compaction. However, no report is currently available on the non-invasive measurements of within-field spatial variability of soil compaction in paddy field conditions.

The main objective of this study was to evaluate a methodology for determining the variation in the thickness of the compacted plough pan within a paddy field using a mobile soil sensing system. This required (i) characterizing paddy field using EC_a measurements under saturated condition (ii) finding and validating the relationship between EC_a and thickness of the plough pan (iii) interpreting the compaction differences in terms of soil-water percolation.

9.2 Materials and methods

9.2.1 Study site

Field 2 located at the Bangladesh Agricultural University, Mymensingh, Bangladesh was selected for the study (chapter 2.4.2). Texture analysis of a composite sample showed that the field has 41 % sand, 45 % silt, 14 % clay at 0 – 0.15 m depth; 45 % sand, 44 % silt, 12 % clay at 0.15 – 0.30 m and 51 % sand, 53 % silt, 6 % clay at 0.30 – 0.45 m depth. Every growing season, the studied paddy field is inundated and subsequently puddled with manual and/or mechanical implements. The water saturated top-soil was homogeneously ploughed and managed.

9.2.2 Sampling the compacted layer

Three replicates of ten undisturbed soil samples were taken within 1 m^2 at three depths (0 – 0.15 m, 0.15 – 0.30 m and 0.30 – 0.45 m). The oven dried (105°C) weight of the soil

samples and the known volume of the sampler (0.75 L) were used to calculate soil bulk density. These bulk density measurements were done under dry field condition in June 2011, which is the commonly used procedure for taking bulk density samples.

The field was afterwards saturated with water and puddled as practiced for rice planting. Soil penetration resistance (PR) was measured by an SC900 soil compaction meter (Spectrum Technologies Inc., Illinois, USA) at ten sampling locations along transect AB. Compaction readings up to a depth of 0.45 m at every 0.025 m depth interval were recorded. At each location three readings were taken within 1 m^2 and averaged. The penetrometer has a 30° conical probe with 12.82 mm diameter and was equipped with an ultrasonic depth sensitivity sensor (ASAE standard small tip). Penetration resistance (in kPa) is measured by an internal load cell and saved in an ASCII text file by the data logging system.

At each sampling location three replicated soil electrical conductivity (EC) measurements were taken from the puddled soil layer (0 - 0.16 m) with a FieldScout direct soil EC meter (Spectrum Technologies Inc., Illinois, USA). The stainless steel probe was inserted directly into the soil at 0.08 m and 0.16 m depths and the average of the two readings was calculated to derive a representative EC of 0 - 0.16 m.

9.2.3 The soil sensing system

To acquire high resolution soil data on paddy field conditions, the FloSSy was used. In the FloSSy, an EMI proximal sensor, the EM38-MK2 (chapter 3.1) was mounted. The raft is trailed by a tractor at a distance of about 1.8 m while it is puddling the paddy field at a speed of approximately 3.5 km h^{-1} (Fig. 9.1). Geo-referenced EC_a data acquired by the system were logged and processed *in-situ* in a field laptop as described in chapter 4.

The EM38-MK2 records the soil EC_a at a particular location from varying soil depths. The sensor consists of two receiver coils at 0.5 and 1.0 m distances from the transmitter coil from which measurements were taken every second. We used both the horizontal (H.5 and H1) and vertical orientations (V.5 and V1). The DOI refers to the depth below the sensor at which 70 % of the cumulative influence of the signal is obtained. Operating the sensor in different orientations, receives dominant influences from soil materials in different depths. This allows the detection of conductivity variation resulting from contrasting soil layers in a

paddy field environment. More technical details and operating principles of the sensor is given in chapter 3.1.

Figure 9.1. (a) FloSSy with: (i) laptop (protected by a plastic sheet), (ii) GPS antenna, (iii) waterproof sensor housing with an EM38-MK2 inside, (iv) floating platform and (v) power tiller; (b) EM38-MK2.

In order to obtain detailed EC_a information, the water saturated paddy field was surveyed two times on two consecutive days, one with the horizontal and one with the vertical orientation of the sensor, in July 2011. For both measurements, the sensor platform was pulled over the soft smooth puddled soil surface. As such four EC_a data sets were obtained: H.5 and H1 in horizontal, and V.5 and V1 in vertical orientations. During both surveys, measurements were taken along 1 m apart (approximately) parallel lines with a resolution of about 0.5 m within a line. During all surveys soil temperature was recorded by a bimetal sensor pushed in the soil to a depth of 0.25 m. Temperature remained stable at about 30 °C. All EC_a measurements were standardized to a reference temperature of 25°C according to chapter 3.1. In the remaining part of this paper all EC_a measurement values refer to the EC_a at 25°C.

9.2.4 Modeling

The cumulative response of the EM38-MK2 (expressed in % of the measured signal) from a layered soil volume below a depth z (in m) beneath the sensor is given in chapter 3.1, both for the vertical $[R_v(z)]$ and the horizontal orientations $[R_h(z)]$. The response functions (equations 3.3 and 3.4) allow modeling the relationship between the conductivity of a soil

layer and EC_a. For a paddy field, we can define the depth to the interface between the puddled layer and the compacted layer as z_{pp}, and the depth to the interface between the compacted layer and the soil material below it as z_{ppb}. Then the thickness of the compacted layer can be calculated as $z_{ppb} - z_{pp}$. The cumulative response from the puddled layer, compacted layer and the uncompacted soil material beneath can be calculated as $1 - R(z_{pp})$, $R(z_{pp}) - R(z_{ppb})$ and $R(z_{ppb})$, respectively. Therefore, for the ten paired EC_a measurements and corresponding z_{ppb} observations on transect AB, the predicted z_{ppb}^* can be modeled by solving a system of non-linear equations, given the apparent conductivity values of the puddled layer ($EC_{a,p}$), compacted layer ($EC_{a,pp}$) and the uncompacted soil beneath ($EC_{a,ppb}$):

$$EC_a = [1 - R(z_{pp})].EC_{a,p} + [R(z_{pp}) - R(z_{ppb}^*)].EC_{a,pp} + R(z_{ppb}^*).EC_{a,ppb} \quad (9.1)$$

The automated FSOLVE function based on the Levenberg–Marquardt algorithm (Marquardt, 1963) in the Matlab computing environment (MathWorks, Natick, MA, USA) was used. The sum of the squared differences between z_{ppb} and z_{ppb}^* was minimized in order to fit the theoretical relationship to the z_{ppb} and EC_a data using:

$$\sum_{i=1}^{n} [z_{ppb} - z_{ppb}^*(i)]^2 = \min \quad (9.2)$$

with *n* being the number of observations. The modeling parameters $EC_{a,pp}$ and $EC_{a,ppb}$ were iteratively adjusted to obtain the smallest sum of the squared differences between z_{ppb} and z_{ppb}^*. Detailed description of the methodology can be found in Saey et al. (2008b).

An independent validation can be performed to evaluate the predictive quality of the model. The Pearson correlation coefficient (*r*), mean estimation error (MEE) and root mean square estimation error (RMSEE) were used as the validation indices. When *r* is close to 1, the z_{ppb} and z_{ppb}^* have a strong positive association. The bias of the model becomes low and

the accuracy of the model becomes high when MEE and RMSEE, respectively approach 'zero'. The MEE and RMSEE were obtained as:

$$\text{MEE} = \frac{1}{n}\sum_{i=1}^{n}[z_{\text{ppb}}{}^{*}(i) - z_{\text{ppb}}(i)] \tag{9.3}$$

$$\text{RMSEE} = \sqrt{\frac{1}{n}\sum_{i=1}^{n}[z_{\text{ppb}}{}^{*}(i) - z_{\text{ppb}}(i)]^{2}} \tag{9.4}$$

with *i* being the number of validation observations. At each location, depth of the compaction layer was observed by PR measurements and the observed depths were compared with the model predictions.

9.2.5 Water percolation measurements

The water percolation rate was measured during paddy growing conditions in August 2011 at 18 locations. At each location, these readings were taken periodically, three times within 1 m^2, with a double ring infiltrometer (0.30 m inner ring diameter and 0.45 m outer ring). The decrease in water level inside the inner ring was measured as a function of time. Measurements continued for three days until the water level stabilized inside the inner ring. Percolation rates were calculated from comparing these data with the evaporation from an open pan located inside the field and surrounded by rice plants.

9.3 Results and discussion

9.3.1 Bulk density measurements

Table 9.1 gives the descriptive statistics of the soil bulk density values for the three depth intervals: 0 – 0.15 m, 0.15 – 0.30 m and 0.30 – 0.45 m. The smallest mean bulk density values were found within 0 – 0.15 m and the largest within 0.15 – 0.30 m; the value was intermediary for the 0.30 – 0.45 m. This indicated the clear difference among the three soil layers where the 0.15 – 0.30 m layer corresponded to the compacted layer. However, the large variation within this layer (between 1.42 and 1.79 Mg m^{-3}) indicated that soil bulk density also varied the most within this layer. These values are similar to those found by Islam et al. (2011a).

Table 9.1 Some descriptive statistics of soil bulk densinty (in Mg m^{-3}) values observed at 10 points on a calibration transect AB (PR = penetration resistance, CV = coefficient of variation).

Soil depth (m)	Mean (Mg m^{-3})	Minimum (Mg m^{-3})	Maximum (Mg m^{-3})	CV (%)
0 - 0.15	1.33	1.19	1.41	5.9
0.15 - 0.30	1.63	1.42	1.79	7.3
0.30 - 0.45	1.46	1.41	1.63	2.9

9.3.2 EC_a measurements

Table 9.2 contains the descriptive statistics of the EC_a measurements. The DOIs of the coil configurations of the EM38-MK2 are: 0.38 m for the H.5 orientation, 0.75 m for both the H1 and V.5 orientations, and 1.50 m for the V1 orientation; each having a different distribution of the depth sensitivity. The mean EC_a values were the largest for the intermediate DOIs: 51 mS m^{-1} and 54 mS m^{-1} for H1 and V.5, respectively. However, the means were lower for both the shallowest and the deepest DOIs: 44 mS m^{-1} for H.5 and 39 mS m^{-1} for V1. These EC_a measurements indicate that the intermediate soil material is more conductive than the shallow and deep soil material. The relative response curves are given by McNeill (1980b) and shown in Fig. 9.2. It is clear that H.5 and H1 respond mostly to the soil material close to the soil surface. On the other hand, with the V.5 reflect the compacted soil material and V1 is mainly influenced by the soil below the compacted layer.

Table 9.2 Some descriptive statistics of EC_a variables (*n* = number of observations, CV = coefficient of variation).

EC_a variable	DOI (m)	*n*	Mean (mS m^{-1})	Minimum (mS m^{-1})	Maximum (mS m^{-1})	CV (mS m^{-1})^2
H.5	0.38	35 673	44	28	60	30.3
H1	0.75	35 673	51	29	75	62.7
V.5	0.75	35 370	54	32	77	62.6
V1	1.5	35 370	39	20	59	46.8

The small variances of the H.5 and V1 coil orientations (Table 9.2) indicate that both the ploughed top-soil and the deep soil had limited variability. On the contrary, the largest

variance for the V.5 coil orientation indicates that the intermediate soil layer accounted for the largest EC_a variation.

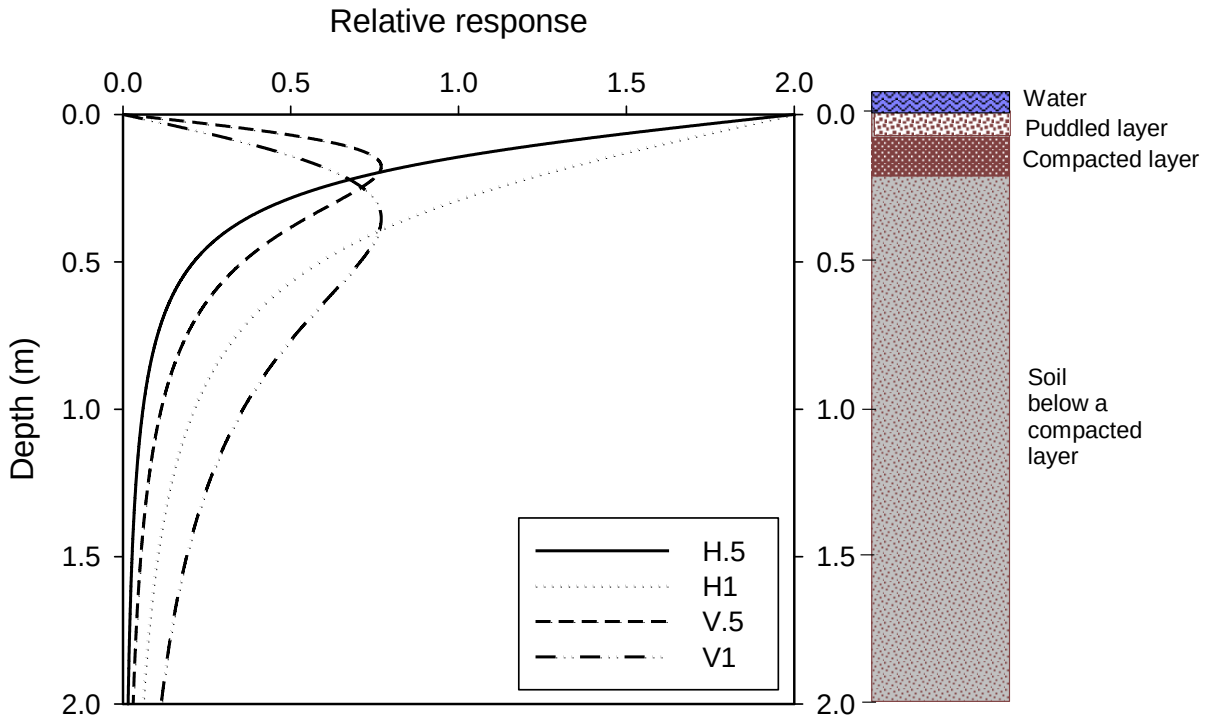

Figure 9.2. Relative response of the four coil configuration as a function of depth (m) for the EM38-MK2 in horizontal (.5 H and 1H) and vertical (.5V and 1V) configurations with 0.5 m and 1 m transmitter-receiver coil separation (left figure) and a typical layered paddy field model showing the different soil layers with indication of approximate layer depths beneath a standing water layer of few centimetres (right figure).

All the EC_a data sets were interpolated with ordinary kriging (Chapter 3.3.2) to create four EC_a maps with a resolution of 0.5 m by 0.5 m. All four variograms were best modelled by an omnidirectional spherical model and the kriged maps are given in Fig. 9.3.

The four EC_a maps show similar patterns of fluctuating values across the field without a systematic trend. However, the shallow EC_a measurements (Fig. 9 3a, 9.3b and 9.3c) reveal a larger variability than the deep measurement (Fig. 9. 3d). Moreover, Fig.9. 2 showed that measurements obtained with the shallow measuring coil configuration in V.5 are insensitive to the upper soil layers and receives a dominant influence from the soil layers which are typically compacted in paddy fields. Hence, it allows detection of conductivity variations in the compacted layer of paddy fields. For a given volume, soil compaction results in a bigger

amount of fine soil pores because of closer packing of soil particles. The finer the soil pores are the larger the concentrations of the pore solution becomes, resulting in larger electrical conductivity values.

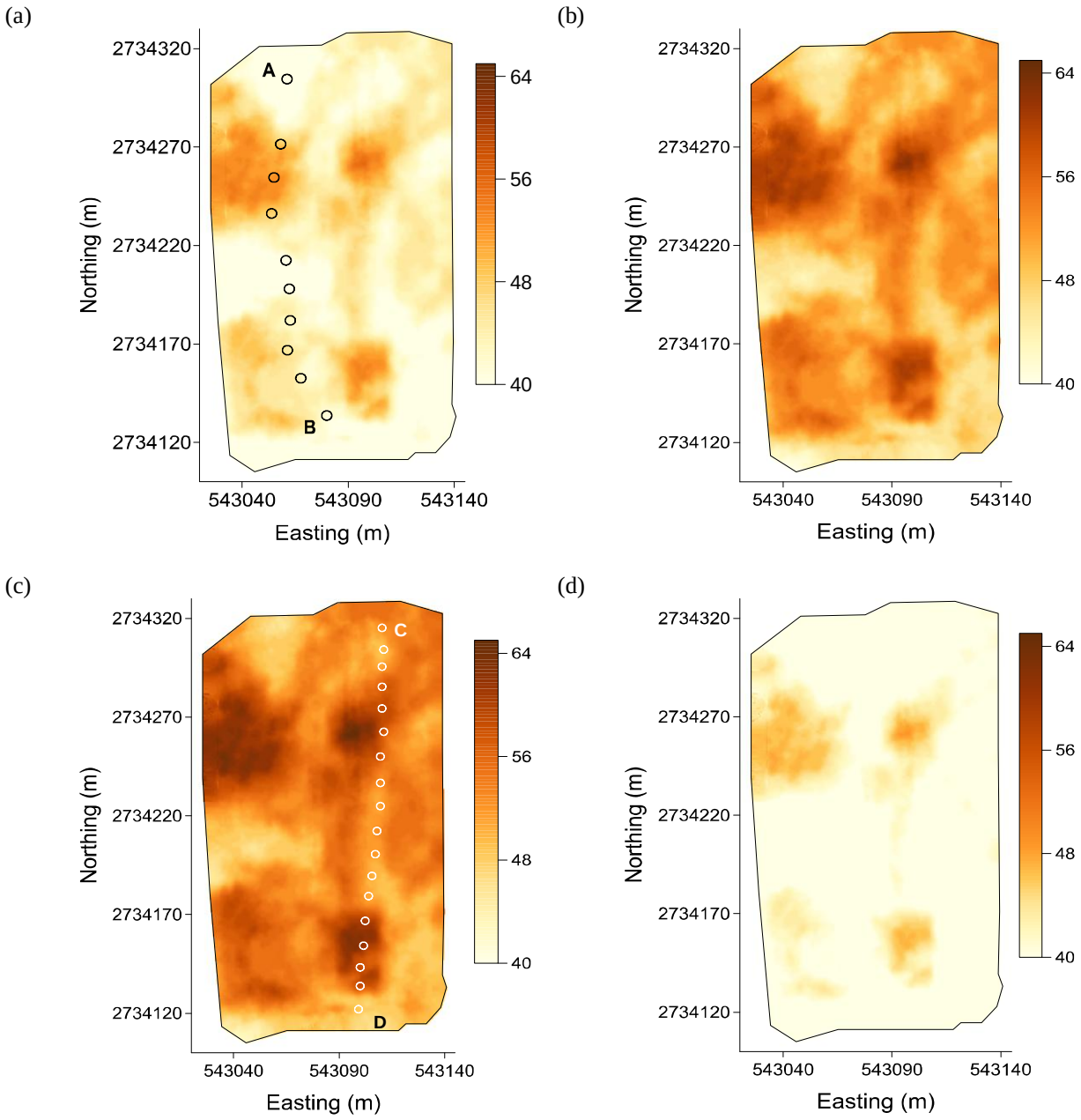

Figure 9.3. Interpolated apparent electrical conductivity (EC_a) in mS m^{-1} using 0.5 and 1.0 m intercoil distances of the EM38-MK2 in both horizontal and vertical orientations: (a) EC_a with H.5, (b) EC_a with H1, (c) EC_a with V.5 and (d) EC_a with V1 coil configuration. AB (n = 10) and CD (n = 18) are two transects for calibration and validation respectively, showing measurement locations as circles.

9.3.3 Relationship between EC_a, bulk density and penetration resistance

Table 9.3 gives the correlation coefficients, *r* between EC_a, bulk density and PR for the three soil depth intervals. For all depth intervals, EC_a in the V.5 coil configuration were stronger correlated than EC_a in the other coil configurations and bulk density. However, the very strong relationship between V.5 and PR, both measured under paddy growing conditions, is clear. This points out that the V.5 measurements are appropriate for detecting differences in soil compaction depth. Therefore, among the four EC_a data sets, the EC_a in the V.5 coil configuration was selected, and in the following parts of this paper all EC_a values refer to the EC_a obtained with the V.5 configuration.

Table 9.3 Pearson correlation coefficient (r) between EC_a, soil bulk density and penetration resistance. Bd = bulk density; PR = penetration resistance; _15, _30 and _45 = measurements obtained from soil depth intervals of 0 – 0.15 m, 0.15 – 0.30 m and 0.30 – 0.45 m, respectively (*n* = 65).

	Bd_15	**Bd_30**	**Bd_45**	**PR_15**	**PR_30**	**PR_45**
H0.5	0.24	0.64	0.61	0.19	0.72	0.75
H1	0.23	0.64	0.61	0.16	0.81	0.76
V.5	0.013	0.71	0.63	0.13	**0.89**	0.83
V1	0.002	0.66	0.56	0.19	0.73	0.75

PR measurements are more sensitive as an indicator of soil compaction than the bulk density measurements taken under dry field conditions. A penetrometer measures the relative soil compaction at much smaller depth intervals than soil bulk density samples could be obtained. A transect (AB) was laid out (Fig. 9.3a) and the PR measurements at the ten locations along the transect AB (Fig. 9.3a) were used to observe the depth of the soil compacted layer. The locations were selected so that the entire range of EC_a was covered. Fig. 9.4 shows PR in respect to soil depth along transect AB. At all locations, soil compaction approached a maximum depth limit (z_{pp}) and remained relatively stable over a depth range of few to tens of centimeters. This stability indicated that the degree of compaction was similar everywhere within the compacted soil layer. Therefore, the distinction between the uncompacted soil layers and depth of the compacted layer z_{ppb} is clearly observable. This depth revealed to be highly variable along transect AB.

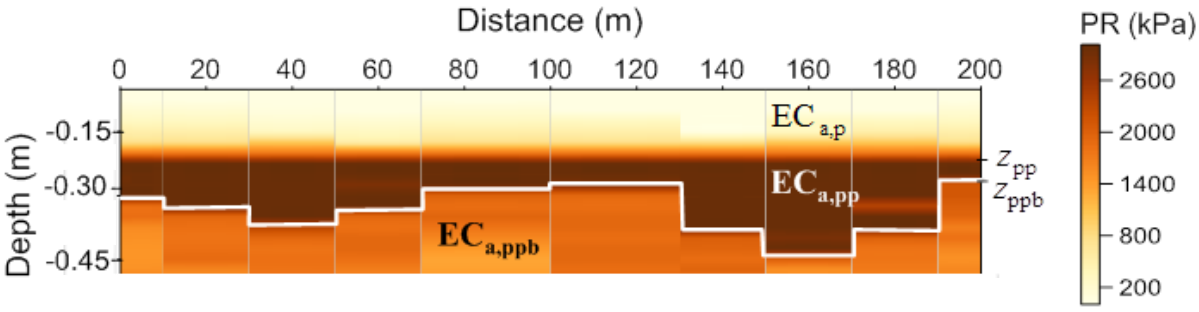

Figure 9.4. The penetration resistance (PR) measurements along transect AB (n = 10); the modeling parameters $EC_{a,p}$ and z_{pp} are constants where $EC_{a,p}$ is the conductivity of the puddled upper layer and z_{pp} is the depth to the interface between the puddled layer and the compacted layer; $EC_{a,pp}$ and $EC_{a,ppb}$ are conductivities of the compacted and the uncompacted layer beneath; z_{ppb} presented as solid line is the depth to the interface between the compacted and the uncompacted layer.

This stability indicated that the degree of compaction was similar everywhere within the compacted soil layer. Therefore, the distinction between the soil layers and depth of the compaction layer z_{ppb} is clearly observable.

9.3.4 Depth modeling

Using the direct soil EC meter and PR measurements, ten paired conductivity and depth measurements along transect AB were obtained from the puddled upper soil layer. The mean conductivity was 21.3 mS m^{-1} ($EC_{a,p}$) with a standard deviation (SD) of 0.8 mS m^{-1} and the mean z_{pp} was 0.16 m with a SD of 0.01 m. These low values of SD indicated a limited variability and therefore, allowed us to take the $EC_{a,p}$ and z_{pp} parameters being constant along the study site. Next, the ten z_{ppb} observations of transect AB were compared with their nearest EC_a measurements recorded with the EM38-MK2. The theoretical McNeill relationship was fitted to the z_{ppb} and EC_a data points by minimizing the sum of the squared differences between z_{ppb} and z_{ppb}^* deduced from equation 9.1 (Fig. 9.5). At each measurement point, iterative adjustment resulted in optimal $EC_{a,pp}$ and $EC_{a,ppb}$ values of 90.6 and 35.6 mS m^{-1} with a R^2 value of 0.89. Then z_{ppb}^* was modeled by using equations.

3.3 and 9.1 given the measured EC_a (from EM38-MK2), the constant $EC_{a,p}$ and z_{pp}; and fitted $EC_{a,pp}$ and $EC_{a,ppb}$.

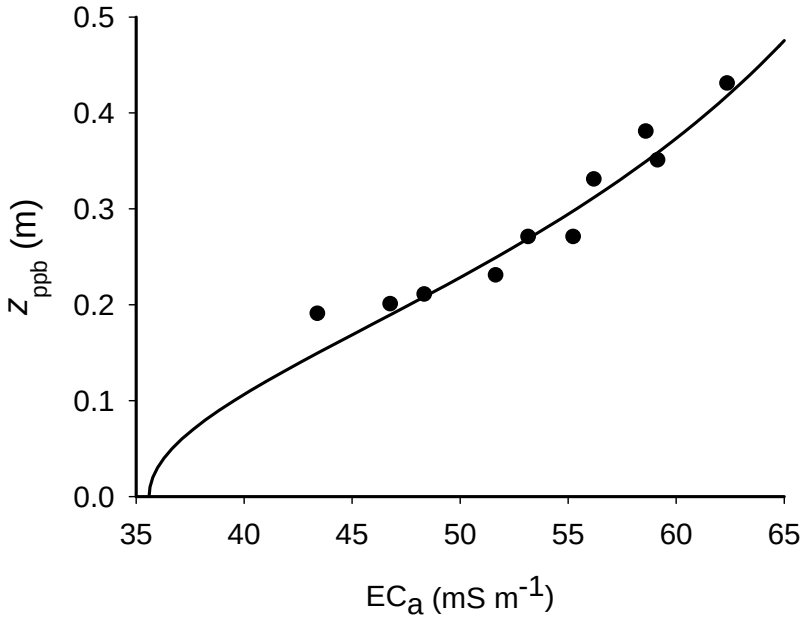

Figure 9.5. z_{ppb} as a function of EC_a along the transect AB with fitted cumulative depth response curve for the EM38-MK2 in 0.5 m intercoil distance in vertical orientation (n = 10).

The accuracy of the model to predict compaction depth was evaluated. Therefore, a validation transect (CD) was laid out (Fig. 9.3c) along which 18 observation locations separated by approximately 10 m were selected. A strong correlation (r = 0.87) between predicted (z_{ppb}^*) and measured depth (z_{ppb}) with low RMSEE and MEE values of 0.03 m and 0.04 m, respectively indicated that the methodology used was highly accurate with a low bias in predicting z_{ppb}^* (Fig. 9.6).

9.3.5 Water percolation

A compacted soil layer should be able to maintain a wet condition in the paddy field by decreasing water losses beyond the rooting zone. Therefore, the percolation measurements taken at 18 locations along the validation transect CD were used to interpret the thickness differences of the compacted layer. Percolation rates ranged from 8 mm day^{-1} to 32 mm day^{-1} with a mean of 18.3 mm day^{-1}. Fig. 9.7 shows the scatter plot of the percolation

measurements and the modeled thickness calculated as $z_{ppb}^{*} - z_{pp}^{*}$ along transect CD. The correlation coefficient, *r* between these two was 0.89. At locations where the compacted layer is thin, there is a higher risk of percolations losses accompanied by leaching losses of nutrients. Therefore, it is clear that increased vertical extent of the compacted layer as predicted by the model also had a strong link with percolation losses.

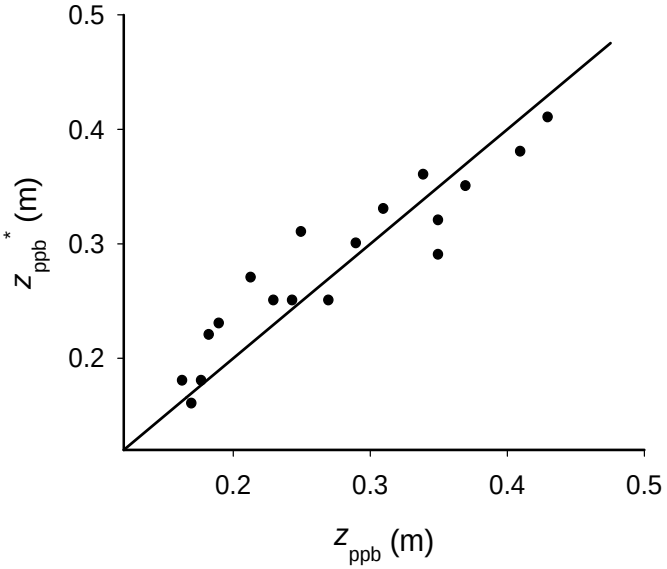

Figure 9.6. Predicted (z_{ppb}^{*}) and observed (z_{ppb}) depth to the interface between the compacted soil layer and the soil beneath the compacted layer along transect CD using 18 observations.

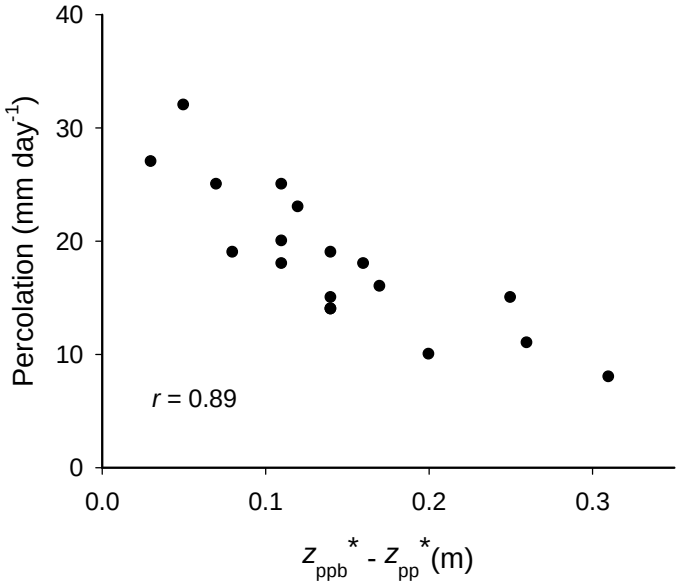

Figure 9.7. Predicted plough pan thickness ($z_{ppb}^{*} - z_{pp}^{*}$) and water percolation measurements observed on 18 locations along the validation transect (CD).

9.4 Conclusions

A uniformly deep compacted soil layer was not present at every location of the puddled paddy field. The EMI based floating sensing system proved to be successful in detailed measuring of the depth differences of the compacted layer within an inundated paddy field. Measurements with the EM38-MK2 in the vertical orientation with 0.5 m transmitter-receiver coil spacing are appropriate for investigating shallow soil depths in paddy fields. Hence, the thickness variability of the compacted soil layer could be modeled accurately showing an inverse relationship with water percolation losses.

To conclude, the combination of high density sensor measurements, coupled with limited direct observations is able to measure the vertical variability of the plough pan of an entire paddy field. This offers new opportunities for precise soil management in paddy rice cultivation system.

10

General conclusions and future research

10.1 Conclusions

Soils are naturally heterogeneous and highly variable. Spatial characterization facilitates understanding and managing the soil in an efficient and sustainable way. Detail soil information is required for this. The flooded conditions in paddy rice fields complicate the determination of soil information using direct methods. The resulting shortage of soil information under crop growing condition complicates its management. This thesis focuses on a novel topic of developing a floating soil sensing system to obtain high resolution soil information. The principal advantages of using this method for soil investigation are its ease and speed of use, potential relationship with soil properties to measure spatial variation in surface and subsoil. Several case studies were conducted in paddy rice fields of Bangladesh to assess the potentials of the system. As conclusion, this final chapter answers the research questions put forward in chapter 1. Some directions of future research are also given.

To reach the general aim, the following research questions were put forward:

Question: *Can a soil sensing system be offered for flooded field conditions?*
Yes.

In order to acquire high resolution soil data efficiently under paddy growing conditions, a Floating Sensing System (FloSSy) was developed and described in chapter 4.

The FloSSy consists of a soil sensor, the EM38 (or, the EM38-MK2) which does not require physical contact with the soil, so the sensor can be operated floating on water. Operating the sensor in the horizontal orientation, results in a depth of influence (DOI: the depth below the sensor at which 70 % of the cumulative influence of the signal is obtained) of about 0.75 m while the vertical orientation results in a DOI of about 1.5 m. Hence, with a water depth between 0.10 m and 0.25 m, sufficient influence of the soil beneath the water layer could be measured with a floating sensor. Consequently, the FloSSy meets the following criteria:

- It was designed to be used in flooded fields, even under seasonal rainy conditions. Therefore, the housing for all electronics and communication cables was made waterproof.
- The system has a GPS to provide the geographic locations of the recorded EC_a measurement.
- It is able to simultaneously store real time raw EC_a and GPS information and convert those to the format required by the user. This required a software component, the FloSSy processor, to function at fully automated on-the-go mode.
- The FloSSy processor displays the traversing path of the sensor in real time. Otherwise, it is impossible in a flooded field to track the previously measured path in order to keep a constant distance between measured lines.
- The sensor carrying platform is built with light weight material that can float on water. At the same time it is stable enough against water waves to prevent accidental turning over.

FloSSy made it possible to measure a field under flooded conditions. This dramatically increases the accessibility of paddy fields for site specific soil management using proximal soil sensing.

Question: *How is the quality of the EC_a data set obtained under flooded conditions?*

The signal of the EM38 sensor can be noisy which complicates the interpretation of the measured EC_a. In arable land this frequently occurs because of artefacts located near the surface soil layer. Chapter 5 entirely addressed this problem.

Under dry field conditions, the sensor platform was pulled over a soil surface wherein the uneven microtopography created a micro-scale variability in the measurements. This complicated the signal interpretation. Modeling the EC_a measurements with variography showed that the structural component of the variogram is small. On the other hand, flooded conditions provided a smooth water surface for the sensing platform which strongly reduced the short

distance variability in the EMI measurements. Consequently, in chapter 5 and 7 the EC_a measured under flooded conditions could be modeled with a strong structural component of the variogram. This gives a more realistic interpretation of soil variability.

Question: *Is there a benefit of surveying a field in flooded conditions compard to dry conditions?*

Yes, EC_a measurements taken under flooded conditions are more reliable.

Soil moisture variation has a strong influence on the sensor signal. This masks the actual soil variation and can result in misinterpretation of the soil property variability. Under flooded conditions soil moisture differences are removed and therefore moisture does not influence the variability of the sensor signal. So EC_a differences could be directly interpreted as soil property variation. This was proven in the studies in chapter 5 for the horizontal orientation and in chapter 7 for the vertical orientation of the EM38 sensor. Comparing dry and wet EC_a measurements showed the influence of the moisture variability. Relationships between soil texture and EC_a obtained under flooded conditions were more stable than those obtained under dry conditions. So, measuring a field under flooded conditions allows the soil EC_a response to be attributed stronger to variations in soil properties.

Although both dry and inundated surveys show a similar spatial structure of the EC_a values, measuring a field under two contrasting moisture conditions provide complementary information regarding the relationship between moisture dynamics and soil texture. This is key information for paddy cultivation because it helps understanding better the water percolation and leaching processes and thereby, adjustment of soil management practices can be benefitted from it.

Question: *Is it complementary to characterize top and sub soil properties?*

Yes.

EC_a surveys should be conducted in both horizontal (H) and vertical (V) orientations of the sensor in order to obtain soil information from both the top and sub-soil layers.

The top soil properties like organic matter content and soil texture can be appropriately identified using the H orientation as was done in chapter 4 and 5, respectively. However, crop management practices like tillage and soil organic matter management should be cautiously taken into account because the contribution of organic matter to explain soil conductivity variation can be important (chapter 4). The V orientation is more appropriate to identify variation in the sub-soil such as soil texture (chapter 7) and compaction (chapter 8). In this case the EC_a obtained in V orientation should be interpreted with caution. In flooded paddy field conditions more than one EC_a survey such as before and after puddling, is appropriate to identify the texture and compaction variations. As texture is a stable property which does not change by puddling practices, the change of compaction by puddling becomes clear in subsequent EC_a measurements. The cost for multiple EC_a surveys is not really a matter of concern as the floating sensing platform of the FloSSy can be easily towed by a typical paddy cultivator when operated for puddling and land preparation practices.

Question: *How does EC_a measured under flooded conditions provide information relevant for paddy field management and crop yield improvement?*

Precise soil management for crop yield improvement is preceded by delineation of management classes. In chapter 6 the EC_a measurements were classified to identify soil management classes. EMI can clearly reflect soil conditions differing in crop yield performances. This is because the soil factors controlling measured EC_a can delineate yield limiting soil factors when weather conditions are normal and input application is not limiting. The key

input for paddy cultivation is water. Therefore, in chapter 7 the EC_a classification was applied to identify water management classes. Management classes based on the unsupervised classification with fuzzy *k*-means serve three functions essential to precise soil management of paddy fields: they provide (i) a basis for soil sampling to assess soil attributes affecting yield; (ii) a means to identify the within class EC_a - yield relation to set yield goals on a class basis or field basis such as in chapter 6; (iii) a prescription map for adjustment of soil management practices. The first two are essential for determining the crop requirements while the last delineates the classes to which they will be applied. The delineation of management classes followed by precise puddling of paddy fields can reduce water losses through percolation. It has been mentioned in chapter 8 that the plough pan restricts water losses through percolation and increasing the degree of compaction of the plough pan is therefore one way of adjusting the soil management practices. However, the ability to delineate potential management classes is not sufficient to implement precise soil management. Therefore, the agronomic relevance of these classes needs to be validated by taking yield and water loss measurements as was done in chapters 6, 7 and 8.

Question: *Can apparent electrical conductivity be used to identify compaction variability?*

Yes.

The identification of soil compaction in paddy fields can be performed successfully with EMI-based measurements. In Chapter 8 we focused on investigating the potentials of the EM38 sensor, to identify differentially compacted areas within a paddy field in crop growing conditions. The dynamic changes of soil compaction could be clearly visualized on the EC_a maps. In practice, the sensing platform can be easily pulled by a cultivator while it is puddling a paddy field. Measuring the field during puddling provides information of soil compaction changes resulting from puddling. The physical process of compaction brings the soil particles in a closer state of contact. As a result, the size of an individual pore is decreased wherein the concentration of solution inside a pore is increased. Since the EM38 signal is

strongly influenced by electrolytes in solution, detection of compaction becomes possible.

Question: *Which sensor and signal is appropriate to model the variability of thickness of the compacted layer?*

Application of EMI technique combined with limited calibration observations is able to accurately model the variability of thickness of the compacted soil layer. The EMI sensor EM38 having a transmitter and one receiver coil at 1 m distance is a single signal instrument, providing one measurement of EC_a. To provide two measurements of EC_a focusing on two soil depths the sensor is operated in vertical (V) and horizontal (H) orientations, respectively. The EM38-MK2 is a multi-signal EMI sensor consisting of two receiver coils at 0.5 and 1 m distances from the transmitter. The theoretical depth of influence of these configurations is: 0.38 m for the H.5 orientation, 0.75 m for both the H1 and V.5 orientations (but with a different distribution of the depth sensitivity) and 1.50 m for the V1 orientation. The 0.75 m H1 and 1.5 m V1 of the EM38-MK2 are comparable to the output of EM38. Chapter 9 focuses on investigating the most appropriate signal to model the depth between the interfaces of soil layers having contrasting compaction. The V.5 orientation of the EM38-MK2 had the strongest link with the observed depths and is appropriate to accurately model the thickness of the compacted soil layer.

The sensor output was calibrated to the depth of the interface between contrasting layers using an empirical curve fitting approach. The procedure incorporated the depth response function proposed by McNeill (1980b) for the V0.5 configuration into the fitting process. At each calibration point the EC_a measurements could be fitted to the depth observations to account for the modelling parameters. The relationship was able to transform the high-resolution EC_a measurements into depth to the interfaces between the contrasting layers. The thickness of the compacted layer could be determined by subtracting the depth to the interface between the compacted layer and the soil material beneath from the depth to the interface between the puddled layer and the compacted layer.

10.2 Impact of conclusions

This thesis clearly illustrated the fact that SSSM for paddy cultivation is possible. FloSSy demonstrated the potential of proximal soil sensing technology to improve the management of paddy rice fields to optimize crop production. As EC_a reflects variation in soil properties, obtaining EC_a data from paddy fields can provide valuable soil information that can be used for SSSM. FloSSy allows recording of georeferenced soil EC_a at a high resolution beneath the standing water layer within paddy fields. This overcomes the major barrier to obtain exhaustive soil information within a paddy field not only in real time but also under crop growing conditions. Furthermore, the variability of soil properties can be indentified more accurately as the quality of EC_a measurements obtained under flooded conditions is better. Soil information obtained in crop growing conditions is more relevant for soil management applications than information obtained under dry conditions. Thus FloSSy makes the characterization of flooded paddy fields possible.

FloSSy provides an opportunity to upgrade the scales of the existing soil maps and to make them suitable for providing soil information detailed enough for SSSM. The existing soil maps of paddy growing countries often are unable to provide detailed information on paddy fields to use for SSSM. For instance, the 1:50 000 choropleth or polygon soil maps of Bangladesh are the most detail source of soil information available to date for making soil management decisions by the end users. However, these maps are not available for the entire country and therefore, the most frequently used maps are 1:100 000 soil maps (Brammer, 1986). The predictive quality of these polygon soil maps is determined by the map scale which is the ratio of the distance on the printed map to the corresponding distance on the land. Concerning the data requirements of SSSM, the map scale is required to be detailed enough to discern within field variations of soil attributes. Currently, the land area that is represented as a management unit on the choropleth map at a given scale on the map is the basis for paddy field management. To illustrate, if we assume a paddy field size of 0.7 ha in Bangladesh, a map prepared at a scale of 1:7 000 could be merely enough to represent the respective field as a single management unit, interestingly, without focusing into further detail for SSSM. In other words, the finest resolution of this map is even coarser than the average size of an individual paddy field (0.5 ha to 0.8 ha) owned by a typical paddy farmer in most paddy growing countries. This explains the underlying reason for assuming the paddy fields on the Brahmaputra floodplain homogeneous (according to soil survey reports) while

introducing several chapters of this thesis. However, using FloSSy it is possible have soil information from sub-metre level within a field to produce detailed soil maps. The scale of these maps is detail enough to decipher a management unit (class) because management classes are delineated based on the structure of spatial continuity of soil property variation. For SSSM, the predictive quality of these maps in relation to soil information resources is not limited to field scale but could be extended to land suitability classification on a regional scale.

In contrast to the available soil information, our research showed that paddy fields are complex dynamic soil systems composed of several layers and textural heterogeneity. Moreover, anthropogenic activities like land preparation (puddling) and organic matter management can frequently complicate the identification of the actual source of EC_a variation. Therefore, the depth and nature of soil manipulation related to crop management aspects needs to be considered carefully before planning an EC_a survey. The research in chapter 4 and 5 focused on top soil properties (field 1) which are manipulated by soil tillage. Eventually, the horizontal orientation of the sensor was considered. Separate EC_a surveys were conducted under flooded conditions: (i) natural field conditions i.e. just after paddy harvest when the field received no land preparation practices or incorporation of crop residues and organic substances for the next crop (chapter 5) and (ii) puddled field conditions i.e. after land preparation and incorporation of organic substances (chapter 4) for planting of the next crop. Interestingly, the EC_a survey results revealed the two different scenarios. Consequently, the reflection of soil management to explain EC_a variation became clear. Soil organic matter variation appeared as the major driving force of EC_a in chapter 4 because the preparatory tillage before conducting the EC_a survey actually influenced the spatial variability of soil organic matter. On the other hand, in chapter 5, textural differences became more important to explain the EC_a variation because the EC_a measurements on the flooded field were done before the preparatory tillage.

In paddy fields, the soil below the ploughed layer is expected to be less manipulated by crop management practices. Therefore, EC_a maps focusing on subsoil depths and thereby investigation of subsoil properties were also taken into account. Chapters 6 and 7 are focused on the delineation of management classes so that the delineated classes could be considered as units for SSSM of paddy rice fields. The vertical orientation of the sensor was appropriate as this orientation is less influenced by materials near the soil surface. Equally, soil sampling

required for validation and explanation of EC_a variation were deeper beneath the ploughed layer. In chapter 6, the management classes were linked to soil bulk density variation because the field (field 2) had already undergone through the usual process of land preparation (puddling) which also influenced bulk density of the soil beneath the ploughed layer. Among the delineated 3 classes, the least productive class (class-1, in terms of paddy yield) reflected the requirement for an additional puddling or higher subsoil compaction to achieve a higher yield. Chapter 7 described a methodological approach to delineate stable management classes for water management within a paddy field (field 1). Therefore, the EC_a survey of the flooded field needed to be in advance of land preparation. This allowed the EC_a measurements to remain uninfluenced by a tillage induced bulk density difference. As such, textural variation of the subsoil could explain the EC_a variation which in turn facilitated the identification of management classes having a difference in water permeability. These management classes would allow the precise management of soil water resources during the developmental stages of crop growth. Considering the two management classes delineated in chapter 7 it would be obvious to practice site specific soil water management approach. Thus, irrigation scheduling for the same paddy crop within the field would be different for the different management classes. In practice, the delineated classes need to be bunded along their class boundary so that irrigation scheduling would be indifferent within a class while different across the classes.

Given a limited soil texture difference, FloSSy allowed to proceed a step further in investigating the soil bulk density differences linked to soil compaction, a key soil property for paddy rice fields. EC_a observations obtained with the FloSSy provided abundant information which could be strongly linked to the soil bulk density and compaction differences and was explained to be a result of puddling differences in chapter 8. The identification of compaction variability of the plough pan is crucial for adjustment of land preparation practices before planting of rice. This facilitates the adjustment of puddling practices and the management of paddy fields in a precise way unprecedented before. As such, a puddling guidance mapping system could be devised for the farmers to focus on particular areas within a field which would require a more intensive puddling to achieve a certain level of subsoil compaction. In chapter 9, modeling the thickness differences of the compacted layer with great accuracy would certainly add an extra value to account in detail for mismanagement of preparatory tillage inputs. Thus, a critical value for the plough pan thickness could be recommended for a particular paddy field, considering the spatial texture

variation, below which puddling could be required and above which the requirements would be relaxed to reduce costs of paddy production inputs.

Finally, it is estimated by IRRI that by the year 2020 the annual demand for rice will reach 820 million tons as world population swells above 8 billion, more than half of whom will be rice consumers. This production increase of almost 50% will have to be achieved on about the same amount of paddy land than is cultivated today - or even less! From a yield sustainability standpoint, traditional wetland rice cultivation has been extremely successful. Moderately stable yields have been maintained for thousands of years without deterioration of the environment. But maintaining the sustainability of rice producing environments in the face of increased demands will require new concepts and agricultural practices, which, in turn, will require increased knowledge of crop and soil management. In this context, the non-invasive soil sensing system FloSSy proved its potential for soil management of paddy fields. As the worldwide floodplain alluvial soils constitute a valuable source of natural resources to support paddy farming, extrapolation of the findings of this research beyond Bangladesh can bring about a significant improvement in paddy cultivation system across the globe.

10.3 Future research

A soil sensor provides a large amount of soil data in a relatively fast and economic way. However, no single sensor can identify all soil properties because every sensor has its potential and limitations. Combining complementary signals is expected to obtain more inferences than can be derived from a single sensor. A multi-sensor approach to have complementary sensor signals should therefore be supported. The research focus should be on combining multiple, simultaneous signals and on the integration of multiple sensors in one sensing configuration. The integration of multiple EC_a measurements can provide information from different soil volumes and can help greater understanding of different soil strata. For instance, the integration of multiple EMI signals from EM38-MK2 and DUALEM-21S could provide precise thickness approximation of the contrasting soil layers. This could eventually reduce the effort of sampling observations for calibration. However, the simultaneous processing of multiple sensor signals, analysis of large amount of data and interpretation would require much effort. New data analyzing techniques should be explored in this context. Methods focusing on information extraction, data fusion and filtering of anomalies in the situation of high resolution multi-dimensional sensor data demand a priority.

Artificial neural networks as a data fusion method and principal component analysis as an information extraction method appear as potential techniques for proximally sensed soil data.

Another idea for future research refers to the areal extent of the study. In this thesis the focus was on within field level. However the potential of the system is not limited and definitely has potential on a landscape and regional level. A major challenge is to integrate the EC_a obtained from different fields and/or at different times in order to determine the appropriate management decisions on a site specific basis. Understanding of soil processes like water percolation, leaching and pore functioning during soil compaction; water balance studies and their simulation modeling can be an approach to achieve this target. With this approach the puddling requirement to achieve a certain level of compaction, water requirement for given paddy field, leaching potential could be quantified and adjusted.

The research could be further extended with additional layers of information on soil and crop attributes. Fusion of available optical e.g. Vis-NIR and chemical e.g. pH sensors could be considered for adaptation and use under wet soil conditions. Likewise, extending the research beyond the boundaries of a field implies going to landscape level. Obtaining detail information on landscape elevation would be essential. Incorporation of LiDAR and remote sensing as source of information on landscape topography appears to be a good option. As the result of soil management practices is judged by evaluating crop productivity and yield, detail information on crop yield should be made available. Yield monitors are able to provide information on crop yield at fine resolution, therefore, can present the whole field scenario in terms of result. Thereafter, a total system analysis could be used including: i) the improvements in economic and/or environmental aspects of crop production, ii) an agro-economical analysis exploring the added value due to improved management of soil, water, machinery, and/or use of agrochemicals, so as to optimize the management practices and to set yield goals in a sustainable and eco-friendly way.

Bibliography

Abdu H., Robinson D.A. and Jones B. 2007. Comparing bulk soil electrical conductivity determination using the DUALEM-1S and EM38-DD electromagnetic induction instruments. Soil Science Society of America Journal, 71: 189-196.

Adamchuk V.I. and Jasa P.J. 2002. On-the-go vehicle-based soil sensors. Precision Agriculture Extension Circular EC 02-178. Lincoln, Nebraska: University of Nebraska Cooperative Extension. USA.

Adamchuk V.I., Hummel J.W., Morgan M.T. and Upadhyaya S.K. 2004. On-the-go soil sensors for precision agriculture. Computers and Electronics in Agriculture, 44: 71-91.

Adamchuk V.I., Viscarra Rossel R.A., Marx D.B. and Samal A.K. 2011. Using targeted sampling to process multivariate soil sensing data. Geoderma, 163: 63-73.

Alam M.L., Saheed S.M., Shinagawa A. and Miyauchi N. 1993. Chemical properties of general soil types of Bangladesh. Memoirs of the Faculty of Agriculture, Kagoshima University, 29: 75-87.

Allred B.J., Ehsani M.R. and Saraswat D. 2005. The impact of temperature and shallow hydrologic conditions on the magnitude and spatial pattern consistency of electromagnetic induction measured soil electrical conductivity. Trans. ASAE, 48: 2123-2135.

Atherton B.C., Morgan M.T., Shearere S.A., Stombawgh T.S. and Ward A.D. 1999. Site-specific farming: a perspective on information needs, benefits and limitations. Journal of Soil and Water Conservation, 54: 455-461.

Bezdek J.C. 1981. Pattern Recognition with Fuzzy Objective Function Algoritms, Plenum Press, New York

Booltink H.W.G., Verhagen J., Bouma J. and Thornton P.K. 1996. Application of simulation models and weather generators to optimize farm management strategies. In: Robert P. C., Rust R. H. and Larson W. E. (Eds.), Precision Agriculture: Proceedings of the Third International Conference on Precision Agriculture. Madison, Wis.: American Society of Agronomy, Crop Science Society of America, and Soil Science Society of America, pp. 343-360.

Bouman B.A.M. and Tuong T.P. 2001. Field water management to save water and increase its productivity in irrigated lowland rice. Agricultural Water Management, 49: 11-30.

Brady N.C. and Weil R.R. 2000. Elements of the nature and properties of soils. Prentice-Hall, Upper Saddle River, NJ.

Brammer H. 1981. Reconnaissance Soil Survey of Dhaka District. Revised Edition. Soil Resources Development Institute, Dhaka, Bangladesh, pp. 6-19.

Brammer H. 1986. Classification of the soils of Bangladesh in the Legend for the FAO/UNESCO soil map of the world. Soil Resources Development Institute, Dhaka 222p.

Brammer H. 1996. The geography of the soils of Bangladesh. The University Press Limited, Dhaka 1000, Bangladesh, p. 25.

Brevik E.C. and Fenton T.E. 2002. Influence of soil water content, clay, temperature, and carbonate minerals on soil electrical conductivity readings taken with an EM-38. Soil Survey Horizons, 43: 9-13.

Brevik E.C. and Fenton T.E. 2004. The effect of changes in bulk density on soil electrical conductivity as measured with the Geonics EM-38. Soil Survey Horizons, 45: 96-102.

Brevik E.C., Fenton T.E. and Lazari A. 2006. Soil electrical conductivity as a function of soil water content and implications for soil mapping. Precision Agriculture, 7: 393-404.

Cannon M.E., McKenzie R.C. and Lachapelle G.P. 1994. Soil salinity mapping with electromagnetic induction and satellite-based navigation methods. Canadian Journal of Soil Science, 74: 335-343.

Carter L.M., Rhoades J.D. and Chesson J.H., 1993. Mechanization of soil salinity assessment for mapping. Paper 93-1557, ASAE, St Joseph, MI, USA.

Casady W.W. and Adamchuk V.I., 2003. Global positioning system and GPS receivers in agriculture. In: Heldman D.R. (Ed.), Encyclopedia of Agricultural, Food, and Biological Engineering, 444-446. New York, New York: Marcel Dekker, Inc. USA.

Chang J., Clay D.E., Carlson C.G., Clay S.A., Malo, D.D., Berg R., Kleinjan J. and Weibold W. 2003. Different techniques to identify management zones impact nitrogen and phosphorus sampling variability. Agronomy Journal, 95: 1550-1559.

Chang J., Clay D.E., Carlson C.G., Reese C.L., Clay S.A. and Ellsbury M.M. 2004. Defining yield goals and management zones to minimize yield and N and P fertilizer recommendation errors. Agronomy Journal, 96: 825-831.

Cline M.G. 1949. Basic principles of soil classifications. Soil Science, 2: 81-91.

Cockx L., Van Meirvenne M. and Hofman G. 2005. Characterization of nitrogen dynamics in a pasture soil by electromagnetic induction. Biology and Fertility of Soils, 42: 24-30.

Cockx L., Van Meirvenne M., Vitharana U.W.A., Verbeke L.P.C., Simpson D., Saey T. and Van Coillie F.M.B. 2009. Extracting topsoil information from EM38DD sensor data using a neural network approach. Soil Science Society of America Journal, 73: 2051-2058.

Cook P.G. and Walker G.R. 1992. Depth profiles of electrical conductivity from linear combinations of electromagnetic induction measurements. Soil Science Society of America Journal, 56:1015-1022.

Cook P.G. and Williams B.G. 1998. Electromagnetic induction techniques. In: Zhang L. and Walker G. (Eds.) Studies in catchment hydrology: The basics of recharge and discharge. CSIRO Publishing, Australia, pp. 1-16.

Corwin D.L. 2004. Geospatial measurements of apparent soil electrical conductivity for characterizing soil spatial variability. In: Alvarez-Benedi J. and Munoz-Carpena R. (Eds.), Soil-Water-Solute Process Characterization. CRC Press, Boca Raton, FL, USA, pp. 639-672.

Corwin D.L. and Lesch S.M. 2003. Application of soil electrical conductivity to precision agriculture: theory, principles, and guidelines. Agronomy Journal, 95: 455-471.

Corwin D.L. and Lesch S.M. 2005a. Apparent soil electrical conductivity measurements in agriculture. Computers and Electronics in Agriculture, 46: 11-43.

Corwin D.L. and Lesch S.M. 2005b.Characterizing soil spatial variability with apparent soil electrical conductivity I. Survey Protocols. Computers and Electronics in Agriculture, 46, 103-133.

Corwin D.L., Lesch S.M. and Farahani H.J. 2008. Theoretical insight on the measurement of soil electrical conductivity. In: Allred B.J., Daniels J.J. and Ehsani M.R. (Eds.), Handbook of Agricultural Geophysics. CRC Press, Boca Raton, USA, pp. 59-83.

Davis J.G., Kitchen N.R., Sudduth K.A. and Drummond S.T. 1997. Using Electromegnatic Induction to Characterize Soils. Better Crops and Plant Food. No. 4. Potash and Phosphate Institute.

De Datta S.K. 1981. Principles and Practices of Rice Production. Wiley-Interscience, New York, pp. 618.

de Gruijter J.J. and McBratney A.B. 1988. A modified fuzzy k-means method for predictive classification. In: Bock H.H. (Ed.), Classification and Related Methods of Data Analysis, Elsevier, Amsterdam, pp. 97-104.

Dilke O.A.W. 1985. Greek and Roman Maps. Thames and Hudson, London.

Dobermann A., Ping J., Adamchuk V.I., Simbahan G.C. and Ferguson R.B. 2003. Classification of crop yield variability in irrigated production fields. Agronomy Journal 95: 1105-1120.

Doolittle J.A., Noble C. and Leinard B. 2000. An electromagnetic induction survey of a riparian area in southwest Montana. Soil Survey Horizons, 41: 27-36.

Doolittle J.A., Sudduth K.A., Kitchen N.R. and Indorante S.J. 1994. Estimating depths to claypans using electromagnetic induction methods. Journal of Soil and Water Conservation, 49: 572-575.

Doolittle J.A., Sudduth K.A., Kitchen N.R. and Indorante S.J. 1994. Estimating depths to claypans using electromagnetic induction methods. Journal of Soil and Water Conservation, 49: 572-575.

Dorling D. and Fairbairn D. 1997. Mapping: Ways of representing the World. Addison Wesley Longman Ltd., Harlow.

Earl R., Taylor J.C., Wood G.A., Bradley I., James I.T., Waine T., Welsh J.P., Godwin R.J. and Knight S.M. 2003. Soil factors and their influence on within-field crop variability, part 1: Field observation of soil variation. Biosystems Engineering, 84: 425-440.

Eswaran H., Moncharoen P., Reich P. and Padmanaban E. 2001. Rice, land and people: the faltering nexus in Asia. Proceedings of the 5th Conference of the East and Southeast Asia. Federation of Soil Science Societies, Krabi, Thailand. Bangkok (Thailand): Department of Agriculture, pp. 38-66.

Ezrin M.H., Amin M.S.M., Anuar A.R. and Aimrun W. 2010. Relationship between rice yield and apparent electrical conductivity of paddy soils. American Journal of Applied Sciences, 7: 63-70.

Ferguson R.B., Hergert G.W., Schepers J.S., Gotway C.A., Cahoon J.E. and Peterson T.A. 2002. Site-specific nitrogen management of irrigated maize: Yield and soil residual nitrate effects. Soil Science Society of America Journal, 66: 544-553.

Gajri P.R., Gill K.S., Singh R. and Gill B.S. 1999. Effect of pre-planting tillage on crop yields and weed biomass in a rice-wheat system on a sandy loam soil in Punjab. Soil and Tillage Research, 52: 83-89.

Geonics Limited. 2003. EM38-ground conductivity meter operating manual. Mississauga, Ontario, Canada.

Gibbons G. 2000. Turning a farm art into science- an overview of precision farming. URL: http://www.precisionfarming.com.

Goering C.E. 1993. Recycling a concept. Agricultural Engineering Magazine. November. St. Joseph, Mich., American Society of Agricultural Engineering.

Goovaerts P. 1997. Geostatistics for Natural Resources Evaluation. Oxford University Press, New York.

Goovaerts P., Webster R. and Dubois J.P. 1997. Assessing the risk of soil contamination in the Swiss Jura using indicator geostatistics. Environmental and Ecological Statistics, 4: 31-48.

Green T.R., Salas J.D., Martinez A. and Erskine R.H. 2007. Relating crop yield to topographic attributes using spatial analysis neural networks and regression. Geoderma, 139: 23-27.

Greenhouse J.P. and Slaine D.D. 1983. The use of reconnaissance electromagnetic methods to map contaminant migration. Ground Water Monitoring Review, 3: 47-59.

Hedley C.B., Yule I.J., Eastwood C.R., Shepherd T.G. and Arnold G. 2004. Rapid identification of soil texture and management zones using electromagnetic induction sensing of soils. Australian Journal of Soil Research, 42: 389-400.

Hemmat A. and Adamchuk V.I. 2008. Sensor systems for measuring soil compaction: review and analysis. Computers and Electronics in Agriculture, 63: 89-103.

Hendrickx J.M.H. and Kachanoski R.G. 2002. Solute content and concentration: Indirect measurement of solute concentration: Nonintrusive electromagnetic induction. In: Dane J. H. and Topp G. C. (Eds.), Methods of Soil Analysis, Part 4: Physical Methods. SSSA, Madison, Wisc. USA, pp. 1297-1306.

Hergert G.W., Pan W.L., Huggins D.R., Grove J.H. and Peck T.R. 1997. Adequacy of current fertilizer recommendations for site-specific management. In: Pierce F.J. and Sadler E.J. (Eds.), The state of site-specific management for agriculture. American Society of Agronomy, Crop Science Society of America, and Soil Science Society of America, Madison, Wisc., USA, pp. 283-300.

Hezarjaribi A. and Sourell H. 2007. Feasibility study of monitoring the total available water content using non-invasive electromagnetic induction-based and electrode based soil electrical conductivity measurements. Irrigation and Drainage, 56: 53-65.

Hollands K.R. 1996. Relationship of nitrogen and topology. In: Robert P.C., Rust R.H. and Larson W.E. (Eds.), Precision agriculture: Proceedings of the third international conference on precision agriculture, Madison, Wisc.: American Society of Agronomy, Crop Science Society of America and Soil Science Society of America, pp. 3-12.

Hummel J.W., Gaultney L.D. and Sudduth K.A. 1996. Soil property sensing for site-specific crop management. Computers and Electronics in Agriculture 14: 121-136.

IRRI. 1987. Physical measurements in flooded rice soils: The Japanese methodologies. International Rice Research Institute, Los Ban˜os, P.O. Box 933, Manila, The Philippines.

IRRI. 2002. World rice statistics, 2002. International Rice Research Institute, Los Ban˜os, P.O. Box 933, Manila, The Philippines.

Isaaks E.H. and Srivastava R.M. 1989. An introduction to applied geostatistics. Oxford University Press. New York.

Islam M.M. and Van Meirvenne M. 2011. FloSSy: A floating sensing system to evaluate soil variability of flooded paddy fields. In: Stafford J.V. (Ed.), Precision Agriculture 2011 Czech Centre for Science and Society, Prague, Czech Republic, pp. 60-66.

Islam M.M., Cockx L., Meerschman E., De Smedt P., Meeuws F. and Van Meirvenne M. 2011a. A floating sensing system to evaluate soil and crop variability within flooded paddy rice fields. Precision Agriculture, 12: 850-859.

Islam M.M., Meerschman E., Cockx L., De Smedt P., Meeuws F. and Van Meirvenne M. 2011b. Comparison of apparent electrical conductivity measurements on a paddy field under flooded and drained conditions. In: Stafford J.V. (Ed.), Precision Agriculture 2011 Czech Centre for Science and Society, Prague, Czech Republic, pp. 43-50.

Islam M.M., Meerschman E., Saey T., De Smedt P., Van De Vijver E. and Van Meirvenne M. 2012. Comparing apparent electrical conductivity measurements on a paddy field under flooded and drained conditions. Precision Agriculture, 13: 384-392.

Islam M.M., Saey T., Meerschman E., De Smedt P., Meeuws F., Van De Vijver E. and Van Meirvenne M. 2011c. Delineating water management zones in a paddy rice field using a floating soil sensing system. Agricultural Water Management, 102: 8-12.

Jain A.K. and Dubes R.C. 1988. Algorithms for clustering data. Prentice-Hall advanced reference series. Prentice-Hall, Inc., Upper Saddle River, NJ.

Jaynes D.B. 1996. Improved soil mapping using electromagnetic induction surveys. In: Proceedings of the 3rd International Conference on Precision Agriculture, Minneapolis, Minnesota, USA. pp. 169-179.

Jaynes D.B., Colvin T.S. and Kaspar T.C. 2005. Identifying potential soybean management zones from multi-year yield data. Computers and Electronics in Agriculture, 46: 309-327.

Jaynes D.B., Novak J.M., Moorman T.B. and Cambardella C.A. 1994. Estimating herbicide partition coefficients from electromagnetic induction measurements. Journal of Environmental Quality, 24: 26-41.

Jenny H. 1941. Factors of soil formation. McGraw-Hill, New York.

Jensen J.R. 2007. Remote sensing of the environment: An earth resource perspective. Prentice Hall, Upper Saddle River, New Zealand.

Kachanoski R.G., de Jong E. and Van Wesenbeeck I.J. 1990. Field scale patterns of soil water storage from non-contacting measurements of bulk electrical conductivity. Canadian Journal of Soil Science, 70: 537-541

Kachanoski R.G., Gregorich E.G. and Van Wesenbeeck I.J. 1988. Estimating spatial variations of soil water content using noncontacting electromagnetic inductive methods. Canadian Journal of Soil Science, 68: 715-722.

Kawasaki K. and Osterkamp T.E. 1988. Mapping shallow permafrost by electromagnetic induction- practical considerations. Cold Regions Science and Technology, 15: 279-288.

Kellogg C.E. 1957. We seek; we learn. In: Stefferud A. (Ed.), The yearbook of agriculture soil. USDA. Washington, DC: US Government Printing Office. pp. 1-11.

Kevien C. and Pocknee S. 2000. Introduction to why management zone. National Environmentally Sound Production Agriculture Laboratory (NESPAL), College of Agricultural and Environmental Science, The University of Georgia.

Killorn R.J., Voss R.D. and Hornstein J.S. 1995. Nitrogen fertilizer management studies, 1987-1991. In: Integrated farm management demonstration program comprehensive report. Ames, Iowa: Iowa State University, pp. 2.3-2.15.

Kogel-Knabner I., Amelung W., Cao Z.H., Fiedler S., Frenzel P., Jahn R., Kalbitz K., Kolbl A. and Schloter M. 2010. Biogeochemistry of paddy soils. Geoderma, 157: 1-14.

Kukal S.S. and Aggarwal G.C. 2003. Puddling depth and intensity effects in rice-wheat system on a sandy loam soil. I. Development of subsurface compaction. Soil and Tillage Research, 72: 1-8.

Kukal S.S. and Sidhu A.S. 2004. Percolation losses of water in relation to pre-puddling tillage and puddling intensity in a puddled sandy loam rice (*Oryza sativa*) field. Soil and Tillage Research, 78: 1-8.

Kyuma K. 2004. Paddy soil science. Kyoto University Press. p. 280. Kyoto, Japan.

Kyuma K. 2005. Paddy soils around the world. In: Toriyama K., Heong K.L. and Hardy B. (Eds.), Rice is Life: Scientific Perspectives for the 21st Century: Proceedings of the World Rice Research Conference. International Rice Research Institute, Tsukuba, Japan, pp. 542-545.

Lark R.M. 1998. Forming spatially coherent regions by classification of multivariate data. International Journal of Geographical Information Science 12: 83-98.

Lark R.M. 2005. Exploring scale-dependent correlation of soil properties by nested sampling. European Journal of Soil Science, 56: 307-317.

LeClerg E.L., Leonard W.H. and Clark A.G. 1962. Field plot technique. 2nd ed. Minneapolis, Minn.: Burgess Publishing Company.

Li Y., Shi Z., Li F. and Li Hong-Yi 2007. Delineation of site-specific management zones using fuzzy clustering analysis in a coastal saline land. Computers and Electronics in Agriculture, 56: 174-186.

Lund E.D., Christy C. and Drummond P. 1999. Practical applications of soil electrical conductivity mapping, p. 771-779, In: Stafford J.V. (Ed.), Precision Agriculture '99, Proceedings of the 2nd European Conference on Precision Agriculture, Odense, Denmark, 11-15 july 1999. Sheffield Academic Press, UK.

Malicki M.A. and Walczak R.T. 1999. Evaluating soil salinity status from bulk electrical conductivity and permittivity. European Journal of Soil Science, 50: 505-514.

Malicki M.A., Campbell E.C. and Hanks R.J. 1989. Investigations on power factor of the soil electrical impedance as related to moisture, salinity, and bulk density. Irrigation Science, 10: 55-62.

Marquardt D. 1963. An algorithm for least-squares estimation of nonlinear parameters. SIAM Journal of Applied Mathematics, 11: 431-441.

Martinez G., Vanderlinden K., Ordonez R. and Muriel J.L. 2009. Can apparent electrical conductivity improve the spatial characterization of soil organic carbon? Vadose Zone Journal, 8: 586-593.

Matheron G. 1962. Traité de Géostatistics Appliqué, Tome 1. Memoires du Bureau de Recherches Geologiques et Minières, Paris.

McBratney A.B. 1992. On variation, uncertainty and informatics in environmental soil-management. Australian Journal of Soil Research, 30: 913-935.

McBratney A.B. and Moore A.W. 1985. Application of fuzzy sets to climate classification. Agricultural and Forest Meteorology, 35: 165-185.

McBride R.A., Gordon A.M. and Shrive S.C. 1990. Estimating forest soil quality from terrain measurements of apparent electrical conductivity. Soil Science Society of America Journal, 54: 290-293.

McDonald A.J., Riha S.J., Duxbury J.M., Steenhuis T.S. and Lauren J.G. 2006. Soil physical responses to novel rice cultural practices in the rice-wheat system: comparative evidence from a swelling soil in Nepal. Soil and Tillage Research, 86: 163-175.

McKenzie N., Bramley R., Farmer T., Janik L., Murray W., Smith C. and McLaughlin C. 2003. Rapid soil measurement- a review of potential benefits and opportunities for the Australian grains industry. Client report for the Grains Research & Development Corporation, GRDC Contract No: CSO00027. GRDC / CSIRO Land and Water, Canberra.

McKenzie R.C., George R.J., Woods S.A., Cannon M.E. and Bennett D.L. 1997. Use of the electromagnetic-induction meter (EM38) as a tool in managing salinization. Hydrogeology Journal, 5: 37-50.

McNeill J.D. 1980a. Electromagnetic terrain conductivity measurement at low induction numbers: Geonics Ltd. Tech. Note TN-6. Mississauga, ON.

McNeill J.D. 1980b. Electrical conductivity of soils and rocks. Technical Note TN-5, Geonics Limited, Missisauga, ON, Canada.

McNeill J.D. 1986. Rapid, accurate mapping of soil salinity using electromagnetic ground conductivity meters: Geonics Ltd. Tech. Note TN-18. Mississauga, ON.

McNeill J.D. 1992. Rapid, accurate mapping of soil salinity by electromagnetic ground conductivity meters. p. 209-229. In: Advances in measurement of soil physical properties: Bringing theory into practice. SSSA Spec. Publ. 30. SSSA, Madison, WI.

Meul M. and Van Meirvenne M. 2003. Kriging soil texture under different types of nonstationarity. Geoderma, 112: 217-233.

Meyer de Stadelhofen C. 1991. Applications of geophysics in the searches of water. (In French.) Lavoisier.

Minasny B. and McBratney A.B. 2006. FuzME version 3. Australian Centre for Precision Agriculture. The University of Sidney NSW.

Mohanty M., Painuli D.K. and Mandal K.G. 2004. Effect of puddling intensity on temporal variation in soil physical conditions and yield of rice (*Oryza sativa* L.) in a Vertisol. Soil and Tillage Research, 76: 83-94.

Moormann F.R and van Breemen N. 1978. Rice: soil, water, land. International Rice Research Institute, Los Ban˜os, Philippines, 185 pp.

Mueller T.G., Hartsock N.J., Stombaugh T.S., Shearer S.A., Cornelius P.L. and Barnhisel R.I. 2003. Soil electrical conductivity map variability in lime stone soils overlain by loess. Agronomy Journal, 95: 496-507.

Mueller T.G., Mijatovic B., Sears B.G., Pusuluri N. and Stombaugh T.S. 2004. Soil electrical conductivity map quality. Soil Science, 169: 841-851.

Mzuku M., Khosla R., Reich R., Inman D., Smith F. and Macdonald L. 2005. Spatial variability of measured soil properties across site-specific management zones. Soil Science Society of America Journal, 69: 1572-1579.

Nadler A. 1982. Estimating the soil water dependence of the electrical conductivity soil solution/electrical conductivity bulk soil ratio. Soil Science Society of America Journal, 46: 722-726.

National Instruments. 2003. LabVIEW: Getting Started with LabVIEW: April 2003 edition. 11500 North Mopac Expressway Austin, Texas 78759-3504 USA.

Panissod C., Dabas M., Jolivet A. and Tabbagh A. 1997. A novel mobile multipole system (MUCEP) for shallow (0-3 m) geoelectrical investigation: the 'Vol-de-canards' array. Geophysical Prospecting, 45: 983-1002.

Pena-Yewtukhiw E.M., Grove J.H. and Beck E.G. 2000. Nonparametric geostatistics/probabilistic sourcing of nitrate to a contaminated well. In: Proceedings of fifth international conference on precision agriculture (cd), Bloomington, MN, USA.

Perumpral J.V. 1987. Cone penetrometer applications: A review. Transactions of the American Society of Agricultural Engineers, 30: 939-944.

Playán E., Pérez-Coveta O., Martínez-Cob A., Herrero J., García-Navarro P., Latorre B., Brufau P. and Garcés J. 2008. Overland water and salt flows in a set of rice paddies. Agricultural Water Management, 95: 645-658.

Prihar S.S., Khera, K.K. and Gajri, P.R. 1975. Effect of puddling with different implements on the water and yield of paddy. J. Res. Punjab Agric. Univ. 13:249-254.

Rhoades J.D. 1990a. Soil salinity: Causes and controls. p. 109-134. In Goudie A.S. (Ed.), Techniques for desert reclamation. John Wiley & Sons, New York.

Rhoades J.D. 1990b. Overview: diagnosis of salinity problems and selection of control practices. p. 18-41. In Tanji K.K. (Ed.), Agricultural salinity assessment and management. ASCE Manuals Pract. No. 71. American Society of Civil Engineers.

Rhoades J.D. 1992. Instrumental field methods of salinity appraisal. In: Advances in Measurement of Soil Physical Properties: Bringing theory into Practice, pp. 231-248, Soil Science Society of America, Madison, WI, USA. Special Publication No. 30.

Rhoades J.D. and Corwin D.L. 1990. Soil electrical conductivity: Effects of soil properties and application to soil salinity appraisal. Communications in Soil Science and Plant Analysis, 21: 837-860.

Rhoades J.D. and Ingvalson R.D. 1971. Determining salinity in field soils with soil resistance measurements. Soil Science Society of America Proceedings, 35: 54-60.

Rhoades J.D., Chanduvi F. and Lesch S.M. 1999. Soil Salinity Assessment: Methods and Interpretation of Electrical Conductivity Measurements. FAO Rep. 57. FAO, Rome, Italy.

Rhoades J.D., Manteghi N.A., Shouse P.J. and Alves W.J. 1989. Soil electrical conductivity and soil salinity: New formulations and calibrations. Soil Science Society of America Journal, 53: 433-439.

Rhoades, J.D., Raats, P.A., Prather, R.J., 1976. Effects of liquid phase electrical conductivity, water content, and surface conductivity. Soil Science Society of America Journal, 40: 651-655.

Roubens M. 1982. Fuzzy clustering algorithms and their cluster validity. European Journal of Operational Research, 10: 294-301.

Saey T., Islam M.M., De Smedt P., Meerschman E., Lehouck A. and Van Meirvenne M. 2012. Using a multi-receiver survey of apparent electrical conductivity to reconstruct a Holocene tidal channel in a polder area. Catena, 95: 104-111.

Saey T., Simpson D., Vermeersch H., Cockx L. and Van Meirvenne M. 2008a. Comparing the EM38DD and DUALEM-21S sensors for depth-to-clay mapping. Soil Science Society of America Journal, 73: 7-12.

Saey T., Simpson D., Vitharana U., Vermeersch H., Vermang J. and Van Meirvenne M. 2008b. Reconstructing the paleotopography beneath the loess cover with the aid of an electromagnetic induction sensor. Catena 74: 58-64.`

Saey T., Van Meirvenne M., De Smedt P., Cockx L., Meerschman E., Islam M.M. and Meeuws F. 2011. Mapping depth-to-clay using fitted multiple depth response curves of a proximal EMI sensor. Geoderma, 162: 151-158.

Saey T., Van Meirvenne M., Vermeersch H., Ameloot N. and Cockx L. 2009. A pedotransfer function to evaluate the soil profile textural heterogeneity using proximally sensed apparent electrical conductivity. Geoderma, 150: 389-395.

Samouelian A., Cousin I., Tabbagh A., Bruand A. and Richard G. 2005. Electrical resistivity survey in soil science: A review. Soil and Tillage Research. 83: 173- 193.

Sanders H.G. 1930. A note on the value of uniformity trials for subsequent experiments. The Journal of Agricultural Science, 20: 63-73.

Schroeder J.J., Neeteson J.J., Oenema O. and Struik P.C., 2000. Does the crop or the soil indicate how to save nitrogen in maize production? Reviewing the state of the art. Field Crops Research, 66: 151-164.

Shainberg I., Rhoades J.D. and Prather R.J. 1980. Effect of exchangeable sodium percentage, cation exchange capacity, and soil solution concentration on soil electrical conductivity. Soil Science Society of America Journal, 44: 469-473.

Sharma P.K. and De Datta S.K. 1985. Puddling influence on soil, rice development and yield. Soil Science Society of America Journal, 49:1451-1457.

Sheets K.R. and Hendrickx J.M.H. 1995. Non-invasive soil water content measurement using electromagnetic induction. Water Resources Research, 31: 2401-2409.

Simpson D., Lehouck A., Verdonck L., Vermeersch H., Van Meirvenne M., Bourgeois J., Thoen E. and Docter R. 2009. Comparison between electromagnetic induction and fluxgate gradiometer measurements on the buried remains of a 17th century castle. Journal of Applied Geophysics, 68: 294-300.

Slavich P.G. and Petterson G.H. 1990. Estimating average rootzone salinity for electromagnetic (EM-38) measurements. Australian Journal of Soil Research, 28: 453-463.

Sommer M. 2006. Influence of soil pattern on matter transport in and from terrestrial biogeosystems-a new concept for landscape pedology. Geoderma, 133: 107-123.

Spies B.R. and Frischknecht F.C. 1991. Electromagnetic Sounding. In: Nabighian M.N. (Ed.), Electromagnetic methods in applied geophysics (vol. 2, application, parts A & B). Society of Exploration Geophysicists, USA, pp. 285-426.

Stafford J.V. 2000. Implementing precision agriculture in the 21st century. Journal of Agricultural Engineering Research, 76: 267-275.

Sudduth K.A., Hummel J.W. and Birrell S.J. 1997. Sensors for site-specific management. In: Pierce, F.J. and Sadler, E.J. (Eds.), The State of Site-Specific Management for Agriculture. ASA-CSSA-SSSA, Madison, WI, USA, pp. 183-210.

Sudduth K.A., Kitchen N.R., Bollero G.A., Bullock D.G. and Wiebold W.J. 2003. Comparison of electromagnetic induction and direct sensing of soil electrical conductivity. Agronomy Journal, 95: 472-482.

Triantafilis J., Ahmed M.F. and Odeh I.O.A. 2002. Application of a mobile electromagnetic sensing system (MESS) to assess cause and management of soil salinization in an irrigated cotton-growing field. Soil Use and Management, 18: 330-339.

Triantafilis J., Laslett G.M. and McBratney A.B. 2000. Calibrating an electromagnetic induction instrument to measure salinity in soil under irrigated cotton. Soil Science Society of America Journal, 64: 1008-1017.

Viscarra Rossel R.A. and McBratney A.B. 1998. Laboratory evaluation of a proximal sensing technique for simultaneous measurement of soil clay and water content. Geoderma, 85: 19-39.

Viscarra Rossel R.A., Fouad Y. and Walter C. 2008. Using a digital camera to measure soil organic carbon and iron contents. Biosystems Engineering, 100: 149-159.

Vitharana U.W.A., Van Meirvenne M., Simpson D., Cockx L. and De Baerdemaeker J. 2008. Key soil and topographic properties to delineate potential management classes for precision agriculture in the European loess area. Geoderma, 143: 206-215.

Webster R. and Oliver M.A. 2007. Geostatistics for Environmental Scientists, Second Edition. John Wiley & Sons, Chichester.

Whelan B.M., McBratney A.B. and Boydell B.C. 1997. The impact of precision agriculture. Proceedings of the ABARE Outlook Conference, 'The Future of Cropping in NW NSW', Moree, UK, July 1997, p. 5.

Williams B.G. and Hoey D. 1987. The use of electromagnetic induction to detect the spatial variability of the salt and clay contents of soil. Australian Journal of Soil Research, 25: 21-27.

Wollenhaupt N.C., Mulla D.J. and Crawford, C.A.G. 1997. Soil sampling and interpolation techniques for mapping spatial variability of soil properties. In: Pierce F.J. and Sadler E.J. (Eds.), The state of site specific management for agriculture, ASA-CSSA-SSSA, Madison, pp. 19-54.

Xie X.L. and Beni G. 1991. A variety measure for fuzzy clustering, IEEE trans. On pattern analysis and machine intelligence., 13: 841-847.

Yang C., Peterson C.L., Shropshire G.J. and Otawa T. 1998. Spatial Variability of Field Topography and Wheat Yield in the Palouse Region of the Pacific Northwest. Transactions of the ASAE, 41: 17-27.

Yoshida S. 1983. Rice. In: Smith, W.H. and Banta S.J. (Eds.), Potential productivity of fiend crops under different environments. International Rice Research Institute, Los Banos, Philippines.

Zalasiewicz J.A., Mathers S.J. and Cornwell J.D. 1985. The application of ground conductivity measurements to geological mapping. Quarterly Journal of Engineering Geology, 18: 139-148.

Zhang N., Wang M. and Wang N. 2002. Precision agriculture- a worldwide overview. Computers and Electronics in Agriculture, 36: 113-132.

Curriculum vitae

CURRICULUM VITAE

Personal information

Name	MOHAMMAD MONIRUL ISLAM
Date of Birth	3 July, 1976
Address	Department of Soil Management, 653 Coupure Links, 9000 Gent, Belgium
Nationality	Bangladesh
e-mails	MohammadMonirul.Islam@UGent.be (office); twshar@gmail.com (personal)
Telephone	+32 9 264 60 42 (office); +32 4 865 15 209 (personal)

Education

2012 **PhD** (public defense on 19th November, 2012) in Applied Biological Sciences: Land and Forest Management, Ghent University, Belgium

2007 **Master of Science** in Physical Land Resources (Soil Science)
Ghent University, Belgium

2006 **Advanced Studies** in Physical Land Resources
Ghent University, Belgium

2003 **Master of Science** in Agronomy
Bangladesh Agricultural University, Bangladesh

2001 **Bachelor of Science** in Agriculture
Bangladesh Agricultural University, Bangladesh

Professional experience

2008-2012 **Researcher**
Department of Soil Management
Ghent University, Belgium

Research focus: Development and application of an electromagnetic induction (EMI) based soil sensing system for flooded paddy rice fields.

2007-2008 **Researcher**
Division of Mechatronics Biostatistics and Sensors,
Department of Biosystems, Katholieke Universiteit Leuven,
Leuven, Belgium

Research focus: Development of an on-the-Go Visible and Near Infrared (Vis-NIR) proximal soil sensing system and modeling of soil-landscape attributes.

2003-2005 **Assistant Professor**
Department of Agronomy
Bangladesh Agricultural University, Bangladesh

2001-2003 **Lecturer**
Department of Agronomy
Bangladesh Agricultural University, Bangladesh

Masters research supervision

A.K.M Mominul Islam, (2009-2010). The potential of a proximal soil sensor to map soil properties of a paddy field in the alluvial plain of Bangladesh. MSc thesis, Ghent University, Belgium.

- Thesis submitted in partial fulfillment to obtain the degree of Master of Science in Physical Land Resources (Soil Science).

Md. Nur-E- Alam Siddique (2009-2010). Potential of soil sensor measurements for soil mapping of Bangladesh. MSc thesis, Ghent University, Belgium.

- Thesis submitted in partial fulfillment to obtain the degree of Master of Science in Physical Land Resources (Soil Science).

Scholarships and awards received

a. *UGent-BOF PhD Scholarship* (2008-2012): The Ghent University scholarship for doing PhD at the Ghent University of Belgium.

b. *IWT Scholarship* (2007-2008): The Belgian government research scholarship for Innovation in Science and Technology (IWT), Division of Mechatronics Biostatistics and Sensors, Department of Biosystems, Katholieke Universiteit Leuven, Belgium.

c. *VLIR-UGent Scholarship* (2005-2007): The VLIR-UOS Inter-University scholarship of the Belgian Government for doing Masters at the Ghent University of Belgium.

d. *Ministry of Science and Technology Scholarship* (2003): *Ministry of Science and Technology Scholarship* of Bangladesh for doing Masters in Agronomy at the Bangladesh Agricultural University.

e. *Professor Jinnat Ara Gold medal* (2001) for securing the top position in the Bachelor of Science (Graduation) examination.

f. *University Grants Commission (UGC) of Bangladesh merit Scholarship* (2000) for academic excellence during Bachelor study at the Bangladesh Agricultural University, Bangladesh.

Scientific Publications

a. Peer reviewed publications indexed in the web of science

Islam, M.M., Meerschman, E., Saey, T., De Smedt, P., Van De Vijver, E., Van Meirvenne, M., Identifying compaction variability in a puddled paddy rice field using a non-invasive proximal soil sensing system. Submitted for publication in: Computers and Electronics in Agriculture.

Islam, M.M., Saey, T., De Smedt, P., Meerschman, E., Van De Vijver, E., Van Meirvenne, M., Modeling the within field variation in the depth of the compaction layer in a paddy field using a proximal soil sensing system. Submitted for publication in: Soil Use and Management.

Saey, T., De Smedt, P., De Clercq, W., Meerschman, E., **Islam, M.M.**, Van Meirvenne, M., 2012. Identifying soil patterns at distinctly different spatial scales with a multi-receiver EMI sensor. Submitted for publication in: Soil Science Society of America Journal.

Meerschman, E., Van Meirvenne, M., Mariethoz, G., **Islam, M.M.**, De Smedt, P., Van De Vijver, E. and Saey, T. Using bivariate multiple-point statistics and proximal soil sensor data to map fossil ice-wedge polygons. Accepted with minor revision in: Geoderma.

Meerschman, E., Van Meirvenne, M., Van De Vijver, E., De Smedt, P., **Islam, M.M.** and Saey, T. Mapping complex soil patterns with multiple-point geostatistics. Accepted with minor revision in: European Journal of Soil Science.

De Smedt, P., Saey, T., Lehouck, A., Stichelbaut, B., Meerschman, E., **Islam, M.M.**, Van De Vijver, E., Van Meirvenne, M., 2012. Exploring the potential of multi-receiver EMI survey for geoarchaeological prospection: a 90 ha dataset. Accepted for publication in: Geoderma.

Van Meirvenne, M., **Islam, M.M**., De Smedt, P., Meerschman, E., Van De Vijver, E., Saey, T., 2012. Key variables for the identification of soil management classes in the aeolian landscapes of north-west Europe. Accepted for publication in: Geoderma.

Islam, M.M., Meerschman, E., Saey, T., De Smedt, P., Van De Vijver, E., Van Meirvenne, M., 2012. Comparing apparent electrical conductivity measurements on a paddy field under flooded and drained conditions. Precision Agriculture. 13, 384-392.

Saey, T., **Islam, M.M.**, De Smedt, P., Meerschman, E., Lehouck, A., Van Meirvenne, M., 2012. Using a multi-receiver survey of apparent electrical conductivity to reconstruct a Holocene tidal channel in a polder area. Catena, 95, 104-111.

Saey, T., De Smedt, P., **Islam, M.M.**, Meerschman, E., Van De Vijver, E., Lehouck, A., Van Meirvenne, M., 2012. Depth slicing of multi-receiver EMI measurements to enhance the delineation of contrasting subsoil features. Geoderma, 189-190: 514-521.

Saey, T., De Smedt, P., Meerschman, E., **Islam, M.M.**, Meeuws, F., Van De Vijver, E., Lehouck, A., Van Meirvenne, M., 2012. Electrical conductivity depth modelling with a multi-receiver EMI sensor for Prospecting Archaeological Features. Archaeological Prospection, 19, 21-30.

Saey, T., Van Meirvenne, M., Dewilde, M., Wyffels, F., De Smedt, P., Cockx, L., Meerschman, E., **Islam, M.M.**, Meeuws, F., 2011. Combining multiple signals of an electromagnetic induction soil sensor to prospect land for metallic objects. Near Surface Geophysics, 9, 309-317.

Saey, T., Van Meirvenne, M., De Smedt, P., Cockx, L., Meerschman, E., **Islam, M.M.**, Meeuws, F., 2011. Mapping depth-to-clay using fitted multiple depth response curves of a proximal EMI sensor. Geoderma, 162: 151-158.

Meerschman, E., Cockx, L., **Islam, M.M.**, Meeuws, F. and Van Meirvenne, M. 2011. Geostatistical assessment of the impact of World War I on the spatial occurrence of soil heavy metals. AMBIO: A Journal of the Human Environment, 40(4), 417-424.

Meerschman, E., Van Meirvenne, M., De Smedt, P., Saey, T., **Islam, M.M.**, Meeuws, F., Van De Vijver, E., Ghysels, G. 2011. Imaging a polygonal network of ice-wedge casts with an electromagnetic induction sensor. Soil Science Society of America Journal, 75,2095-2100.

Islam, M.M., Saey, T., Meerschman, E., De Smedt, P., Meeuws, F., Van De Vijver, E., Van Meirvenne, M., 2011. Delineating water management zones in a paddy rice field using a floating soil sensing system. Agricultural Water Management, 102, 8-12.

Islam, M.M., Cockx, L., Meerschman, E., De Smedt, P., Meeuws, F., Van Meirvenne, M., 2011. A floating sensing system to evaluate soil and crop variability within flooded paddy rice fields. Precision Agriculture. 12(6), 850-859.

b. Peer reviewed publications

Alam, M.K., Salam, M.A., **Islam, M.M.**, Yesmin, S., Rahman, M.R., 2005. Effect of seedling age on the performance of two varieties of transplant aman rice under the system of rice intensification. Bangladesh Journal of Crop Science. 16(2): 229-235.

Nahar, K., **Islam, M.M.**, Hossain, I., 2005. Study on seed and seedling health status of farmers saved rice seed cv. BR 1 from bogra district. Bangladesh Journal of Seed Science and Technology. 8(1&2):1-5.

Ahmed, I.M., Anwar, M.P., **Islam, M.M.**, Islam, M.A., Sarkar, M.A.R., 2004. Effect of row ratio and transplanting time of restorer and cytoplasmic male sterility lines on seed production of BRRI hybrid dhan. Bangladesh Journal of Crop Science. 13-15: 63-69.

Rahman, M.M., **Islam, M.M.**, Aktar, F.M.F., 2004. Effect of hill spacing and nitrogen level on seed yield and yield attributes of transplant aman rice. Bangladesh Journal of Crop Science. 13-15: 95-101.

Islam, M.M., Sarkar, M.A.R., Ahmed, M., 2004. Effect of seedling age and plant spacing on the yield and yield attributes of BRRI Dhan 29. Bangladesh Journal of Crop Science. 13-15: 83-88.

Islam, M.M., Sarkar, M.A.R., 2004. Effect of fertilizer management and spacing on the yield and yield attributes of bororice. Bangladesh Journal of Agricultural Sciences. 31 (2): 227-232.

Islam, M.M., Bhuiyan, M.M.H., Islam, F., Nahar, K., Rahman, B.M.Z., 2003. Response of late transplant aman rice to various forms and timing of nitrogenous fertilizer application. Bangladesh Journal of Agricultural Sciences. 30 (1): 51-55.

Sobhan, M.A., Anwar, M.P., **Islam**, **M.M.**, Islam, M.A., 2003. Effect of number of seedling and spacing on the yield of hybrid rice variety sonarbangla-1. Bangladesh Journal of Environmental Science. 9:132-137.

Islam, M.M., Khan, M.S.K., Rahman, B.M.Z., Islam, F., Nahar, K., 2003. Effect of nitrogen on growth, yield and quality of wheat. Bangladesh Journal of Agricultural Sciences. 30 (1): 43-49.

Islam, M.M., Amin, M.R., Islam, M.A., Islam, F., Nahar, K., 2003. Effect of nitrogenous fertilizer on yield and quality of aromatic rice. Bangladesh Journal of Agricultural Sciences. 30 (2): 287-293.

Rahman, B.M.Z., Anwar, M.P., Shahin, S.M., Islam, F., **Islam, M.M.**, 2002. Response of wheat to phosphorus and boron nutrition. Bangladesh Journal of Agricultural Sciences. 29 (1): 159-164.

Paul, S., Anwar, M.P., **Islam**, **M.M.**, Debnath, K. Nahar, K., 2002. Effect of different forms of urea, and nitrogen levels on yield of three transplant aman rice varieties. Progressive Agriculture. 13 (1&2): 15-17.

c. Non-refereed Publications

Islam, M.M. 2003. Enhancement of Growth and Yield of Boro Rice through Modification of SRI (System of Rice Intensification) Technique in Terms of Fertilizer Management, Spacing and Seedling Age. MSc thesis, Department of Agronomy, Bangladesh Agricultural University, Mymensingh-2202, Bangladesh.

Islam, M.M. 2007. Identifying Management Zones within an Agricultural Field in the Sandy Area of Flanders. MSc thesis, Department of Soil Management, Ghent University, Belgium.

d. Books

Islam, A.K.M. M., Van Meirvenne M., **Islam M.M.**, 2011. Proximal soil sensing system for paddy field variability mapping: The potential of a proximal soil sensor for soil properties mapping. VDM Verlag Dr. Müller GmbH & Co. KG, Saarbrücken, Germany, ISBN-13: 978-3639375619.

Bhuiya M.S.U., **Islam M.M.**, Uddin M.R., Salam M.A., Rahman M.M., 2005. Introductory Agronomy. Oracle Publications, 38/2A, Banglabazar, Dhaka-1100, Bangladesh.

e. Book chapters

Islam, M. M. and Van Meirvenne M. 2011. FloSSy: a floating sensing system to evaluate soil variability of flooded paddy fields. In: Stafford J.V. (Ed.), Precision Agriculture 2011. Czech Centre for Science and Society, Prague, Czech Republic. ISBN: 978-80-904830-5-7, pp. 60-66.

Islam, M. M., Meerschman, E., Cockx, L., De Smedt, P., Meeuws, F., Van Meirvenne, M., 2011. In: Stafford J.V. (Ed.), Precision Agriculture 2011. Czech Centre for Science and Society, Prague, Czech Republic. ISBN: 978-80-904830-5-7, pp. 43-50.

f. Articles in Conference Proceedings

Van Holm, L., Cockx, L., **Islam, M.M.**, Van Meirvenne, M., Mertens, J., Bries, J., Merckx, R., 2008. Identifying Management zones within a field in the sandy area of Flanders. In: Proceedings of the International Conference on Agricultural Engineering & Industry Exhibition (AgEng 2008), Hersonissos (Crete), Greece, 23-25 June, 2008.

Islam, M.M., Van Meirvenne, M., Loonstra, E., Meerschman, E., De Smedt, P., Meeuws, F., Van De Vijver, E., Saye, T. 2011. Key properties for delineating soil management zones. In: Adamchuk V.I. and Viscarra Rossel, R.A. (Eds.), Proceeding of the second Global Workshop on Proximal Soil Sensing, pp. 52-55. Montreal, Canada: McGill University, 15-18 May 2011.

g. Abstracts in Conference Proceedings

Islam, M.M., Van Meirvenne, M., 2011. A floating sensing system to evaluate soil variability of flooded paddy fields. In: Proceedings of the thematic day of the soil science society of Belgium, Brussels, Belgium, 7 December, 2011.

Van Meirvenne M., Saey T., Simpson D., **Islam M.M.**, Ameloot N., 2009. Proximal soil sensing in support of soil inventory and archaeological prospection. In: Proceedings of the 69th Annual *Meeting* of the *German Geophysical* Society, *Kiel*, *Germany,* 23-*26 March, 2009*.

h. Poster in symposium

Van Meirvenne, M., **Islam, M.M.**, 2011. Detailed soil mapping of paddy fields using the mobile soil sensor FloSSy. Event on FBE your partner in development cooperation, Faculty of Bioscience Engineering, Ghent University, Gent 9000, Belgium, 8 December, 2010.